AIR FORCE INSTITUTE OF TECHNOLOGY

AIR UNIVERSITY
UNITED STATES AIR FORCE
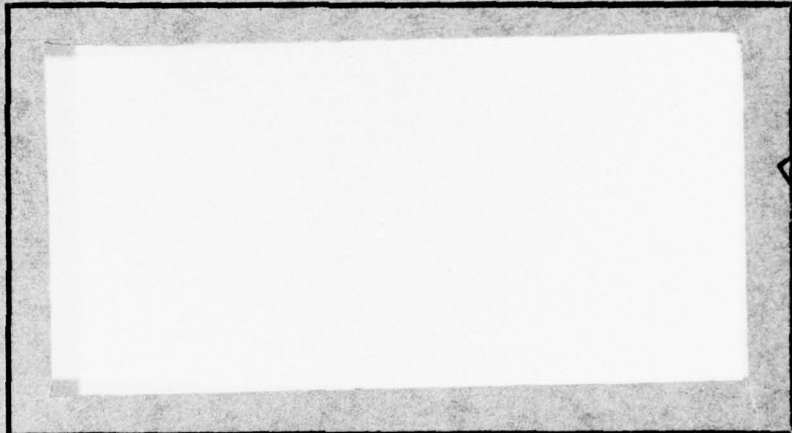
SCHOOL OF ENGINEERING

WRIGHT-PATTERSON AIR FORCE BASE, OHIO

DDC
JAN 16 1978
F

OPTIMAL ATTITUDE CONTROL OF

AN ORBITING SATELLITE

CONTAINING FLEXIBLE APPENDAGES

THESIS

AFIT/GA/AA/77D-1   Vincent T. Cilmi
                    Captain   USAF

OPTIMAL ATTITUDE CONTROL OF
AN ORBITING SATELLITE
CONTAINING FLEXIBLE APPENDAGES.

Master's THESIS,

Presented to the Faculty of the School of Engineering

of the Air Force Institute of Technology

Air University

in Partial Fulfillment of the

Requirements for the Degree of

Master of Science

by

Vincent T. Cilmi, BAE

Captain   USAF

Graduate Astronautical Engineering

December 1977

116 p.

Preface

This report presents the results of my investigation into three methods for obtaining the optimal control requirements of satellites with flexible appendages. A new method using integral coordinate techniques was introduced in this thesis and was found to provide quite acceptable optimal control results.

This project required that I become fairly involved with the concepts of modern control theory, stability analysis, and dynamics of flexible vehicles. In this regard, I am indebted to Dr. Leonard Meirovitch for his many publications which provided background information in these areas. I am especially grateful to Dr. Robert A. Calico, my thesis advisor, for suggesting the original idea for this thesis and for the guidance he provided throughout this project.

Finally, I would like to thank my wife, Maria, and our daughters, Maria Angela, Kristina, and Diana for their patience and understanding during the past eighteen months.

Contents

List of Figures

List of Tables

Symbols

a	distance from satellite center of mass to oscillators
A	symmetrical rigid body moment of inertia about the x axis
A'	moment of inertia of rigid body and antenna in the undeformed state about the x axis
$\underline{A}$	dynamics matrix of the uncontrolled system
B	symmetrical rigid body moment of inertia about the y axis
B'	moment of inertia of rigid body and antenna in the undeformed state about the y axis
$\underline{B}$	control input matrix
$\beta_i l$	eigenvalues corresponding to the natural frequencies of vibration for a cantilevered beam
C	moment of inertia about the z axis
d	damping coefficient
dm	differential mass element
dz	differential displacement in the z direction
D	Rayleigh's dissipation function
EI	bending stiffness modulus
$\underline{F}$	feedback gain matrix
h	distance from center of mass to antenna connection point
H	Hamiltonian
$\hat{i}, \hat{j}, \hat{k}$	unit vectors of the x,y,z system
I_m	moment of inertia matrix of mass oscillators

I_{B-m}	Principle moment of inertia matrix of rigid body
K	spring stiffness acting on mass oscillators
l	length of antenna
L	Lagrangian
m	mass of antenna
M	mass of rigid body
P_i	generalized momentum terms
$\dot{P}_i$	time derivative of generalized momentum terms
$\underline{P}$	steady state solution matrix to Riccati equation
q_i	generalized coordinate terms
$\dot{q}_i$	time derivative of generalized coordinate
$\underline{Q}$	state weighting matrix
$\bar{r}$	radius vector from center of mass to differential mass on rigid body
$\bar{r}_m$	radius vector from center of mass to mass oscillator
$\underline{R}$	control weighting matrix
RA	moment of inertia ratio
$\overline{RC}$	radius vector from center of earth to center of mass of satellite
RI	inertia type term
S_{z_i}	used for notation simplification
t	time
T	kinetic energy
T_2	kinetic energy terms quadratic in generalized velocities
T_1	kinetic energy terms linear in generalized velocities

T_0	kinetic energy terms in generalized coordinates alone
$(\ )^T$	transpose of a matrix
u	antenna displacement in the x direction for the discrete system model
$\dot{u}$	antenna velocity in the x direction
$u_{1,2,3,4}$	mode displacements in the x direction
$\bar{u}$	integral coordinate defined for x direction
$\bar{u}(t)$	control vector
$U(z,t)$	superposition of total normal mode motion in the x direction
v	antenna displacement in the y direction
$\dot{v}$	antenna velocity in the y direction
$v_{1,2,3,4}$	mode displacements in the y direction
$\bar{v}$	integral coordinate defined for y direction
V	potential energy
$\bar{V}$	velocity vector
$V(z,t)$	superposition of the total normal mode motion in the y direction
$\bar{x}(t)$	state vector
x_1	state element
x,y,z	body fixed axis at center of mass of satellite
X,Y,Z	orbital axis at center of mass of satellite
X_1,Y_1,Z_1	inertial axis fixed at center of earth
z	displacement along antenna in z direction
Zeta	damping ratio
δ_{ij}	Kronecker delta

$\theta_{1,2,3}$	angular displacements
$\dot{\theta}_{1,2,3}$	angular rates
p	mass per unit length of antenna
Φ_i	normal mode eigenfunctions for cantilevered beam
$\bar{\omega}$	angular velocity vector of satellite
ω_n	natural frequency
$\omega_{1,2,3,4}$	mode natural frequencies
Ω, Ω_s	satellite initial spin rate about the z axis
$\Omega_x, \Omega_y, \Omega_z$	angular velocities of the x,y,z system

Abstract

This thesis investigated three methods for obtaining optimal control requirements for satellites having flexible appendages. A discrete method, modal method, and a new integral coordinate method for obtaining control requirements were examined. Mathematical formulation was performed on a satellite configuration consisting of a symmetrical rigid body with two flexible antennas extending in opposite directions along the spin axis. System equations of motion were derived using Hamilton's equations. Modern optimal control theory, involving the minimization of a quadratic cost functional and the numerical solution to the steady state matrix Riccati equation, was applied to the system. An example problem was presented and numerically solved. The resulting controlled states and control requirements for each method were compared and a discussion of the advantages and disadvantages of the different techniques was presented. The results of this thesis indicate that the integral coordinate technique provides a valid and useful means of obtaining realistic estimates of control requirements for the class of satellites under consideration. The report goes on to recommend further investigation of the integral coordinate method for other spacecraft and satellite configurations.

OPTIMAL ATTITUDE CONTROL OF

AN ORBITING SATELLITE

CONTAINING FLEXIBLE APPENDAGES

I. Introduction

Background

In order to meet functional requirements, space vehicles
are frequently required to maintain a fixed orientation with
respect to either an orbiting frame of reference or some
inertial reference frame. In the early years of space ex-
ploration spacecraft tended to be small, mechanically simple,
and essentially rigid. Today, however, satellite configura-
tions are highly complex with many flexible devices, such as
antennas, booms, and solar panels, which greatly affect the
attitude dynamics of the body. The stability and control
requirements for such modern space systems are of particular
importance to the designer.

In recent years, numerous papers have been presented to
determine the effect that flexible appendages have on the
stability of space systems. Of particular interest are the
papers of Meirovitch and Calico (Ref 1; Ref 2), who extend
the Liapunov direct method of stability analysis to predict
the stability of various spacecraft configurations. Their
basic strategy was to define integral coordinates to evaluate
the system Hamiltonian and test for stability by using the
Hamiltonian as a Liapunov functional. Their research pro-
vided a simplified, alternative means of predicting stability

1

of satellites with flexible appendages. In the area of satellite attitude control, methods of analysis are complex requiring a thorough investigation of a particular vehicle configuration in order to obtain a prediction of optimal control requirements. By using techniques similar to those developed by Meirovitch and Calico for predicting stability, this thesis will examine the control requirements for satellites with flexible appendages, and attempt to provide a new method for obtaining the optimal control for these space systems.

Problem Definition

It is well known that a rigid satellite is stable when spun about its axis of maximum moment of inertia. However, the addition of flexible appendages to spin stabilized space systems can result in an undesirable wobbling, or coning motion, of the vehicle. To keep the attitude of flexible satellites in proper orientation a means of controlling the system is required. Frequently, active attitude controllers employing momentum exchange or mass explusion devices are utilized to resist attitude perturbations. The active controller can take various forms, such as a momentum wheel, or as a reaction jet controller of the spin axis orientation (Ref 3:87). Regardless of what control device is physically implemented, the designer of flexible satellites must have a good a priori knowledge of the amount of control which will be required to regulate a particular satellite.

The overall direction of this thesis will be to provide

2

a new, relatively simple, method for estimating the required optimal control to maintain a particular spacecraft attitude. The new method will be based on the technique of integral coordinates previously employed by Meirovitch and Calico (Ref 1) to predict satellite stability. By using this simplified technique, the time and effort required to obtain an estimate for the optimal control will be significantly reduced over current complex methods employing modal analysis. Having a simple means of obtaining the control for flexible satellites would be of great benefit to the spacecraft designer, since it provides a tool that is relatively easy to employ upon which a control decision could be made during preliminary design.

General Problem Formulation

An objective of this thesis is to develop a new method for obtaining the optimal control of a satellite having flexible appendages. The particular satellite to be investigated consists of a symmetrical rigid body with two flexible antennas extending in the positive and negative directions of the z axis as depicted in Figure 1. Mathematical analysis is performed on a discrete model (Figure 2a) and a continuous model (Figure 2b) of this satellite configuration. The discrete model will be examined using spring-mass-damper oscillators to discretize the system and the continuous model will be investigated using both a modal analysis approach and a simplified method of integral coordinates. The kinetic and potential energies will be derived for the
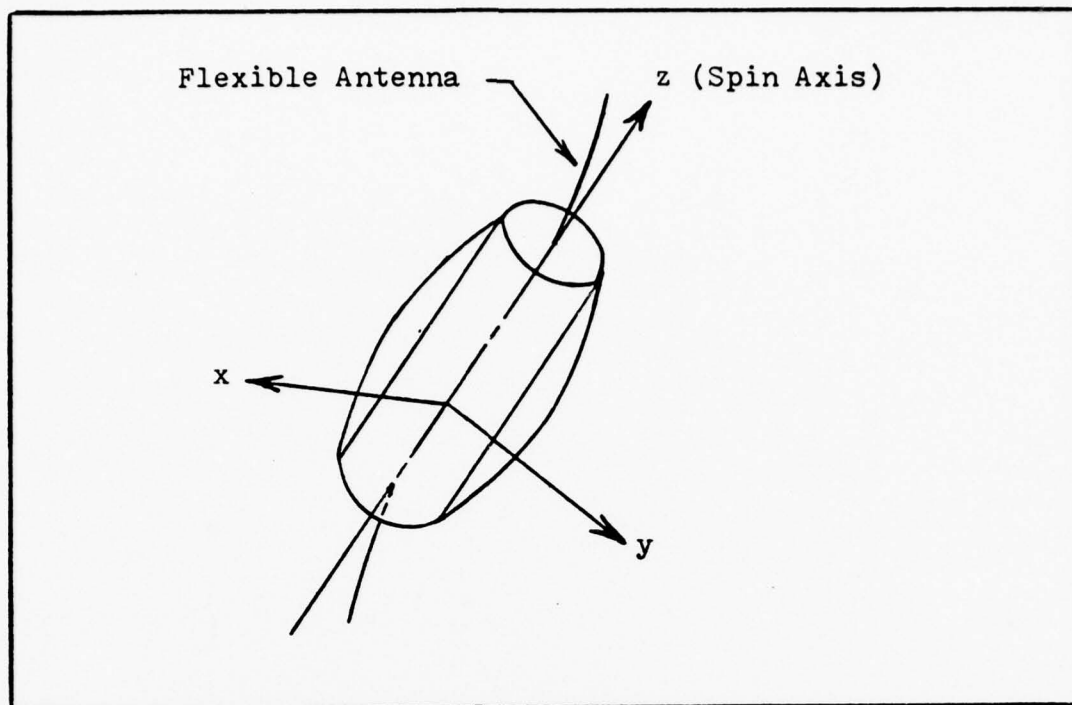
Figure 1.   Satellite Configuration
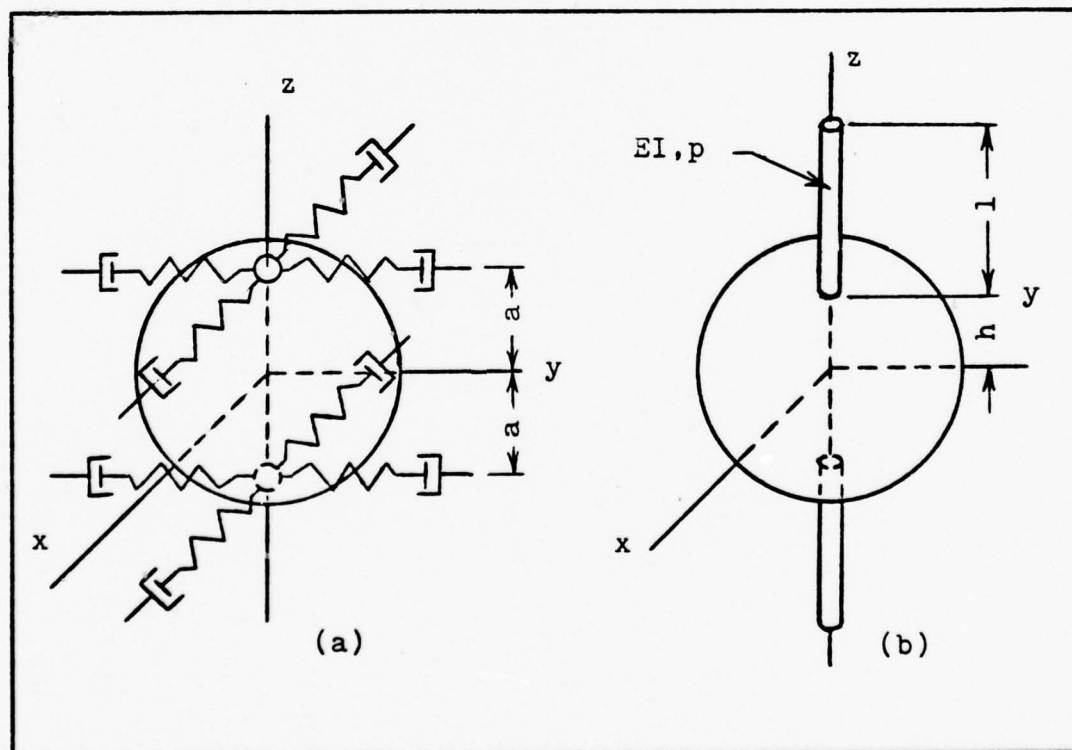
Figure 2.   Models: a) Discrete; b) Continuous

4

discrete and continuous models of this system. After deriving these energy expressions, the system Hamiltonian and Lagrangian will be formed and utilized in obtaining the satellite equations of motion. Once having the equations of motion, control will be introduced into the problem along with the constraint that the satellite spin axis will maintain a fixed orientation with respect to inertial space. To ascertain the amount of control required to keep a nulled satellite position, an optimal control problem will be formulated using discrete, modal, and integral coordinate methods. The results obtained for the three methods will be compared and an analysis will be made regarding the effectiveness of using integral coordinate techniques for determing optimal control of satellites containing flexible appendages.

Assumptions

This thesis will examine high spin stabilized satellites in earth orbit. Since the system is spinning at a relatively high rate, it can be shown that the torque due to gravity is quite small. For this reason, it will be assumed that the flexible satellite under consideration is moment-free for short time periods. This assumption is valid since the actual gravity torque on the system would have an insignificant effect on the attitude dynamics of the satellite as compared to the effects associated with such things as the system mass distribution, system elastic properties and dynamic coupling thereto, relative motion of internal mechanisms,

5

rate of conversion of mechanical energy into heat by dissi-
pative mechanisms, and external forces of various forms
(Ref 4:1597). For this investigation, it will be assumed
that the satellite is spin stabilized about the z axis, and
that the mass distribution, elastic properties of the system,
and conversion of mechanical energy into heat by dissipative
mechanisms contribute the dominant perturbations in the
attitude dynamics of the body. It will also be assumed that
the angular momentum of the relative motion of the satellite
to the earth is constant and neglegible compared to the
angular momentum of the rigid body motion. This assumption
is reasonable since this study examines high spin stabilized
satellites. For simplicity, the center of mass of the sat-
ellite will be assumed to move in a circular orbit. Since
the gravity potential is approximately a constant in a
circular orbit it will not affect the attitude dynamics of
the body over short time periods. Therefore, the potential
energy will consist entirely of elastic strain energy of the
flexing antennas. For ease of calculation, identical uniform
antennas are assumed. Antisymmetric motion of the satellite
antennas will be assumed to simplify the expression for the
kinetic energy. It can be shown that the antisymmetric
motion assumption would represent the worst possible case
in regards to the stability of the flexible satellite system
in question (Ref 5:202). Additionally, the antisymmetric
motion assumption implies that the center of mass remains
fixed relative to the main rigid body (Ref 6:1535). To

further simplify the kinetic energy expression, it will be assumed that the satellite will undergo small perturbations from the null position. This is a valid assumption since it can be shown that for an inherently stable configuration wobbling of the satellite due to perturbations will be contained in a small region near the equilibrium position. For an inherently unstable configuration with no controller, any perturbation will cause the cone angle of the wobble to increase until the body begins to tumble in space (Ref 4:1598). Since small angular and vibrational displacement perturbations are assumed, angular and displacement terms in the kinetic energy expression higher than second order will be ignored. The control required to maintain the satellite system in a desired orientation will depend upon several state measurements. It will be assumed that any state displacement required to implement the control feedback gains can be measured or somehow obtained during actual operations of the satellite. The modal investigation will be assumed to perfectly model the actual satellite system, and will provide the reference for evaluating the effectiveness of the new integral coordinate technique.

Sequence of Presentation

The remainder of this report is organized as follows. Chapter II presents the mathematical formulation of the satellite system. The equations of motion are derived for the discrete, modal, and integral coordinate techniques of the uncontrolled satellite systems. The equations of motion

are checked by performing an eigenvalue stability analysis and comparing the results with previous investigations on satellites of the same configuration. In Chapter III, control is introduced into the system and the optimal control problem is formulated. Closing this chapter is a brief discussion of how control feedback gains may be obtained. In Chapter IV a presentation of the control results is given. The effectiveness of the integral coordinate technique for obtaining an estimation of satellite optimal control requirements is analyzed. The conclusions to be drawn from this investigation are presented in Chapter V. A brief summary of the investigation is presented in Chapter VI. Also included in this final chapter are recommendations for utilizing integral coordinate techniques for satellites with flexible appendages.

II. Mathematical Formulation

Satellite in Earth Orbit

As previously indicated the specific satellite config-
uration under investigation consists of a symmetrical rigid
body with two flexible appendages extending out the negative
and positive z axes (Figure 1). When the satellite is in
the undeformed state, the x, y, and z body fixed axes rep-
resent the principle moment-of-inertia axes. The mass mo-
ments of inertia for the symmetrical rigid body section are
A, B=A, and C about the x, y, and z axes respectively. The
satellite orientation in earth orbit is depicted in Figure 3.
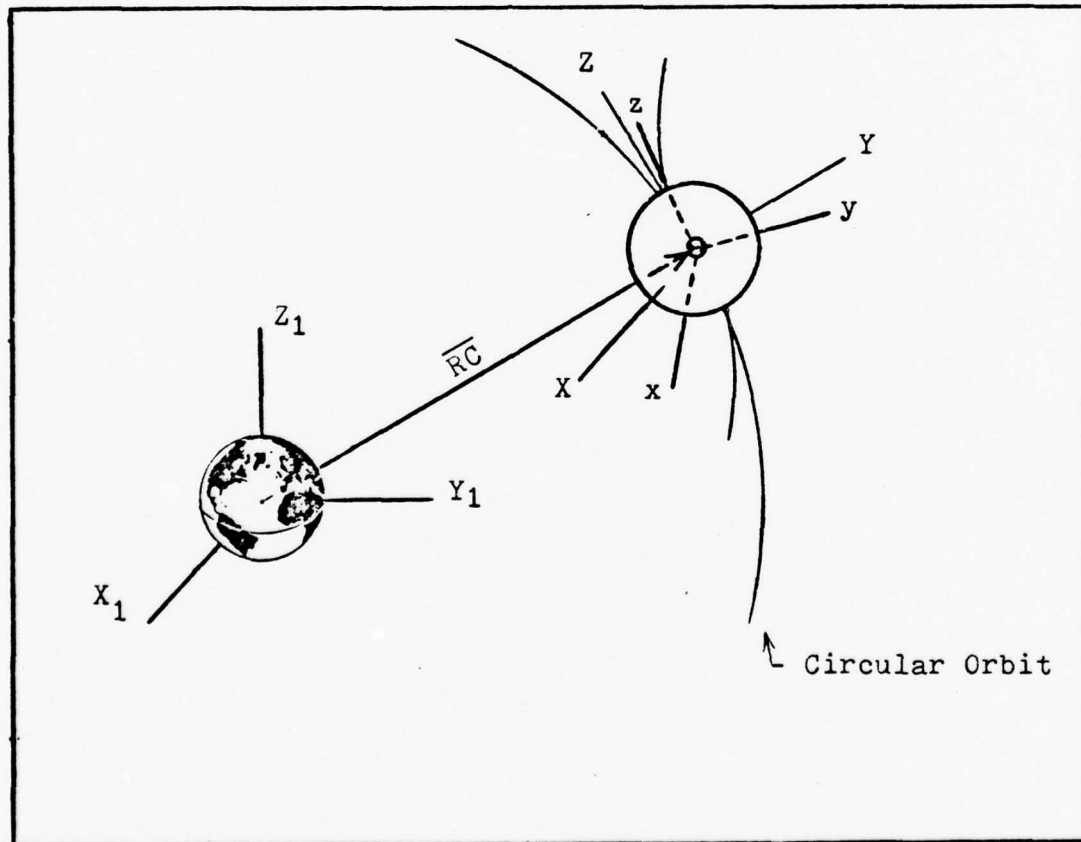
Figure 3. Satellite in Earth Orbit

The center of the earth is considered an inertial reference point with axes X_1, Y_1, and Z_1. The radius vector RC, which is constant in magnitude for a circular orbit, is measured from the center of the earth to the center of mass of the satellite.

Discrete Method - Equations of Motion

The discrete model of the satellite is illustrated in Figure 2a. The model consists of a symmetrical rigid body with spring-mass-damper oscillators simulating the flexible antennas. The oscillators each have a mass m and are symmetrically placed a distance a along the z axis. The motion of the two oscillators is denoted by u_1, v_1, u_2, and v_2, and the angular velocity components of the X,Y,Z system by Ω_x, Ω_y, and Ω_z. The complete motion of the system is described by ten generalized coordinates: three coordinates for the motion of the center of mass of the satellite, three coordinates for the angular orientation of the body, and four coordinates for the position of the two oscillators with respect to the x,y,z system. Under the assumption that the center of mass of the satellite moves around the earth in a circular orbit and at a constant angular velocity, the degrees of freedom of the system can be reduced by three. The assumption that the antennas move in antisymmetric motion implies that $u_1 = -u_2 = u$ and $v_1 = -v_2 = v$. This assumption allows a further reduction in the number of generalized coordinates by two. Before the equations of motion for these generalized coordinates can be derived, expressions

10

for the kinetic and potential energies must be established.

The general expression of the kinetic energy for the satellite system can be written as

$$T = \tfrac{1}{2} \int (\overline{V} \cdot \overline{V}) dm \qquad (1)$$

where $\overline{V}$ is the inertial velocity of an element of mass dm. For this discrete model, $\overline{V}$ can be written in component terms for the rigid body and mass oscillators and the integral evaluated over their respective domains. The general expression for the kinetic energy becomes

$$T = \tfrac{1}{2} A'\Omega_x^2 + \tfrac{1}{2} B'\Omega_y^2 + \tfrac{1}{2} C\Omega_z^2 + m(\dot{u}^2 + \dot{v}^2) + m\Big[v^2\Omega_x^2$$

$$+ u^2\Omega_y^2 + (u^2 + v^2)\Omega_z^2 - 2a\dot{v}\Omega_x + 2a\dot{u}\Omega_y - 2(\dot{u}v -$$

$$u\dot{v})\Omega_z - 2uv\Omega_x\Omega_y - 2av\Omega_y\Omega_z - 2au\Omega_x\Omega_z\Big] + \text{Const.} \qquad (2)$$

where $A' = A + 2ma^2$, $B' = B + 2ma^2$, and C are the mass moments of inertia of the undeformed body about the x, y, and z axes respectively. The derivation of equation (2) is given in Appendix A.

Since the effect of gravity forces is assumed negligible, the potential energy consists entirely of elastic strain energy. For the discrete system model the potential energy expression is

$$V = K(u^2 + v^2) \qquad (3)$$

where K is the spring stiffness of the oscillators in both the x and y directions. Here, the spring stiffness coefficient K was chosen to be equal in both directions since uniform antennas were assumed.

11

Energy dissipation in the system is due totally to damping in the antenna rods. In the discrete model, dissipation is modelled by placing damping pods on the oscillators. The equation expressing the effects of damping is given by Rayleigh's dissipation function

$$D = d(\dot{u}^2 + \dot{v}^2) \tag{4}$$

where d is the damping coefficient in the x and y directions.

Before proceeding to formulate the equations of motion, it is desired to express the orbitally referenced angular velocities Ω_x, Ω_y, and Ω_z in terms of Euler angles and rates. Figure 4 illustrates the 3-2-1 rotation used in the transformation to Euler angles.
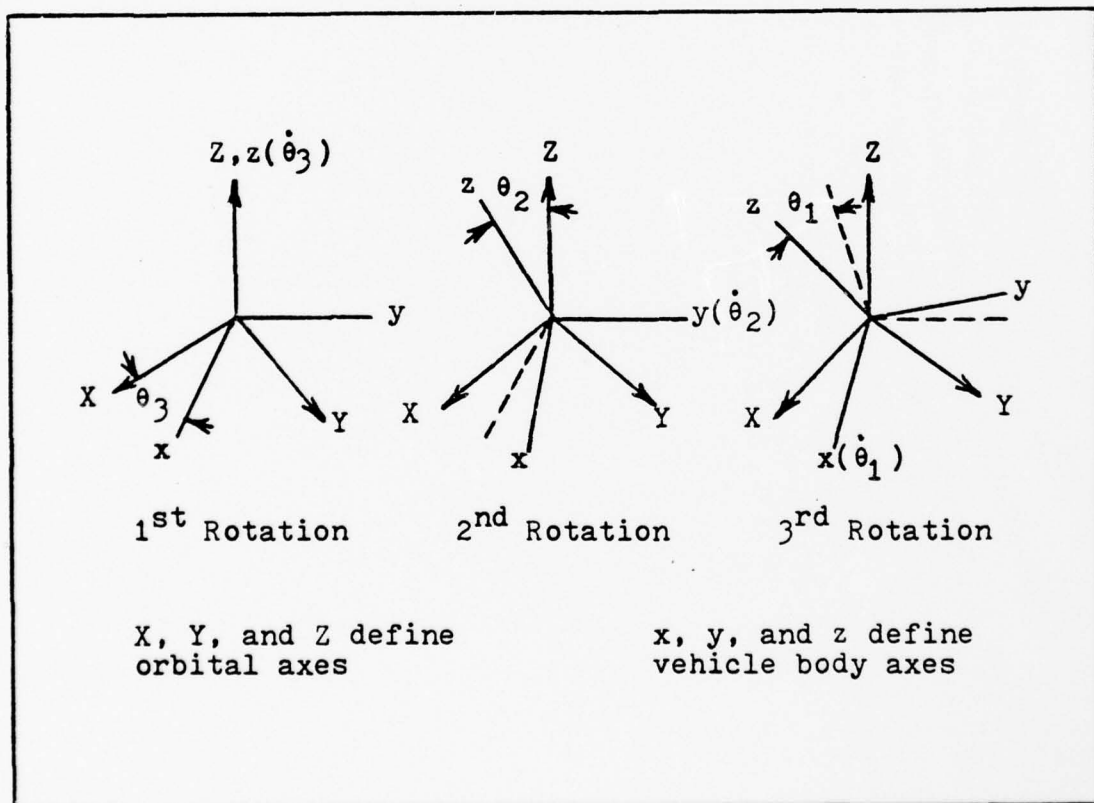
Figure 4. Satellite Rotational Motion

12

In Appendix B it is shown that the orbitally referenced angular velocities are related to Euler angles by

$$\bar{\omega} = \begin{bmatrix} \Omega_x \\ \Omega_y \\ \Omega_z \end{bmatrix} = \begin{bmatrix} 1 & 0 & -\sin\theta_2 \\ 0 & \cos\theta_1 & \sin\theta_1 \cos\theta_2 \\ 0 & -\sin\theta_1 & \cos\theta_1 \cos\theta_2 \end{bmatrix} \begin{bmatrix} \dot{\theta}_1 \\ \dot{\theta}_2 \\ \dot{\theta}_3 \end{bmatrix} \quad (5)$$

Since small angular displacements in θ_1 and θ_2 about a zero angle equilibrium point was assumed, equation (5) can be linearized by using the Taylor series expansion of the sine and cosine. For small angles Taylor series expansion yields

$$\sin\theta_{1,2} \cong \theta_{1,2}$$

and

$$\cos\theta_{1,2} \cong 1 - \frac{\theta_{1,2}^2}{2} \quad (6)$$

Substituting relations (6) into equation (5) yields

$$\bar{\omega} = \begin{bmatrix} \Omega_x \\ \Omega_y \\ \Omega_z \end{bmatrix} = \begin{bmatrix} 1 & 0 & -\theta_2 \\ 0 & 1 - \frac{\theta_1^2}{2} & \theta_1(1 - \frac{\theta_2^2}{2}) \\ 0 & -\theta_1 & (1 - \frac{\theta_1^2}{2})(1 - \frac{\theta_2^2}{2}) \end{bmatrix} \begin{bmatrix} \dot{\theta}_1 \\ \dot{\theta}_2 \\ \dot{\theta}_3 \end{bmatrix} \quad (7)$$

where $\dot{\theta}_1$ and $\dot{\theta}_2$ are angular velocities associated with small perturbation angles, and $\dot{\theta}_3$ is equal to the initial spin rate Ω about the z axis plus any small perturbation in spin about this axis. If equation (7) is substituted into the kinetic energy equation (2) and the assumption of small

13

state perturbations is applied, terms of higher than second order in the resulting kinetic energy expression can be ignored, yielding

$$
\begin{aligned}
T = \ & \tfrac{1}{2} A' \dot{\theta}_1{}^2 + \tfrac{1}{2} B' \dot{\theta}_2{}^2 + \tfrac{1}{2} C \dot{\theta}_3{}^2 + m(\dot{u}^2 + \dot{v}^2) - 2ma\dot{v}\dot{\theta}_1 \\
& + 2ma\dot{u}\dot{\theta}_2 - A'\Omega\theta_2\dot{\theta}_1 + B'\Omega\theta_1\dot{\theta}_2 + C(\Omega\dot{\theta}_3 - \Omega\theta_1\dot{\theta}_2) \\
& + 2ma\Omega\theta_2\dot{v} + 2ma\Omega\theta_1\dot{u} - 2m\Omega(\dot{u}v - u\dot{v}) - 2ma\Omega v\dot{\theta}_2 \\
& - 2ma\Omega u\dot{\theta}_1 + \tfrac{1}{2} A'\Omega^2\theta_2{}^2 + \tfrac{1}{2} B'\Omega^2\theta_1{}^2 + \tfrac{1}{2} C(\Omega^2 - \theta_1{}^2\Omega^2 \\
& - \theta_2{}^2\Omega^2) + m\Omega^2(u^2 + v^2) - 2ma\Omega^2 v\theta_1 + 2ma\Omega^2 u\theta_2 \qquad (8)
\end{aligned}
$$

Since the expressions for the kinetic energy and the potential energy depend on generalized coordinates and velocities alone, and not explicitly on time, the system is considered to be non-natural (Ref 7:77). For such a non-natural system it can be shown that the Hamiltonian assumes the form

$$
H = T_2 - T_0 + V \qquad (9)
$$

where T_2 represents those kinetic energy terms which are quadratic in the generalized velocities, T_0 represents kinetic energy terms which are independent of the generalized velocities, and V is the potential energy of the satellite system (Ref 7:84,91). Therefore, the Hamiltonian becomes

$$
\begin{aligned}
H = \ & \tfrac{1}{2} A' \dot{\theta}_1{}^2 + \tfrac{1}{2} B' \dot{\theta}_2{}^2 + \tfrac{1}{2} C \dot{\theta}_3{}^2 + m(\dot{u}^2 + \dot{v}^2) - 2ma\dot{v}\dot{\theta}_1 \\
& + 2ma\dot{u}\dot{\theta}_2 - \tfrac{1}{2} A'\Omega^2\theta_2{}^2 - \tfrac{1}{2} B'\Omega^2\theta_1{}^2 - \tfrac{1}{2} C(\Omega^2 - \Omega^2\theta_1{}^2 \\
& - \Omega^2\theta_2{}^2) - m\Omega^2(u^2 + v^2) + 2ma\Omega^2 v\theta_1 - 2ma\Omega^2 u\theta_2 \\
& \hspace{7cm} + K(u^2 + v^2) \quad (10)
\end{aligned}
$$

14

Also required for the formulation of the equations of motion is the Lagrangian which is defined by

$$L = T - V \tag{11}$$

For this particular system the Lagrangian is given by

$$
\begin{aligned}
L \; = \; & \tfrac{1}{2} A' \dot{\theta}_1{}^2 + \tfrac{1}{2} B' \dot{\theta}_2{}^2 + \tfrac{1}{2} C \dot{\theta}_3{}^2 + m(\dot{u}^2 + \dot{v}^2) - 2ma\dot{v}\dot{\theta}_1 \\
& + 2ma\dot{u}\dot{\theta}_2 - A'\Omega\theta_2\dot{\theta}_1 + B'\Omega\theta_1\dot{\theta}_2 + C(\Omega\dot{\theta}_3 - \Omega\theta_1\dot{\theta}_2) \\
& + 2ma\Omega\theta_2\dot{v} + 2ma\Omega\theta_1\dot{u} - 2m\Omega(\dot{u}v - u\dot{v}) - 2ma\Omega v\dot{\theta}_2 \\
& - 2ma\Omega u\dot{\theta}_1 + \tfrac{1}{2} A'\Omega^2\theta_2{}^2 + \tfrac{1}{2} B'\Omega^2\theta_1{}^2 + \tfrac{1}{2} C(\Omega^2 - \theta_1{}^2\Omega^2 \\
& - \theta_2{}^2\Omega^2) + m\Omega(u^2 + v^2) - 2ma\Omega^2 v\theta_1 + 2ma\Omega^2 u\theta_2 \\
& \hspace{8cm} - K(u^2 + v^2) \tag{12}
\end{aligned}
$$

The system equations of motion can now be formulated by either applying Lagrange's equations, which yield five second order differential equations, or Hamilton's equations, which yield ten first order differential equations. Hamilton's equations are used in this thesis to provide five first order differential equations of the generalized coordinates (θ_1, θ_2, θ_3, u, and v) and five first order differential equations of the generalized momentum (P_{θ_1}, P_{θ_2}, P_{θ_3}, P_u, and P_v). The generalized momentum is defined

$$P_i \equiv \frac{\partial L}{\partial \dot{q}_i} \qquad i = 1, ---, 5 \tag{13}$$

For a holonomic system subject to forces not derivable from a potential function, Hamilton's equations of motion take on a special form. In particular, when the nonconservative forces in the system are derivable from Rayleigh's dissipation function, Hamilton's equations become

15

$$\dot{q}_i = \frac{\partial H}{\partial P_i}, \qquad \dot{P}_i = -\frac{\partial H}{\partial q_i} - \frac{\partial D}{\partial \dot{q}_i} \qquad i = 1,\text{---},5 \qquad (14)$$

where Rayleigh's dissipation function D is expressed in equation (4) (Ref 7:95). A detailed derivation of the ten first order differential equations is presented in Appendix C. These equations of motion are summarized below:

$$\dot{\theta}_1 = \frac{P_{\theta_1} + aP_v}{A} + \Omega\theta_2$$

$$\dot{\theta}_2 = \frac{P_{\theta_2} - aP_u}{B} + (\frac{C}{B} - 1)\Omega\theta_1$$

$$\dot{\theta}_3 = \frac{P_{\theta_3}}{C} - \Omega$$

$$\dot{u} = -\frac{aP_{\theta_2}}{B} + \frac{B'P_u}{2mB} + \Omega v - \frac{Ca\Omega\theta_1}{B}$$

$$\dot{v} = \frac{aP_{\theta_1}}{A} + \frac{A'P_v}{2mA} - \Omega u$$

$$\dot{P}_{\theta_1} = (1 - \frac{C}{B})C\Omega^2\theta_1 + (1 - \frac{C}{B})\Omega P_{\theta_2} + \frac{C}{B}a\Omega P_u$$

$$\dot{P}_{\theta_2} = -C\Omega^2\theta_2 - \Omega P_{\theta_1}$$

$$\dot{P}_{\theta_3} = 0$$

$$\dot{P}_u = \Omega P_v - 2Ku - 2D\dot{u}$$

$$\dot{P}_v = -\Omega P_u - 2Kv - 2D\dot{v} \qquad (15)$$

Note that equation (15) can be expressed in state notation as

$$\dot{\overline{x}}(t) = \underline{A}\overline{x}(t) \tag{16}$$

where   x(t) is a 10 x 1 state vector

$\underline{A}$ is a constant coefficient 10 x 10 matrix

A stability analysis of the discrete system can now be accomplished by evaluating the eigenvalues and eigenvectors of the $\underline{A}$ matrix. This task was performed in this thesis to check the validity of the equations of motion shown in equation (15). Validity was confirmed by comparing stability results numerically calculated in this thesis to the stability results obtained by Meirovitch in Ref. 4 for the same satellite system. Although Ref. 4 used Lagrange's equations to formulate the equations of motion, the stability results for various system parameters were identical to the stability results obtained by using Hamilton's equations. Figures (5) and (6) depict ratio of spin rates obtained from Ref. 4 and from this thesis for particular satellite parameter sets. Additionally, eigenvalue stability analysis was in close agreement with that obtained in Ref 4. Figure 7 illustrates the stability regions obtained in Ref. 4 and in this thesis. Note that for these stability plots, stable regions are under the curve while unstable regions are above the curve. While not meant to be an exact proof, the similarity of stability results obtained in this analysis tends to support the validity of the equations of motion given by equation (15).

17
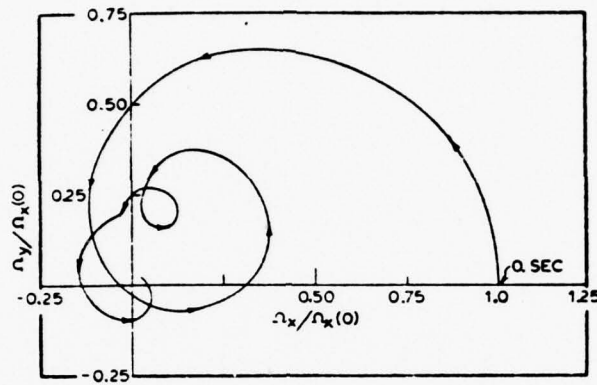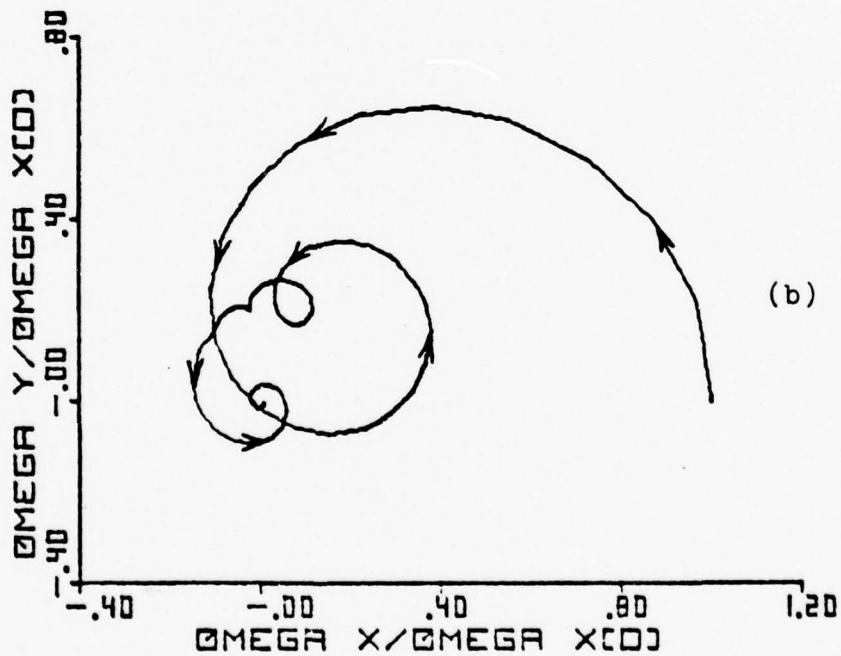
Figure 5.   Stable System Response: a) (Ref 4); b) Thesis
            Investigation

18
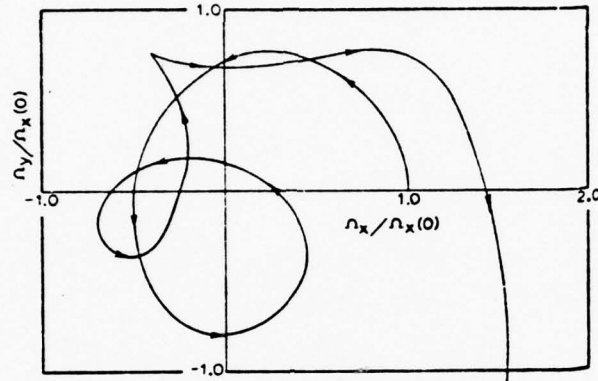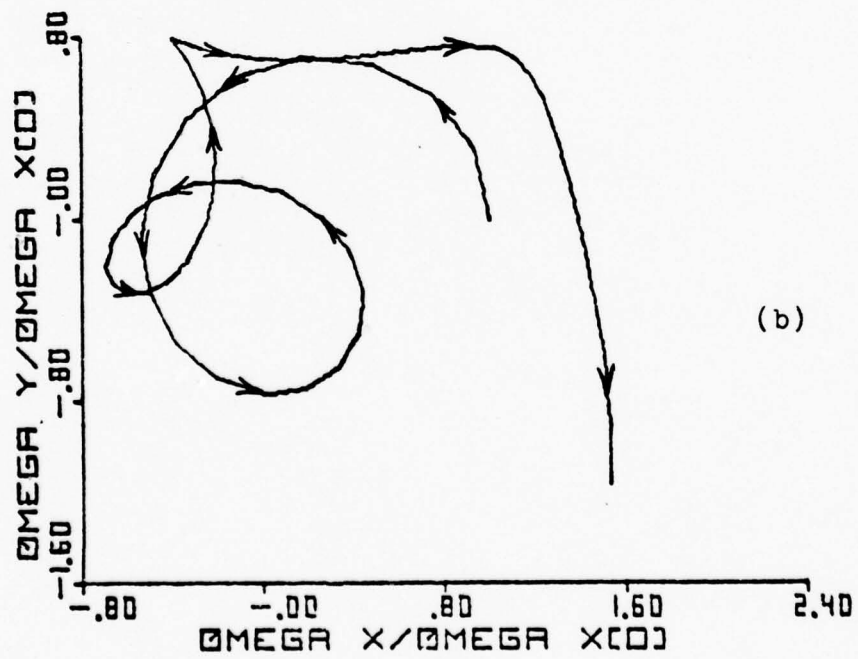
Figure 6. Unstable System Response: a) (Ref 4); b) Thesis
           Investigation

19

Parameter stability plot: discrete system $R_1 = 2ma^2/A$, $\zeta > 0$;

continuous system $R_2 = (2/A)\int_h^{h+l} z^2 dm$, $\alpha > 0$, $l = 1$, $h = 2$.
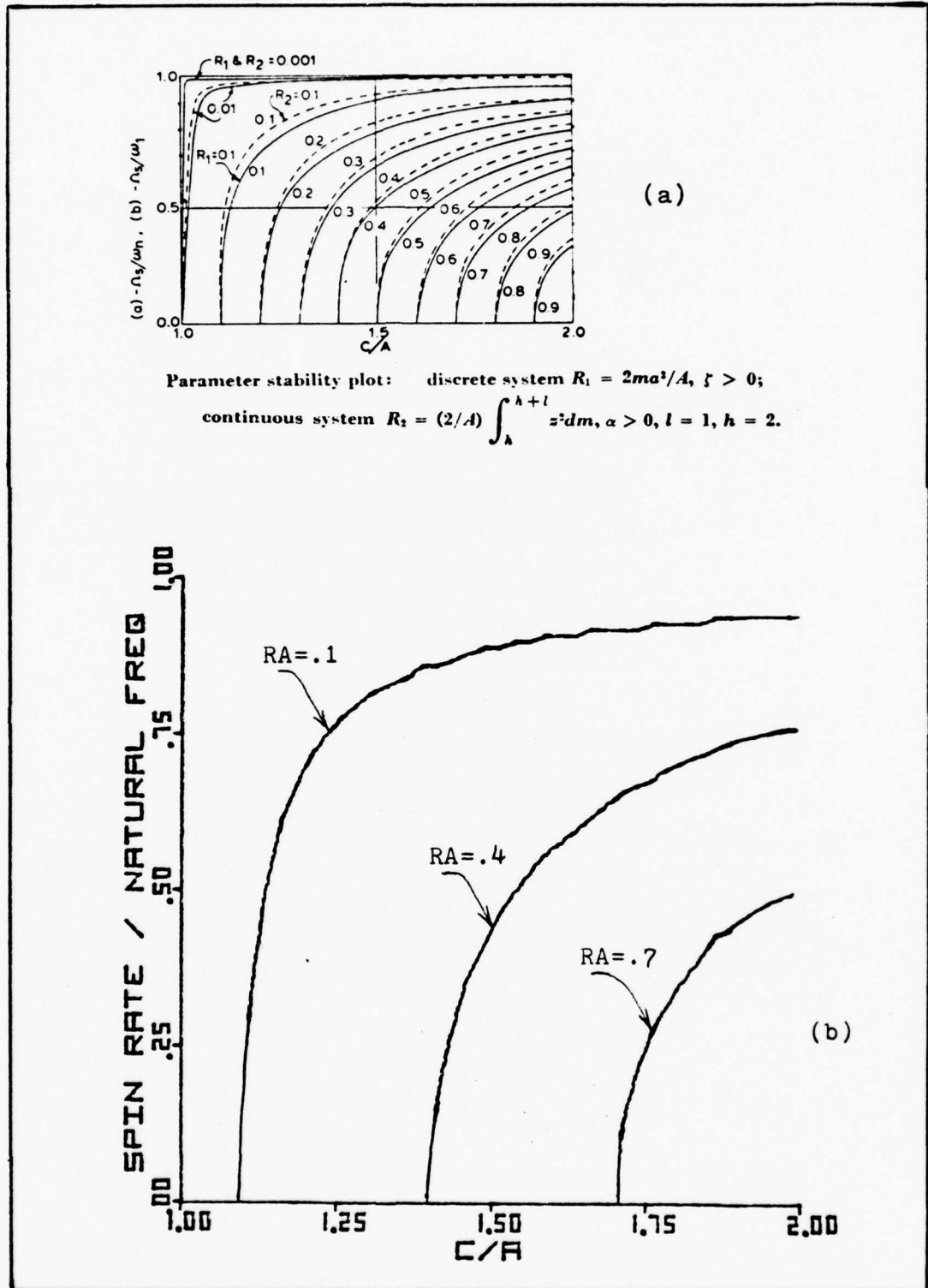
Figure 7. Stability Plot - Discrete System: a) (Ref 4);
b) Thesis Investigation

20

From this point in the investigation, some type of control could be introduced into the discrete system to keep a perturbed satellite in a proper or desired orientation. However, before proceeding with the control investigation, the equations of motion of both the modal analysis and integral coordinate techniques will be derived. After obtaining these attitude motion equations, control will be introduced and the results of each method will be presented and compared.

Continuous Modal Method - Equations of Motion

The continuous model of the satellite system is illustrated in Figure 2b. This model consists of two flexible uniform rods of length 1 connected to a symmetric rigid main body. The rods are attached at a distance h from the center of mass of the system. Each antenna rod has a mass per unit length of p and a total mass of m = p x 1. Proceeding as in the discrete system analysis, the kinetic and potential energy expressions will now be formulated.

The general expression for the kinetic energy is given by equation (1). Using the same assumptions as in the discrete system analysis, the kinetic energy for the continuous system can be written as

$$
\begin{aligned}
T = \; & \tfrac{1}{2} A' \Omega_x^2 + \tfrac{1}{2} B' \Omega_y^2 + \tfrac{1}{2} C \Omega_z^2 + \int_h^{h+1} \Big[\dot{u}^2 + \dot{v}^2 \\
& + v^2 \Omega_x^2 + u^2 \Omega_y^2 + (u^2 + v^2)\Omega_z^2 - 2z\dot{v}\Omega_x + 2z\dot{u}\Omega_y \\
& - 2(\dot{u}v - u\dot{v})\Omega_z - 2uv\Omega_x\Omega_y - 2zv\Omega_y\Omega_z - 2zu\Omega_x\Omega_z \Big] p\,dz \\
& \qquad\qquad\qquad\qquad\qquad\qquad\qquad + \text{Const.} \qquad (17)
\end{aligned}
$$

21

In equation (17) A' and B' are the mass moments of inertia about the x and y axes and includes the mass of the rods in the undeformed position. If the transformation presented on page 13 is again performed, the kinetic energy can be written in terms of Euler angles and rates. If the assumption of small state perturbations is applied, terms of higher than second order can be ignored, resulting in the following expression for the kinetic energy

$$
\begin{aligned}
T = & \frac{1}{2} A'(\dot{\theta}_1{}^2 - 2\theta_2\dot{\theta}_1\Omega + \theta_2{}^2\Omega^2) + \frac{1}{2} B'(\dot{\theta}_2{}^2 + 2\dot{\theta}_2\theta_1\Omega \\
& + \theta_1{}^2\Omega^2) + \frac{1}{2} C(\dot{\theta}_3{}^2 - 2\theta_1\dot{\theta}_2\Omega + 2\dot{\theta}_3\Omega - \theta_1{}^2\Omega^2 - \\
& \theta_2\Omega^2 + \Omega^2) + \int_h^{h+1}\left[\dot{u}^2 + \dot{v}^2 + (u^2 + v^2)\Omega^2 - \right. \\
& 2z\dot{v}(\dot{\theta}_1 - \theta_2\Omega) + 2z\dot{u}(\dot{\theta}_2 + \theta_1\Omega) - 2(\dot{u}v - u\dot{v})\Omega - \\
& \left. 2zv(\dot{\theta}_2\Omega + \theta_1\Omega^2) - 2zu(\dot{\theta}_1\Omega - \theta_2\Omega^2\right]pdz + \text{Const.} \quad (18)
\end{aligned}
$$

Breaking the kinetic energy into T_2 terms (quadratic in generalized velocities), T_1 terms (linear in generalized velocities), and T_0 terms (containing generalized coordinates alone) yields

$$
\begin{aligned}
T_2 = & \frac{1}{2} A'\dot{\theta}_1{}^2 + \frac{1}{2} B'\dot{\theta}_2{}^2 + \frac{1}{2} C\dot{\theta}_3{}^2 + \int_h^{h+1}\left[\dot{u}^2 + \dot{v}^2\right. \\
& \left. - 2z\dot{v}\dot{\theta}_1 + 2z\dot{u}\dot{\theta}_2\right]pdz
\end{aligned}
$$

$$
\begin{aligned}
T_1 = & -A'\Omega\theta_2\dot{\theta}_1 + B'\Omega\theta_1\dot{\theta}_2 + C(\Omega\dot{\theta}_3 - \Omega\theta_1\dot{\theta}_2) \\
& + \int_h^{h+1}\left[2z\Omega\theta_2\dot{v} + 2z\Omega\theta_1\dot{u} - 2\Omega(\dot{u}v - u\dot{v})\right. \\
& \left. - 2z\Omega v\dot{\theta}_2 - 2z\Omega u\dot{\theta}_1\right]pdz
\end{aligned}
$$

22

$$T_0 = \tfrac{1}{2}A'\Omega^2\theta_2{}^2 + \tfrac{1}{2}B'\Omega^2\theta_1{}^2 + \tfrac{1}{2}C\Omega^2(1 - \theta_1{}^2 - \theta_2{}^2)$$
$$+ \int_h^{h+1}\left[(u^2 + v^2)\Omega^2 - 2z\Omega^2 v\theta_1 + 2z\Omega^2 u\theta_2\right]pdz \qquad (19)$$

For the continuous system the potential energy expression, which is considered to be caused only by the elasticity of the rods, is

$$V = \int_h^{h+1} EI\left[\left(\frac{\partial^2 u}{\partial z^2}\right)^2 + \left(\frac{\partial^2 v}{\partial z^2}\right)^2\right]dz \qquad (20)$$

where it is assumed that the bending stiffness of the rods are identical in both the x and y directions (Ref 8:229).

The damping in the system is again given by Rayleigh's dissipation function. For the continuous system the dissipation function has the form

$$D = \int_h^{h+1} d(\dot{u}^2 + \dot{v}^2)dz \qquad (21)$$

where d is the damping coefficient in the x and y directions.

The general form of the Hamiltonian and the Lagrangian remain as given by equations (9) and (11). For the continuous system the Hamiltonian can be written as

$$H = \tfrac{1}{2}A'\dot\theta_1{}^2 + \tfrac{1}{2}B'\dot\theta_2{}^2 + \tfrac{1}{2}C\dot\theta_3{}^2 + \int_h^{h+1}\left[\dot{u}^2 + \dot{v}^2\right.$$
$$- 2z\dot{v}\theta_1 + 2z\dot{u}\theta_2\Big]pdz - \tfrac{1}{2}A'\Omega^2\theta_2{}^2 - \tfrac{1}{2}B'\Omega^2\theta_1{}^2$$
$$+ \tfrac{1}{2}C\Omega^2(\theta_1{}^2 + \theta_2{}^2 - 1) - \int_h^{h+1}\left[(u^2 + v^2)\Omega^2\right.$$
$$- 2z\Omega^2 v\theta_1 + 2z\Omega^2 u\theta_2\Big]pdz + \int_h^{h+1} EI\left[\left(\frac{\partial^2 u}{\partial z^2}\right)^2\right.$$
$$\left. + \left(\frac{\partial^2 v}{\partial z^2}\right)^2\right]dz \qquad (22)$$

23

The corresponding Lagrangian can be written as

$$L = \tfrac{1}{2} A' \dot{\theta}_1^2 + \tfrac{1}{2} B' \dot{\theta}_2^2 + \tfrac{1}{2} C \dot{\theta}_3^2 + \int_h^{h+1} [\dot{u}^2 + \dot{v}^2$$

$$- 2z\dot{v}\dot{\theta}_1 + 2z\dot{u}\dot{\theta}_2] p dz - A'\Omega\theta_2\dot{\theta}_1 + B'\Omega\theta_1\dot{\theta}_2 +$$

$$C\Omega(\dot{\theta}_3 - \theta_1\dot{\theta}_2) + \int_h^{h+1} [2z\Omega\theta_2\dot{v} + 2z\Omega\theta_1\dot{u} -$$

$$2\Omega(\dot{u}v - u\dot{v}) - 2z\Omega v\dot{\theta}_2 - 2z\Omega u\dot{\theta}_1] p dz + \tfrac{1}{2} A'\Omega^2\theta_2^2$$

$$+ \tfrac{1}{2} B'\Omega^2\theta_1^2 + \tfrac{1}{2} C\Omega^2(1 - \theta_1^2 - \theta_2^2) + \int_h^{h+1} [(u^2$$

$$+ v^2)\Omega^2 - 2z\Omega^2 v\theta_1 + 2z\Omega^2 u\theta_2] p dz -$$

$$\int_h^{h+1} EI\left[\left(\frac{\partial^2 u}{\partial z^2}\right)^2 + \left(\frac{\partial^2 v}{\partial z^2}\right)^2\right] dz \qquad (23)$$

It can be noted that in equations (22) and (23) elastic displacements appear in integrals defined over the elastic domain. The spatial and time dependency of u and v presents some difficulty in analyzing the continuous system in that the Hamiltonian and Lagrangian contain both continuous and discrete coordinates as well as spatial derivatives of the continuous coordinates. Such systems are termed hybrid, that is, they give rise to both ordinary and partial differential equations in describing the motion. In order to circumvent this, the system will be discretized by approximating elastic displacements by means of modal analysis.

In this thesis the first four natural modes of antenna motion are investigated. Using the antisymmetric motion assumption, the modal amplitudes in the x and y directions can be described by u_1, u_2, u_3, u_4, v_1, v_2, v_3, and v_4. Using

24

the assumption that attitude motion need only be considered, the complete attitude orientation of the satellite can be described by eight natural mode displacements and three angular rotations of the body. The modal analysis treats the elastic antennas as flexible beams subject to the boundary condition that the beams are rigidly attached to the satellite at one end and free at the other. The elastic motion of the individual antenna can be considered to consist of a superposition of the normal modes of a beam having the same mass and stiffness distribution as the flexible antenna (Ref 4:1601). In terms of an equation, the overall motion in the u and v directions is described by

$$U(z,t) = \sum_{i=1}^{n} \Phi_i(z)u_i(t)$$

$$V(z,t) = \sum_{i=1}^{n} \Phi_i(z)v_i(t) \qquad (24)$$

where z represents any point along the beam. Here, the normal modes or eigenfunctions Φ_i associated with a uniform cantilever beam satisfy the differential equation

$$EI \frac{d^4\Phi_i}{dz^4} - p\omega_i^2\Phi_i = 0 \qquad i = 1,---,n \qquad (25)$$

where the effects of shear deformations and rotary inertia are neglected (Ref 9:198). For a uniform beam the quantities EI and p are constants. In equation (25) ω_i is the natural frequency of the ith mode. Additionally, the

boundary conditions on equation (25) for a clamped-free beam
translate to

$$\Phi_i = 0, \quad \frac{d\Phi_i}{dz} = 0 \quad z = h$$

$$EI \frac{d^2\Phi_i}{dz^2} = 0, \quad d(EI \frac{d^2\Phi_i}{dz^2}) / dz = 0 \quad z = h + l \quad (26)$$

Previous solutions to the problem associated with equations
(25) and (26) yield eigenfunctions

$$\Phi_i = \frac{[\sin \beta_i l - \sinh \beta_i l][\sin \beta_i(z - h) - \sinh \beta_i(z - h)]}{\sqrt{pl} \, \sin \beta_i l \, \sinh \beta_i l} +$$

$$\frac{[\cos \beta_i l + \cosh \beta_i l][\cos \beta_i(z - h) - \cosh \beta_i(z - h)]}{\sqrt{pl} \, \sin \beta_i l \, \sinh \beta_i l} \quad (27)$$

in which

$$(\beta_i l)^4 = \frac{\omega_i^2 pl}{EI} , \quad (28)$$

where $\beta_i l$ is determined by

$$\cos \beta_i l \, \cosh \beta_i l = -1 \quad (29)$$

Values of $\beta_i l$ for various beams are readily obtainable from
reference text books in structures. For the clamped-free
beam these values are

$$\beta_1 l = 1.875$$

$$\beta_2 l = 4.694$$

$$\beta_3 l = 7.855$$

$$\vdots$$

$$\beta_i l \cong \frac{2i - 1}{2}\pi \quad (30)$$

26

In addition, the eigenfunctions of equation (27) are orthogonal and can be normalized with respect to the mass per unit length function p such that

$$\int_{h}^{h+1} p\Phi_i(z)\Phi_j(z)dz = \delta_{ij} \qquad (31)$$

where δ_{ij} represents the Kronecker delta (Ref 1:35).

Using the above modal analysis techniques, integral terms in the Hamiltonian and Lagrangian can be discretized. For example,

$$\int_{h}^{h+1} u^2 p\,dz = \sum_{i=1}^{n} u_i^2$$

$$\int_{h}^{h+1} \dot{u}^2 p\,dz = \sum_{i=1}^{n} \dot{u}_i^2$$

$$\int_{h}^{h+1} \dot{u}v p\,dz = \sum_{i=1}^{n} \dot{u}_i v_i$$

$$\int_{h}^{h+1} upz\,dz = (ml^2)^{\frac{1}{2}} \sum_{i=1}^{n} S_{zi} u_i$$

$$\int_{h}^{h+1} 2z\dot{\theta}_2 \dot{u} p\,dz = 2\dot{\theta}_2 (ml^2)^{\frac{1}{2}} \sum_{i=1}^{n} S_{zi} \dot{u}_i \qquad (32)$$

where

$$S_{zi} = \frac{2^{\frac{1}{2}}[(h/l)\beta_i l(\sin\beta_i l - \sinh\beta_i l) - (\cos\beta_i l + \cosh\beta_i l)]}{(\beta_i l)^2 \sin\beta_i l \sinh\beta_i l}$$

(Ref 1:54)   (33)

Additionally, it can be shown (Ref 8:220) that

$$\int_{h}^{h+1} EI\left[\left(\frac{\partial^2 u}{\partial z^2}\right)^2 + \left(\frac{\partial^2 v}{\partial z^2}\right)^2\right]dz = \sum_{i=1}^{n} \omega_i^2 u_i^2 + \sum_{i=1}^{n} \omega_i^2 v_i^2 \quad (34)$$

27

Since higher order modes will contribute minimally to the overall antenna motion, this investigation will restrict analysis to the first four natural modes of motion. With this in mind, the expression for the Hamiltonian becomes

$$H = \tfrac{1}{2} A' \dot{\theta}_1^2 + \tfrac{1}{2} B' \dot{\theta}_2^2 + \tfrac{1}{2} C\dot{\theta}_3^2 + \sum_{i=1}^{4} \dot{u}_i^2 + \sum_{i=1}^{4} \dot{v}_i^2$$

$$- 2\dot{\theta}_1 (ml^2)^{\frac{1}{2}} \sum_{i=1}^{4} S_{zi}\dot{v}_i + 2\dot{\theta}_2 (ml^2)^{\frac{1}{2}} \sum_{i=1}^{4} S_{zi}\dot{u}_i$$

$$- \tfrac{1}{2} A'\Omega^2\theta_2^2 - \tfrac{1}{2} B'\Omega^2\theta_1^2 + \tfrac{1}{2} C\Omega^2(\theta_1^2 + \theta_2^2 - 1)$$

$$- \Omega^2 \sum_{i=1}^{4} u_i^2 - \Omega^2 \sum_{i=1}^{4} v_i^2 + 2\theta_1\Omega^2(ml^2)^{\frac{1}{2}} \sum_{i=1}^{4} S_{zi}v_i$$

$$- 2\theta_2\Omega^2(ml^2)^{\frac{1}{2}} \sum_{i=1}^{4} S_{zi}u_i + \sum_{i=1}^{4} \omega_i^2(u_i^2 + v_i^2) \qquad (35)$$

Similarly the Lagrangian becomes

$$L = \tfrac{1}{2} A' \dot{\theta}_1^2 + \tfrac{1}{2} B' \dot{\theta}_2^2 + \tfrac{1}{2} C\dot{\theta}_3^2 + \sum_{i=1}^{4} (\dot{u}_i^2 + \dot{v}_i^2)$$

$$+ 2(ml^2)^{\frac{1}{2}} \sum_{i=1}^{4} S_{zi}(\dot{u}_i\theta_2 - \dot{v}_i\theta_1) - A'\Omega\theta_2\dot{\theta}_1 + B'\Omega\theta_1\dot{\theta}_2$$

$$+ C\Omega(\dot{\theta}_3 - \theta_1\dot{\theta}_2) + 2\Omega(ml^2)^{\frac{1}{2}} \sum_{i=1}^{4} S_{zi}(\dot{v}_i\theta_2 + \dot{u}_i\theta_1 -$$

$$v_i\dot{\theta}_2 - u_i\dot{\theta}_1) + 2\Omega \sum_{i=1}^{4} (\dot{u}_i v_i - u_i\dot{v}_i) + \tfrac{1}{2} A'\Omega^2\theta_2^2 +$$

$$\tfrac{1}{2} B'\Omega^2\theta_1^2 + \tfrac{1}{2} C\Omega^2(1 - \theta_1^2 - \theta_2^2) + \Omega^2 \sum_{i=1}^{4} (u_i^2 + v_i^2)$$

$$+ 2\Omega^2(ml^2)^{\frac{1}{2}} \sum_{i=1}^{4} S_{zi}(u_i\theta_2 - v_i\theta_1) - \omega_i^2 \sum_{i=1}^{4} (u_i^2 + v_i^2)$$

$$\qquad (36)$$

One is now in a position to obtain the equations of
motion for the continuous system by the modal method. The
generalized momentum is again given by

$$P_k = \frac{\partial L}{\partial \dot{q}_k} \qquad k = 1, ---, 11 \tag{37}$$

With Rayleigh's dissipation function D given by equation
(21), Hamilton's equations become

$$\dot{q}_k = \frac{\partial H}{\partial P_k}, \qquad \dot{P}_k = -\frac{\partial H}{\partial q_k} - \frac{\partial D}{\partial \dot{q}_k} \qquad k = 1, ---, 11 \tag{38}$$

The resulting 22 first order differential equations of
motion are derived in Appendix D and summarized below

$$\dot{\theta}_1 = \theta_2 + \frac{P_{\theta 1}}{D_a}$$

$$\dot{\theta}_2 = (\frac{C}{D_b} - 1)\,\theta_1 + \frac{P_{\theta 2}}{D_b} - \frac{(ml^2)^{\frac{1}{2}}}{D_b} \sum_{i=1}^{4} S_{z_i} P_{u_i}$$

$$\dot{v}_j = -\Omega u_j + \frac{(ml^2)^{\frac{1}{2}}}{D_a} S_{z_j} P_{\theta 1} + \frac{ml^2}{D_a} S_{z_j} \sum_{i=1}^{4} S_{z_i} P_{v_i}$$
$$+ \frac{P_{v_j}}{2} \qquad j = 1, ---, 4$$

$$\dot{u}_j = \Omega v_j - \frac{(ml^2)^{\frac{1}{2}}}{D_b} S_{z_j} P_{\theta 2} - \frac{(ml^2)^{\frac{1}{2}}}{D_b} C\Omega S_{z_j} \theta_1 + \frac{P_{u_j}}{2}$$
$$+ \frac{ml^2}{D_b} S_{z_j} \sum_{i=1}^{4} S_{z_i} P_{u_i} \qquad j = 1, ---, 4$$

$$\dot{P}_{\theta 1} = (1 - \frac{C}{D_b})C\Omega^2\theta_1 + (1 - \frac{C}{D_b})\Omega P_{\theta 2} + \frac{(ml^2)^{\frac{1}{2}}}{D_b} C\Omega \sum_{i=1}^{4} S_{z_i} P_{u_i}$$

$$\dot{P}_{\theta 2} = -C\Omega^2\theta_2 - \Omega P_{\theta 1}$$

29

$$\dot{P}_{v_j} = -2\omega_j^2 v_j + \frac{2d}{p}\Omega u_j - \frac{2d}{p}\left(\frac{ml^2}{D_a}\right)^{\frac{1}{2}} S_{zj} P_{\theta_1} - \Omega P_{u_j}$$

$$- \frac{d}{p}\left[P_{v_j} + \frac{2ml^2}{D_a} S_{zj} \sum_{i=1}^{4} S_{zi} P_{v_i}\right] \quad j = 1,---,4$$

$$\dot{P}_{u_j} = -2\omega_j^2 u_j - \frac{2d}{p}\Omega v_j + \frac{2d}{p}\left(\frac{ml^2}{D_b}\right)^{\frac{1}{2}} S_{zj}(C\Omega\theta_1 + P_{\theta_2}) + \Omega P_{v_j}$$

$$- \frac{d}{p}\left[P_{u_j} + \frac{2ml^2}{D_b} S_{zj} \sum_{i=1}^{4} S_{zi} P_{u_i}\right] \quad j = 1,---,4$$

$$\dot{\theta}_3 = \frac{P_{\theta_3}}{C} - \Omega$$

$$\dot{P}_{\theta_3} = 0 \tag{39}$$

The relations appearing in equation (39) were verified in much the same manner as the discrete system equations. Noting that θ_3 and P_{θ_3} uncouple from the system, an eigen-value stability analysis was performed on the remaining 20 x 20 constant coefficient matrix. Again, the results obtained in this analysis correspond to the modal method results obtained in Ref. 4 for the continuous system. This correspondence of results is illustrated in Figure 8 where similar stability plots are depicted for various system parameters. In Figure 8, stable regions are below the curve and unstable regions are above the curve.

For this investigation, the equations of motion obtained by the above modal technique will serve as a true model of the satellite system. Later in this thesis, control will be added to the system and results obtained using

30

Parameter stability plot: discrete system $R_1 = 2ma^2/A,\ \zeta > 0$; continuous system $R_2 = (2/A)\int_h^{h+l} z^2 dm,\ \alpha > 0,\ l = 1,\ h = 2$.
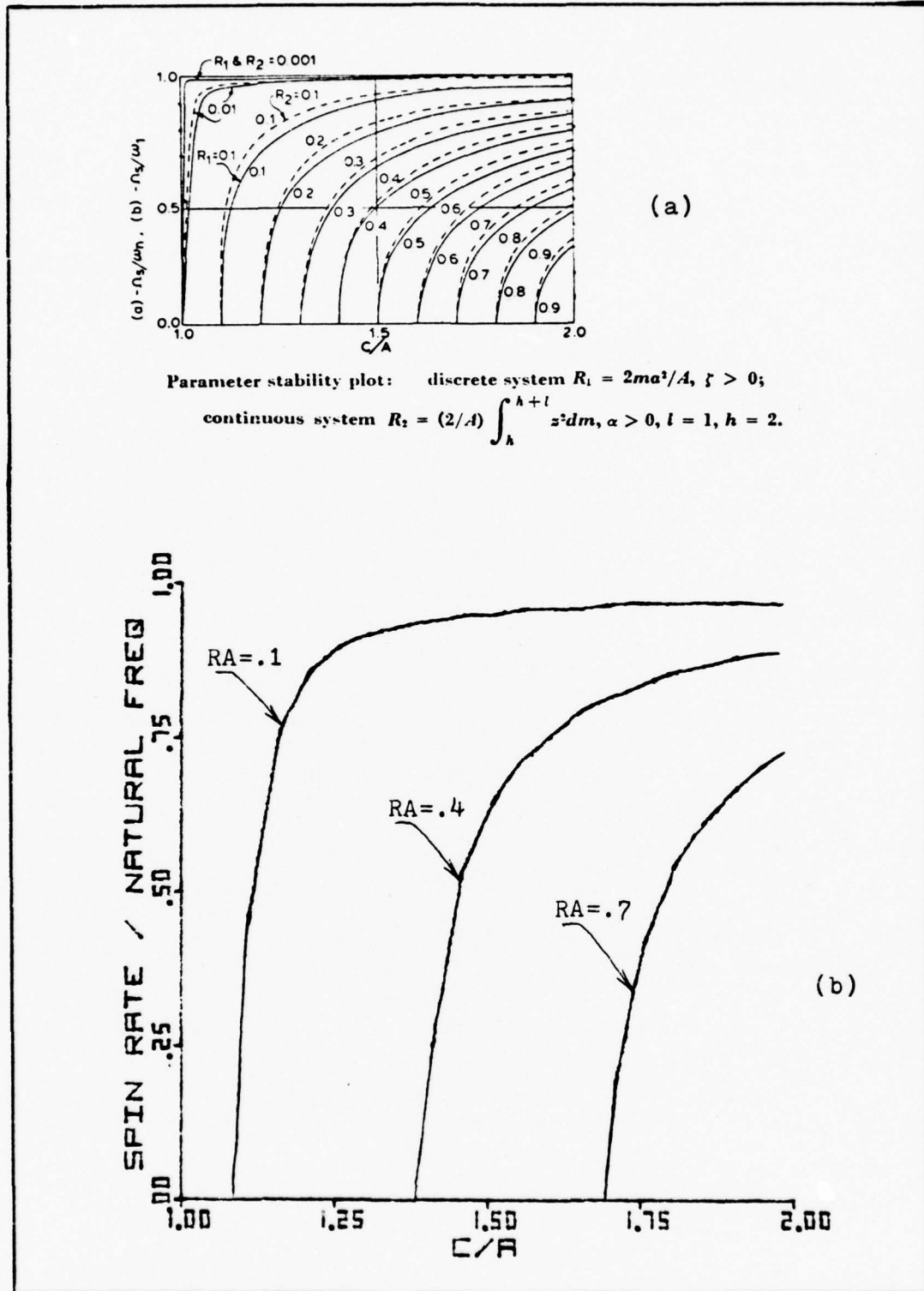
Figure 8. Stability Plot - Continuous System a) (Ref 4)
b) Thesis Investigation

31

integral coordinate equations of motion, which are derived
in the next section, are compared to results obtained by
this so-called true model.

Integral Coordinate Method - Equations of Motion

As can be noted, the modal analysis method of the pre-
vious section leads to a rather large and complex system
of differential equations. Additionally, modal analysis
does leave some question as to the accuracy of results
since series truncation is utilized. In this section, a
method of integral coordinates will be introduced which will
significantly reduce the number of differential equations
to be solved. Although the integral coordinate technique
has fewer differential equations, the system is still based
on a continuous representation with results maintaining a
high degree of correctness.

The model for the satellite system remains that given
by Figure 2b. Since the model is continuous, the general
expressions for the system Hamiltonian and Lagrangian are
once again given by equations (22) and (23). In order to
circumvent the problems associated with evaluating the spa-
tially dependent integrals in equations (22) and (23), new
coordinates will be selected. To this end, the following
integral coordinates are defined

$$\bar{u} = \int_h^{h+1} puzdz \ , \qquad \dot{\bar{u}} = \int_h^{h+1} p\dot{u}zdz$$

$$\bar{v} = \int_h^{h+1} pvzdz \ , \qquad \dot{\bar{v}} = \int_h^{h+1} p\dot{v}zdz \qquad (40)$$

32

For the integral coordinate formulation, it can be surmised that the general coordinates will be θ_1, θ_2, θ_3, $\bar{u}$, and $\bar{v}$. The immediate advantage of this approach is in its simplicity. The continuous system may now be investigated using the same number of generalized coordinates as in the discrete system, while maintaining the completeness of the more complex modal analysis investigation.

In conjunction with the definitions given in equation (40), integral terms in equations (22) and (23) which are quadratic in u or v may be handled by using Schwarz's inequality. This inequality relationship is

$$\left(\int_h^{h+1} pvz\,dz\right)^2 \leq \int_h^{h+1} pz^2\,dz \int_h^{h+1} pv^2\,dz \quad \text{(Ref 1:59) (41)}$$

or

$$\int_h^{h+1} pv^2\,dz \geq \frac{\left(\int_h^{h+1} pvz\,dz\right)^2}{\int_h^{h+1} pz^2\,dz} \tag{42}$$

Approximating by using the equality sign above, and recalling the definition of $\bar{v}$ yields

$$\int_h^{h+1} pv^2\,dz \cong \frac{\bar{v}^2}{\int_h^{h+1} pz^2\,dz} \tag{43}$$

Similarly,

$$\int_h^{h+1} pu^2\,dz \cong \frac{\bar{u}^2}{\int_h^{h+1} pz^2\,dz} \tag{44}$$

33

If the same procedure is followed for integrals with quadratic terms in $\dot{u}$ and $\dot{v}$, substitution into equation (22) for the Hamiltonian yields

$$H = \tfrac{1}{2} A'\dot{\theta}_1^2 + \tfrac{1}{2} B'\dot{\theta}_2^2 + \tfrac{1}{2} C\dot{\theta}_3^2 + \frac{\dot{u}^2}{RI} + \frac{\dot{v}^2}{RI} - 2\dot{\theta}_1\dot{\bar{v}} + 2\dot{\theta}_2\dot{\bar{u}}$$

$$- \tfrac{1}{2} A'\theta_2^2\Omega^2 - \tfrac{1}{2} B'\theta_1^2\Omega^2 - \tfrac{1}{2} C\Omega^2(1 - \theta_1^2 - \theta_2^2)$$

$$+ (\omega_1^2 - \Omega^2)\left[\frac{\bar{u}^2}{RI} + \frac{\bar{v}^2}{RI}\right] + 2\theta_1\Omega^2\bar{v} - 2\theta_2\Omega^2\bar{u} \qquad (45)$$

where

$$RI = \int_h^{h+1} pz^2 dz$$

$$A' = A + 2m(h + \tfrac{1}{2})^2 + \frac{2ml^2}{12}$$

$$B' = A' \qquad\qquad (46)$$

Similarly, substitution into equation (23) for the Lagrangian yields the following

$$L = \tfrac{1}{2} A'\dot{\theta}_1^2 + \tfrac{1}{2} B'\dot{\theta}_2^2 + \tfrac{1}{2} C\dot{\theta}_3^2 + \frac{\dot{u}^2}{RI} + \frac{\dot{v}^2}{RI} - 2\dot{\theta}_1\dot{\bar{v}} + 2\dot{\theta}_2\dot{\bar{u}}$$

$$- A'\theta_2\dot{\theta}_1\Omega + B'\theta_1\dot{\theta}_2\Omega - C\theta_1\dot{\theta}_2\Omega + C\dot{\theta}_3\Omega + 2\theta_2\Omega\dot{\bar{v}} + 2\theta_1\Omega\dot{\bar{u}}$$

$$- 2\dot{\theta}_2\Omega\bar{v} - 2\dot{\theta}_1\Omega\bar{u} + \tfrac{1}{2} A'\theta_2^2\Omega^2 + \tfrac{1}{2} B'\theta_1^2\Omega^2 + \tfrac{1}{2} C\Omega^2(1 -$$

$$\theta_1^2 - \theta_2^2) + (\Omega^2 - \omega_1^2)\left[\frac{\bar{u}^2}{RI} + \frac{\bar{v}^2}{RI}\right] + 2\theta_2\Omega^2\bar{u} - 2\theta_1\Omega^2\bar{v}$$

$$(47)$$

For simplicity, the term $(\dot{u}v - u\dot{v})$ in the Lagrangian has been intentionally neglected due to its small overall effect

on the system. The differential equations of motion for
the above integral coordinate technique can now be formu-
lated by again applying Hamilton's equations given in equa-
tions (13) and (14). With Rayleigh's dissipation function
defined by equation (21), it is shown in Appendix E that
the integral coordinate equations of motion become

$$
\dot{\theta}_1 = \frac{P_{\theta_1} + RI\ P_{\overline{v}}}{A' - 2RI} + \Omega\theta_2 + \frac{2\Omega\overline{u}}{A' - 2RI}
$$

$$
\dot{\theta}_2 = \frac{P_{\theta_2} - RI\ P_{\overline{u}}}{B' - 2RI} + \left(\frac{C}{B' - 2RI} - 1\right)\Omega\theta_1 + \frac{2\Omega\overline{v}}{B' - 2RI}
$$

$$
\dot{\overline{u}} = \frac{B'RI\ P_{\overline{u}}}{2(B' - 2RI)} - \frac{RI\ P_{\theta_2}}{B' - 2RI} - \frac{C\Omega RI\ \theta_1}{B' - 2RI} - \frac{2\Omega RI\ \overline{v}}{B' - 2RI}
$$

$$
\dot{\overline{v}} = \frac{A'RI\ P_{\overline{v}}}{2(A' - 2RI)} + \frac{RI\ P_{\theta_1}}{A' - 2RI} + \frac{2\Omega RI\ \overline{u}}{A' - 2RI}
$$

$$
\dot{P}_{\theta_1} = \left(1 - \frac{C}{B' - 2RI}\right)C\Omega^2\theta_1 + \left(1 - \frac{C}{B' - 2RI}\right)\Omega P_{\theta_2}
$$

$$
+ \frac{C\Omega RI\ P_{\overline{u}}}{B' - 2RI} - \frac{2C\Omega^2\overline{v}}{B' - 2RI}
$$

$$
\dot{P}_{\theta_2} = -\Omega P_{\theta_1} - C\Omega^2\theta_2
$$

$$
\dot{P}_{\overline{u}} = -\frac{2\Omega P_{\theta_1}}{A' - 2RI} - \frac{2\Omega RI\ P_{\overline{v}}}{A' - 2RI} - \frac{4\Omega^2\overline{u}}{A' - 2RI} + 2(\Omega^2 - \omega_1^2)\ \frac{\overline{u}}{RI}
$$

$$
+ \frac{d}{p(B' - 2RI)}\ (2C\Omega\theta_1 + 2P_{\theta_2} - B'P_{\overline{u}} + 4\Omega\overline{v})
$$

$$
\dot{P}_{\overline{v}} = -\frac{2\Omega P_{\theta_2}}{B' - 2RI} + \frac{2\Omega RI\ P_{\overline{u}}}{B' - 2RI} - \frac{2C\Omega^2\theta_1}{B' - 2RI} - \frac{4\Omega^2\overline{v}}{B' - 2RI} +
$$

$$
2(\Omega^2 - \omega_1^2)\ \frac{\overline{v}}{RI} - \frac{d}{p(B' - 2RI)}\ (A'P_{\overline{v}} - 2P_{\theta_1} - 4\Omega\overline{u})
$$

35

$$\dot{\theta}_3 = \frac{P_{\theta_3}}{C} - \Omega$$

$$\dot{P}_{\theta_3} = 0 \tag{48}$$

The equations of motion are now derived for the three
methods under investigation. In the next chapter, control
will be introduced into the problem. After the introduction
of control, the control requirements for the three methods
will be determined and the effectiveness of the integral
coordinate technique for obtaining control feedback gains
will be analyzed.

III. Control

Up to now the only control on the satellite has been the passive attitude control inherent in spin stabilized systems. Active attitude control of the satellite is required for two reasons. For one, even though a stable spinning satellite will tend to resist attitude perturbations, in time, its spin axis will move away from a desired direction due to the influence of a gravity gradient, aerodynamic force, or other such perturbative force. Secondly, active attitude control is required to reorient the spin axis of the satellite if a change in pointing direction is required during flight. In this thesis, the satellite will be initially displaced slightly from a null position to simulate the effect of either a perturbative force or a desired change in spin axis orientation. To effect the attitude change, control will be applied to the angular velocities $\dot{\theta}_1$ and $\dot{\theta}_2$ of the satellite system. A momentum exchange or a mass explusion device could be utilized to impart this change in angular velocities, although, the actual physical mechanism is immaterial to this investigation.

Optimal Control

Modern control theory techniques will be applied to obtain an estimation of the optimal control required to produce desired attitude changes in the satellite system. In this thesis, control is considered optimal in the sense that minimum angular velocity control is used to minimize

state deviations. For all three methods under investigation, the uncontrolled satellite is described by equation (16). Since the system is linear and time-invariant, the differential equation for the controlled satellite system is given by the matrix equation

$$\dot{\bar{x}}(t) = \underline{A}\bar{x}(t) + \underline{B}\bar{u}(t) \quad \text{(Ref 10:148)} \quad (49)$$

where

$\underline{A}$ is a (n x n) plant matrix

$\underline{B}$ is a (n x r) input matrix

$\bar{x}(t)$ is a (n x 1) state vector

$\bar{u}(t)$ is a (r x 1) control vector

Optimal control is now sought such that a quadratic cost functional involving the weighted components of the states plus the control is minimized when the final time is unspecified. In terms of an equation, the quadratic cost function is given by

$$J = \frac{1}{2}\int_{0}^{\infty}(\bar{x}^{T}(t)\underline{Q}\bar{x}(t) + \bar{u}^{T}(t)\underline{R}\bar{u}(t))dt \quad (50)$$

where $\underline{Q}$ and $\underline{R}$ are positive definite symmetric weighting matrices on the states and control vectors respectively (Ref 10:149). If $\underline{Q}$ is large it would imply that the corresponding state components will be rapidly regulated. If there are large entries in $\underline{R}$, this would imply that energy in the corresponding control element will be kept small. In this thesis, both $\underline{Q}$ and $\underline{R}$ are set equal to the identity matrix, $(\underline{I})$, implying equal weighting for the states and

the control. For the cost function and state relationship presented above, it can be shown that a statement of the optimal control is given by

$$\overline{u}(t) = - \underline{R}^{-1}\underline{B}^{T}\underline{P}\overline{x}(t) \tag{51}$$

where the determination of the optimal control involves the solution of $\underline{P}$ by the matrix Riccati equation (Ref 10:151). The matrix Riccati equation is given by the following differential equation

$$\underline{\dot{P}} + \underline{PA} + \underline{A}^{T}\underline{P} - \underline{PBR}^{-1}\underline{B}^{T}\underline{P} = 0 \tag{52}$$

where the steady state solution can be determined by setting $\underline{P}$ equal to zero. Defining the feedback gain matrix as

$$\underline{F} = - \underline{R}^{-1}\underline{B}^{T}\underline{P} \tag{53}$$

the closed-loop system matrix differential equations can be written

$$\dot{\overline{x}}(t) = (\underline{A} + \underline{BF})\overline{x}(t) \tag{54}$$

For the closed-loop system, stability can be determined by numerically calculating the eigenvalues and eigenvectors associated with the time-invariant matrix coefficient on $\overline{x}(t)$ in equation (54). A block diagram of the closed-loop system is illustrated in Figure 9.
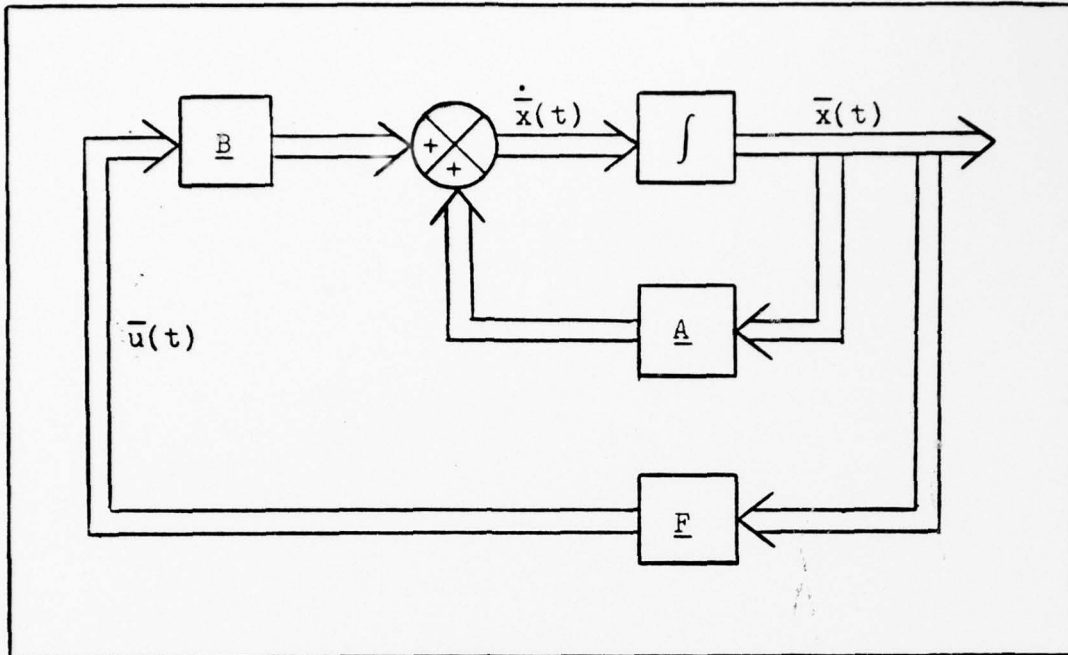
Figure 9. Closed-Loop System of Control Feedback

Control Feedback Gains

In order to obtain control feedback gains for the
three methods investigated, values of $\underline{R}$ and $\underline{B}$ were selected
and steady state solutions to the matrix Riccati equation
were numerically determined. The AFIT Subprogram OPTCON
(Ref 11) and the Aerospace Medical Research Laboratory
Subroutine MRIC (Ref 12) were used in obtaining the numer-
ical solutions to the steady state Riccati equation. With
the ability to obtain feedback gain matricies for particular
initial conditions and satellite parameters, it is now
possible to obtain and compare control requirements for the
three techniques being investigated.

40

IV. Results and Analysis

In chapter II the dynamics of the satellite were formulated for the three techniques being investigated. A means of controlling the system was introduced in chapter III. In this chapter, specific examples are examined and the results for the various techniques are presented.

For each method being investigated, optimal control was determined by numerically obtaining control feedback gains, F, based on equations (52) and (53). As previously mentioned, Subroutine MRIC and Subprogram OPTCON were utilized to obtain feedback gains for the system. These feedback gains were substituted into the general closed-loop system differential equation (54), which describes the satellite's controlled motion. The closed-loop differential equation was then integrated forward in time by using the CC6600 Subroutine ODE (Ref 13). For the example which follows, the satellite's angular displacements and antenna motion are plotted versus time for both uncontrolled and controlled situations.

Example 1

In this example a stable satellite configuration was examined. The following initial conditions, satellite parameters, and weighting matrices apply to all three methods.

Initial Conditions:

$$\theta_1 = 0^\circ$$
$$\theta_2 = 3^\circ = .0523598776 \text{ Radians}$$

41

$$u = 0 \text{ ft} = \bar{u} = u_1 = u_2 = u_3 = u_4$$

$$v = 0 \text{ ft} = \bar{v} = v_1 = v_2 = v_3 = v_4$$

$$t = 0 \text{ sec}$$

Satellite Parameters:

$$\Omega_s = 50 \text{ Rad/sec}$$

$$\omega_n = \omega_1 = 60 \text{ Rad/sec}$$

$$\Omega_s/\omega_n = .833$$

$$C = 60 \text{ slugs-ft}^2$$

$$C/A = 1.5$$

$$B = A$$

$$RA = .1$$

$$a = 2 \text{ ft}$$

$$h = 2 \text{ ft}$$

$$l = 1 \text{ ft}$$

$$\text{Zeta} = d/2m\omega_n = .5$$

$$d/p = 10$$

Weighting Matrices:

$$\underline{Q} = [I]$$

$$\underline{R} = [I]$$

Discrete System Results

For the discrete system model, Figures 10 and 11 illustrate the satellite's motion for the uncontrolled system. It can be noted that for an inherently stable system, the antenna displacements of u and v tend to dampen out over a period of time. The damped motion of the antenna was characteristic for any value of zeta greater than zero. Recalling that θ_1 and θ_2 are angular measurements of

42
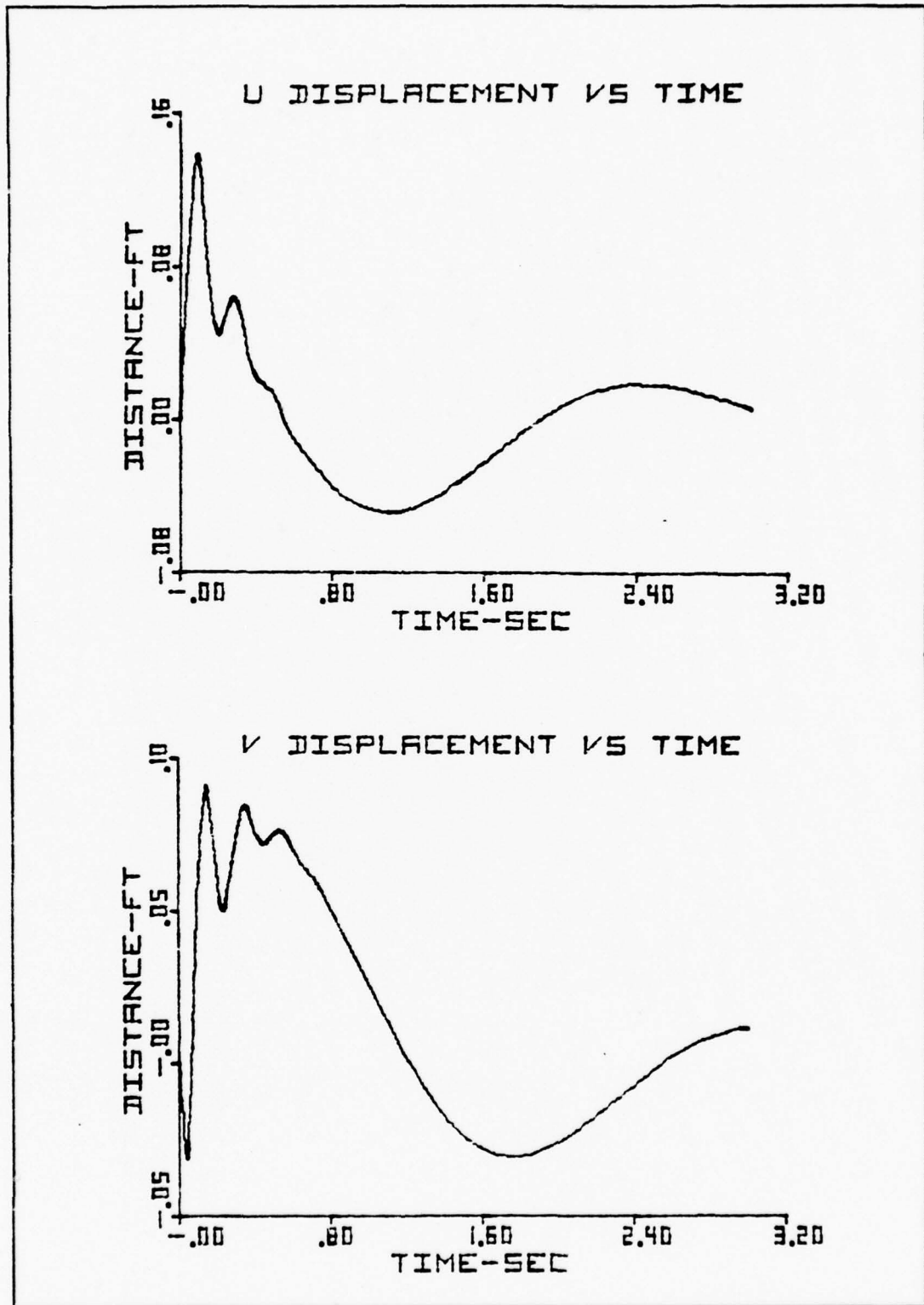
Figure 10. Uncontrolled Antenna Motion - Discrete System

43
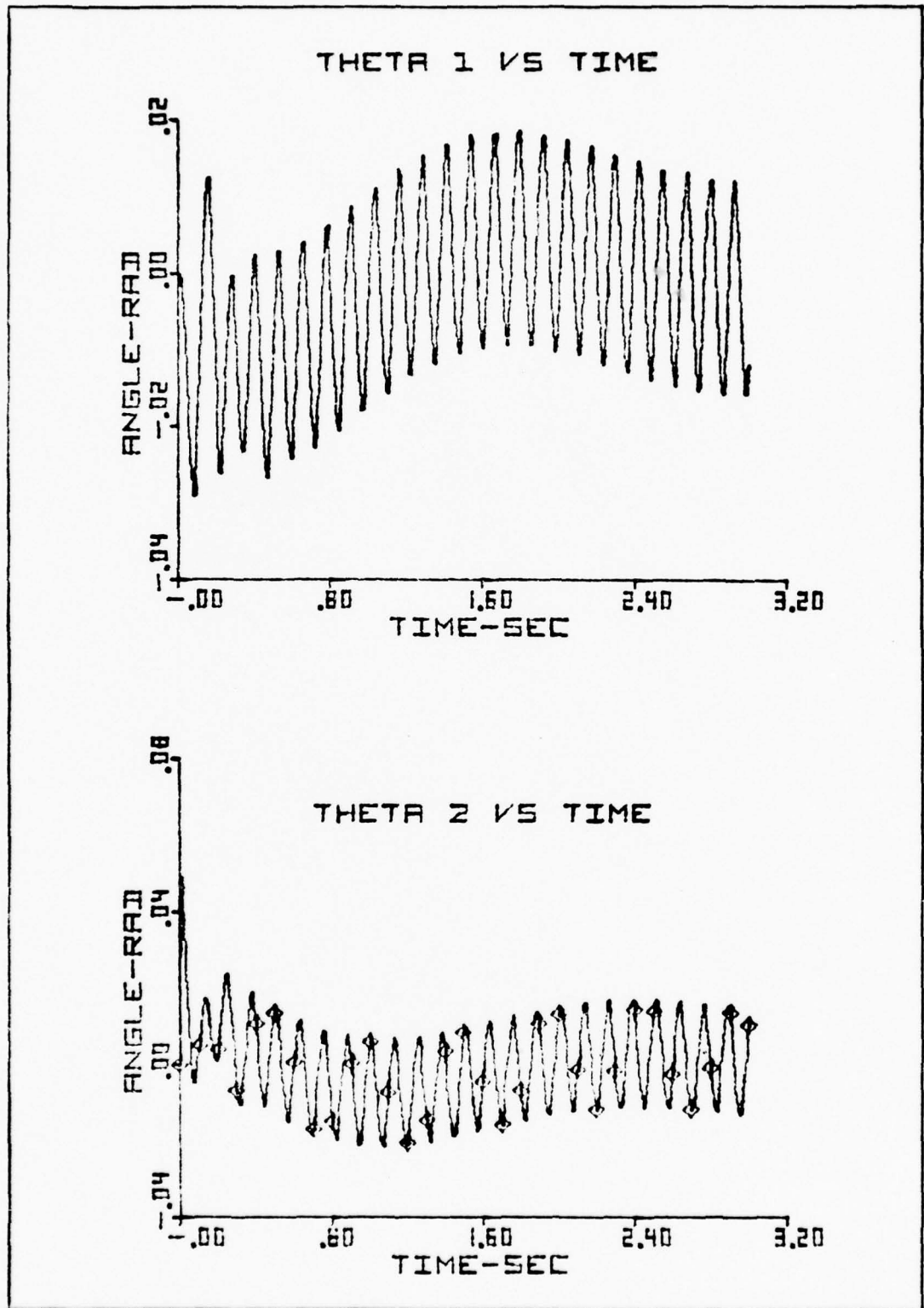
Figure 11.   Uncontrolled Angular Motion - Discrete System

44

the body fixed axis with respect to an inertial axis, it can be seen from Figure 11 that the spin axis assumes a new pointing direction. A controller is required to drive these angular displacements back to zero so that the spin axis is once again oriented to the null position. Table I provides the feedback gains required to control the system.

Table I.

Discrete Feedback Matrix

	Col 1	Col 2	Col 3	Col 4
Row 1	-3.7003E+02	-4.5512E+00	-2.7374E-05	-1.0320E+01
Row 2	-2.7374E-05	7.2990E-06	-5.4318E+02	7.0958E-06
	Col 5	Col 6	Col 7	Col 8
Row 1	9.9053E-01	2.2624E-02	-1.2334E-01	4.7534E-01
Row 2	-1.8106E-01	-7.0379E-08	9.8347E-01	-4.4572E-07

The optimal control at any instant of time is just the matrix multiplication of the feedback gain, $\underline{F}$, times the current state vector.

$$\bar{u}(t) = \underline{F}\bar{x}(t) \tag{55}$$

Recalling that θ_3 and P_{θ_3} uncouple for all three methods investigated, the states of the discrete system can be described by an (8 x 1) vector written in the following order.

$$\bar{x}(t) = \begin{array}{l} x_1 = \theta_1 \\ x_2 = v \\ x_3 = \theta_2 \\ x_4 = u \end{array}$$

45

$$x_5 = P_{\theta_1}$$
$$x_6 = P_v$$
$$x_7 = P_{\theta_2}$$
$$x_8 = P_u \qquad (56)$$

Figure 12 illustrates the angular displacements and antenna motion of the controlled discrete system. As can be observed, the satellite is returned to the desired null orientation in just over one second. For this particular set of satellite parameters, the stability of the closed-loop system is shown by the all negative eigenvalues illustrated in Table II.

Table II.

Discrete Closed-Loop Eigenvalues

Real	Imaginary
-.33957E+01	-.52787E+01
-.33957E+01	.52787E+01
-.54171E+02	-.10598E+03
-.54171E+02	.10598E+03
-.19348E+03	-.19573E+03
-.19348E+03	.19573E+03
-.27159E+03	-.27615E+03
-.27159E+03	.27615E+03
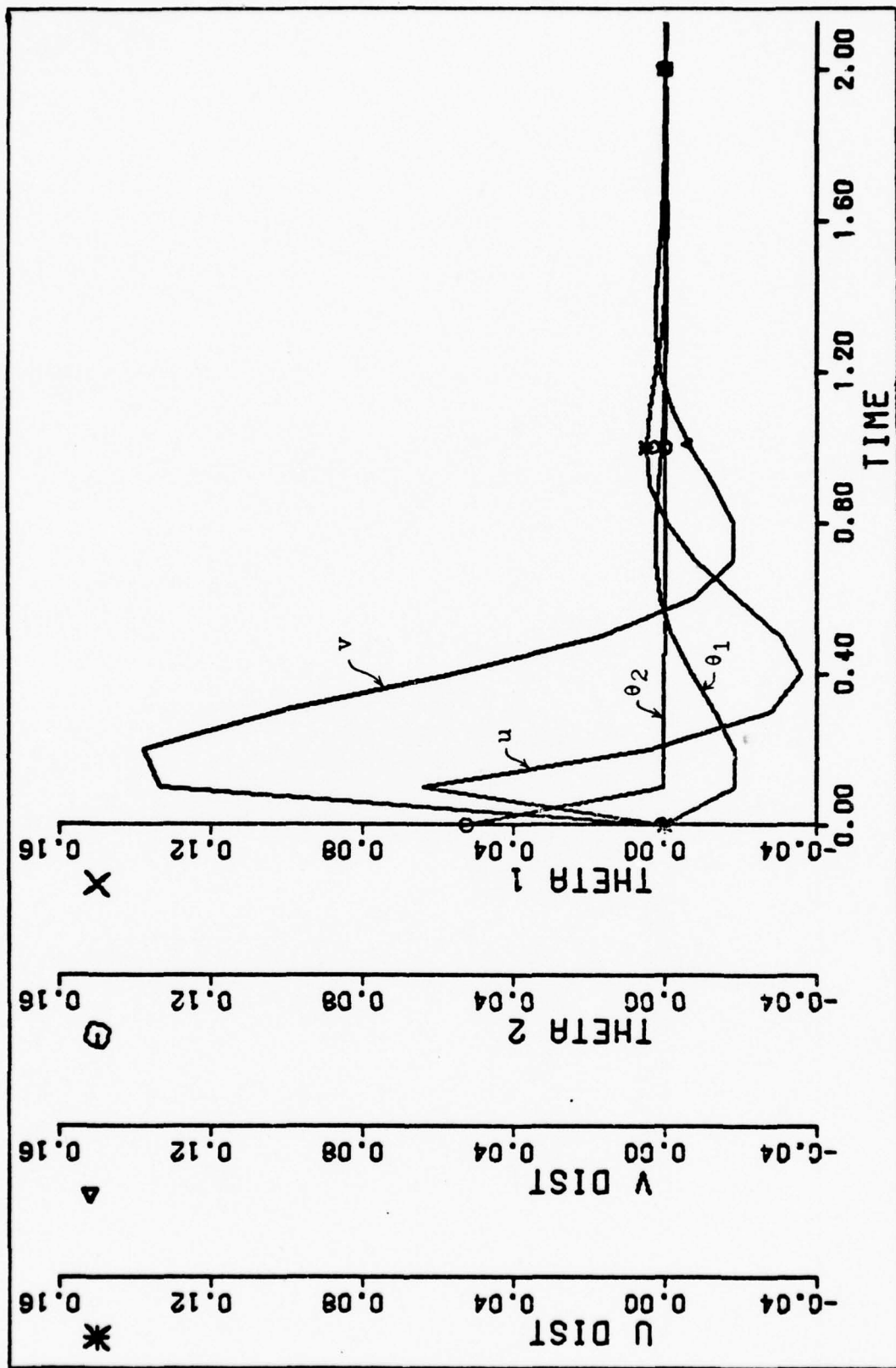
Figure 12. Controlled States - Discrete System

47

Modal Analysis Results

The modal analysis investigation of the continuous system model was the second method applied to this example problem. In order to obtain an insight into the unforced satellite motion, the equations of motion were numerically integrated and the uncontrolled states were plotted against time. Figure 13 illustrates the uncontrolled angular displacements of θ_1 and θ_2. A breakdown of the uncontrolled motion for the first four modes of antenna vibration is presented in Figures 14 through 17. As expected, the first mode significantly dominates the antenna motion. The magnitude of the overall uncontrolled modal displacements in the u and v directions is illustrated in Figure 18. For the controlled system, the set of feedback gains appearing in Table III were obtained using AMRL Subroutine MRIC. The order of the states corresponding to the feedback gains of Table III and the modal analysis method is as follows:

$$\bar{x}(t) = \begin{array}{ll} x_1 = \theta_1 & x_{11} = P_{\theta_1} \\ x_2 = \theta_2 & x_{12} = P_{\theta_2} \\ x_3 = v_1 & x_{13} = P_{v_1} \\ x_4 = v_2 & x_{14} = P_{v_2} \\ x_5 = v_3 & x_{15} = P_{v_3} \\ x_6 = v_4 & x_{16} = P_{v_4} \\ x_7 = u_1 & x_{17} = P_{u_1} \\ x_8 = u_2 & x_{18} = P_{u_2} \\ x_9 = u_3 & x_{19} = P_{u_3} \\ x_{10} = u_4 & x_{20} = P_{u_4} \end{array} \qquad (57)$$

48
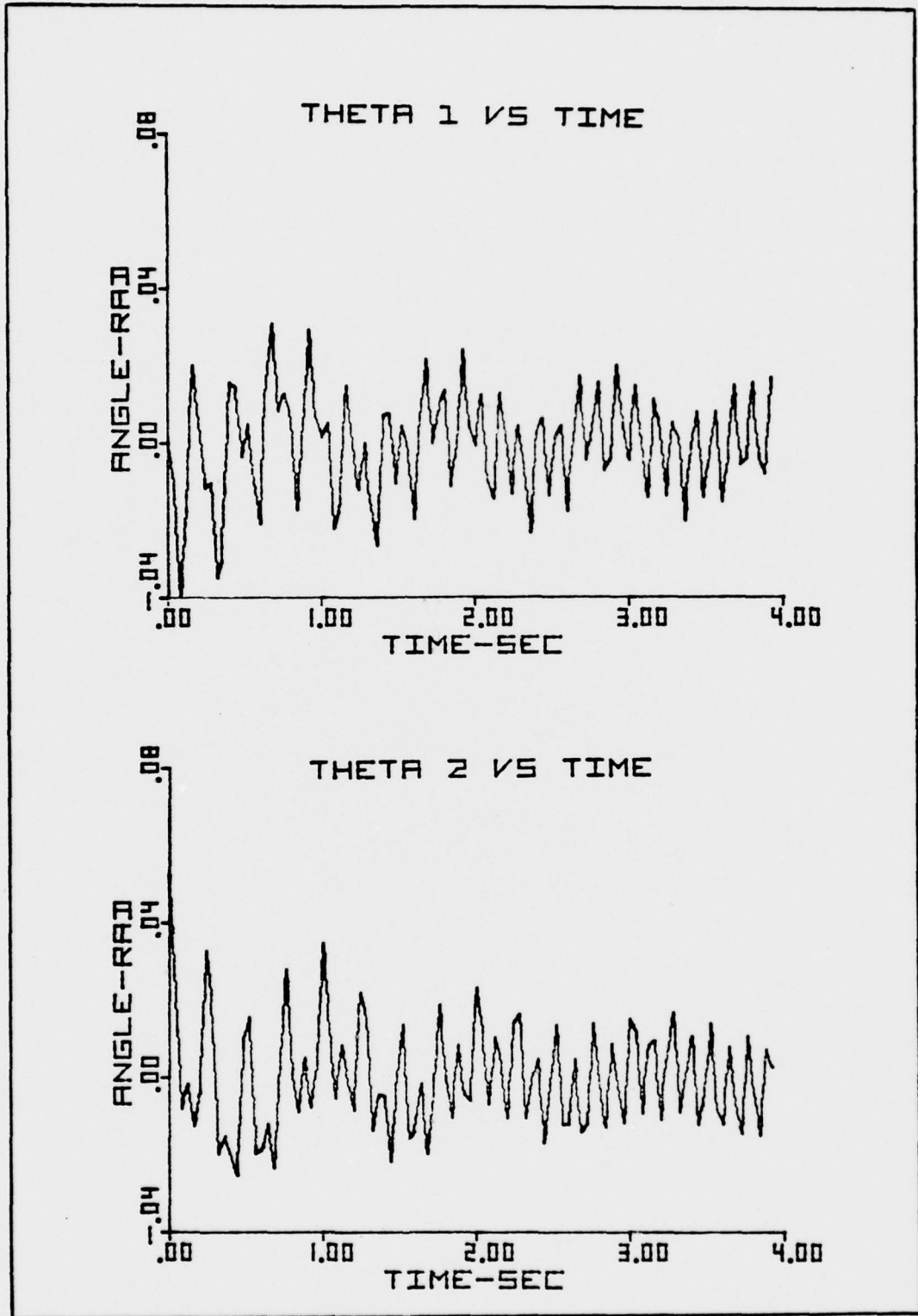
Figure 13.   Uncontrolled Angular Motion - Modal Analysis

49
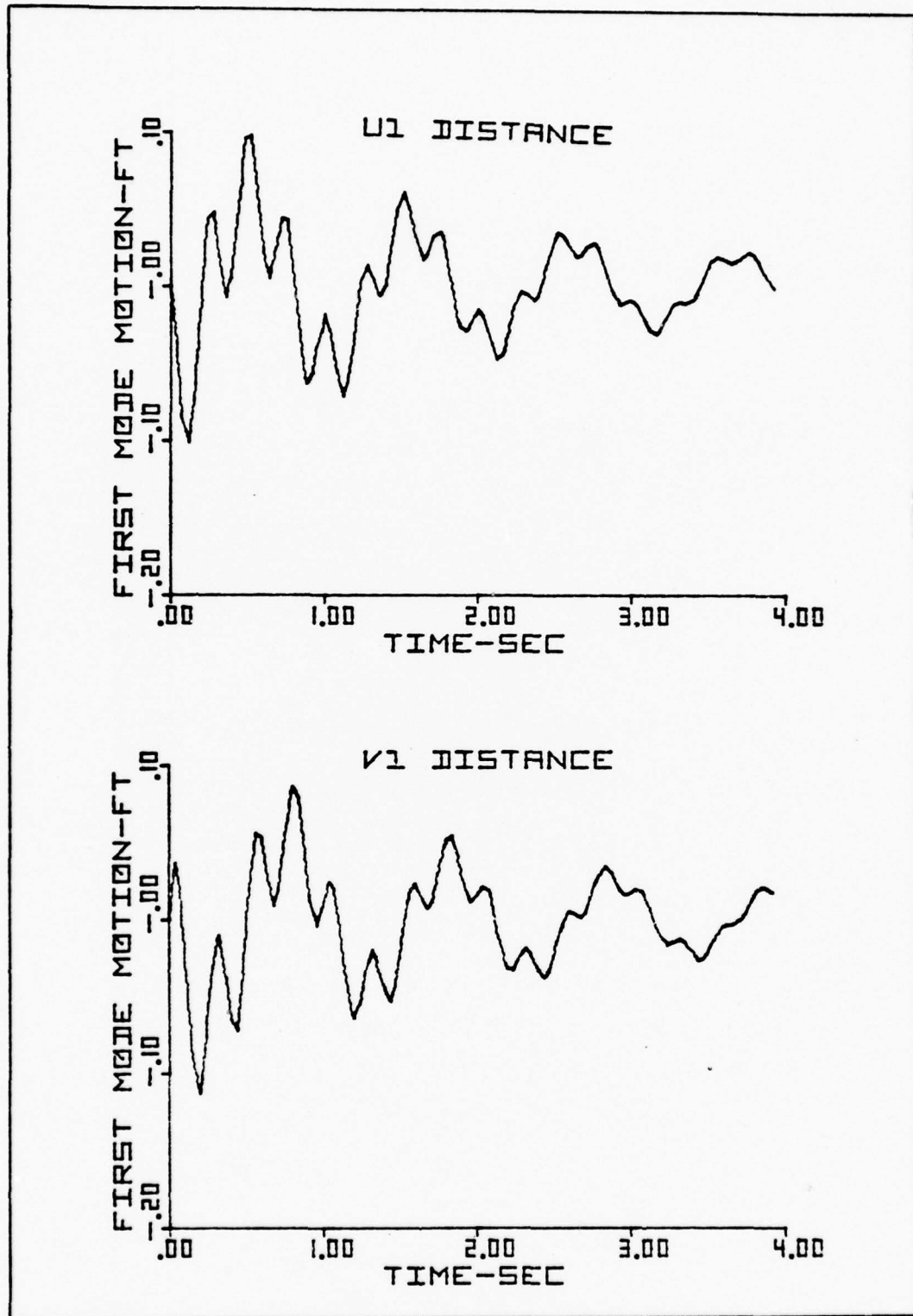
Figure 14. Uncontrolled First Mode Antenna Motion
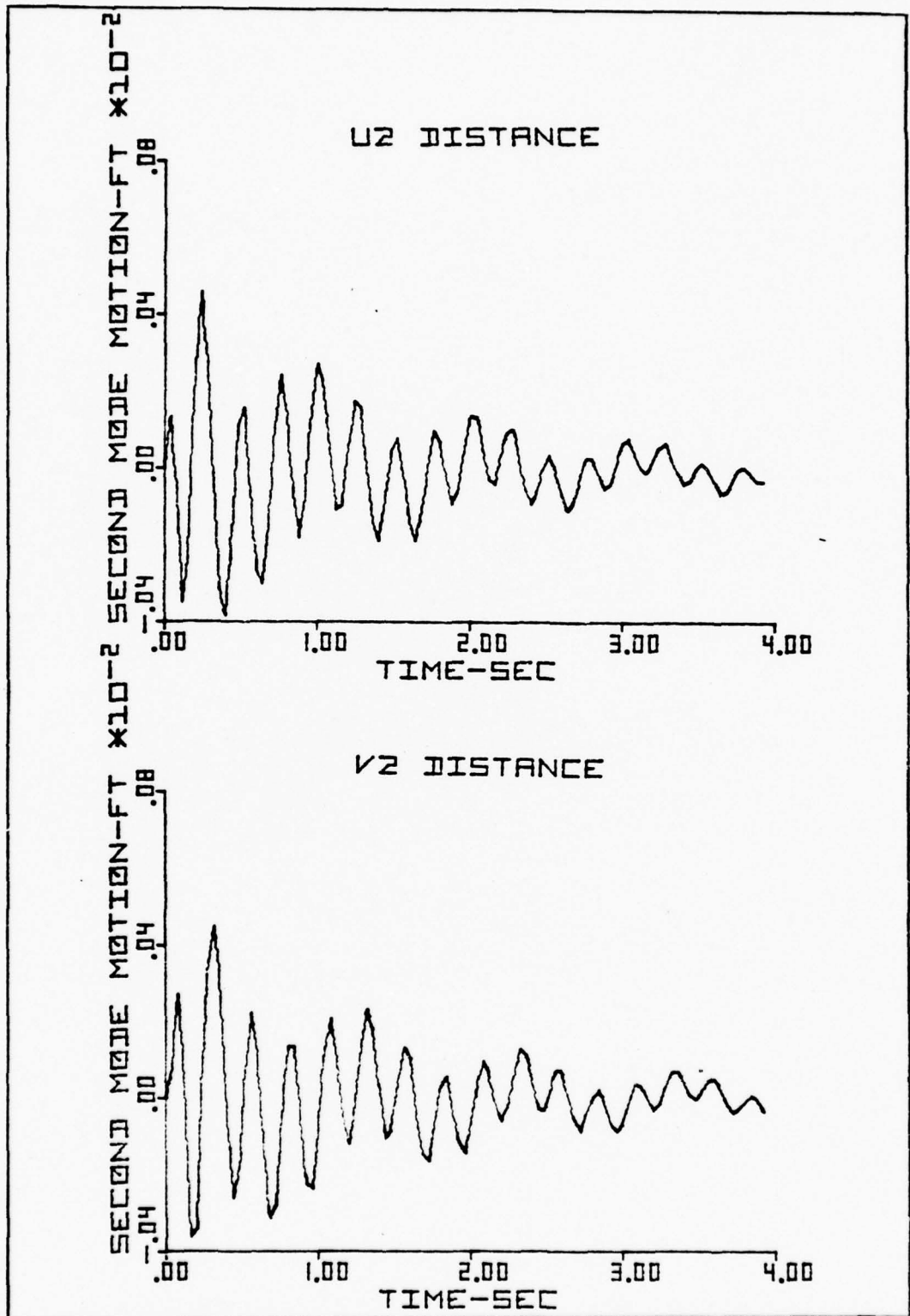
Figure 15. Uncontrolled Second Mode Antenna Motion

51
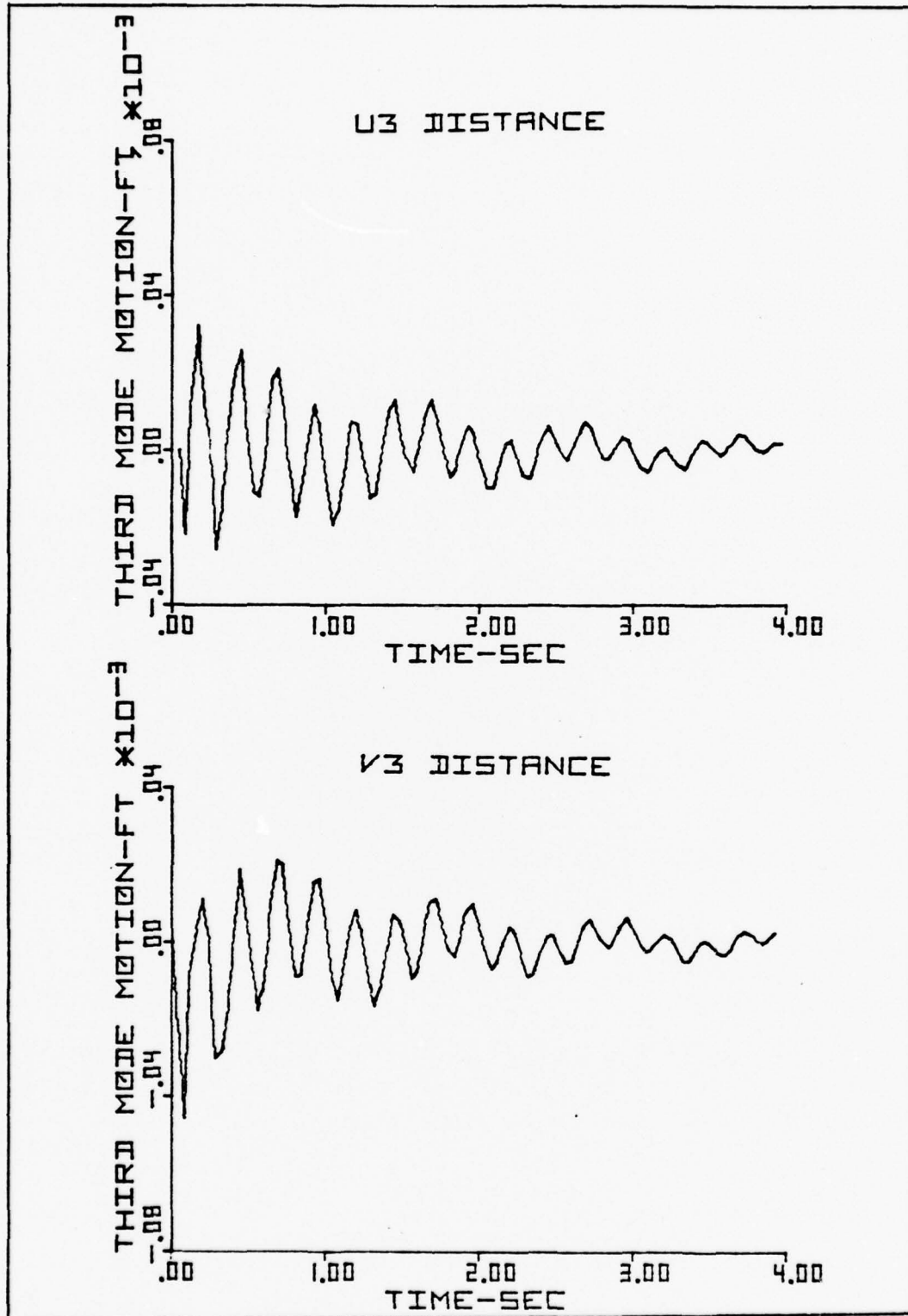
Figure 16. Uncontrolled Third Mode Antenna Motion

52
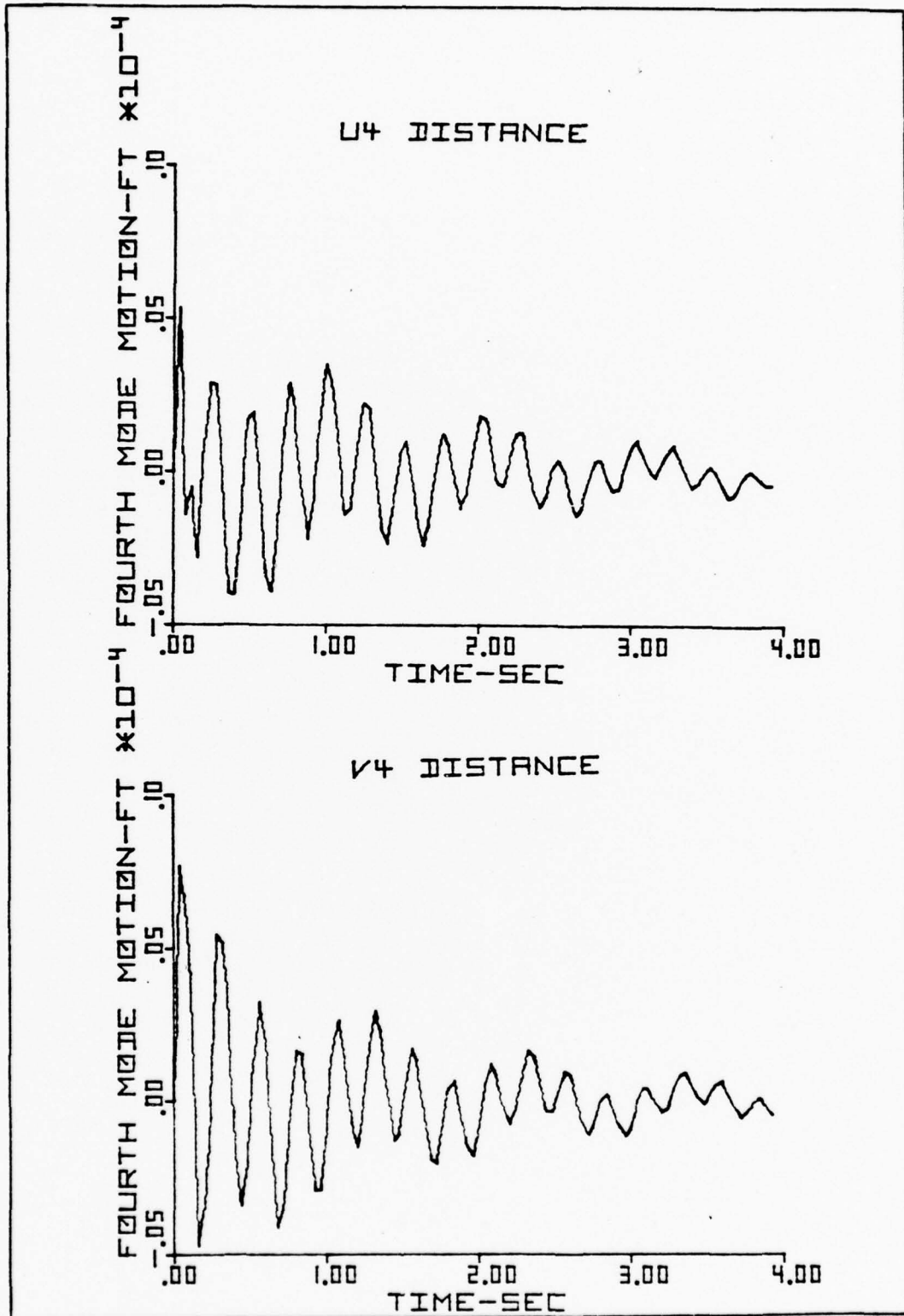
Figure 17.   Uncontrolled Fourth Mode Antenna Motion

53
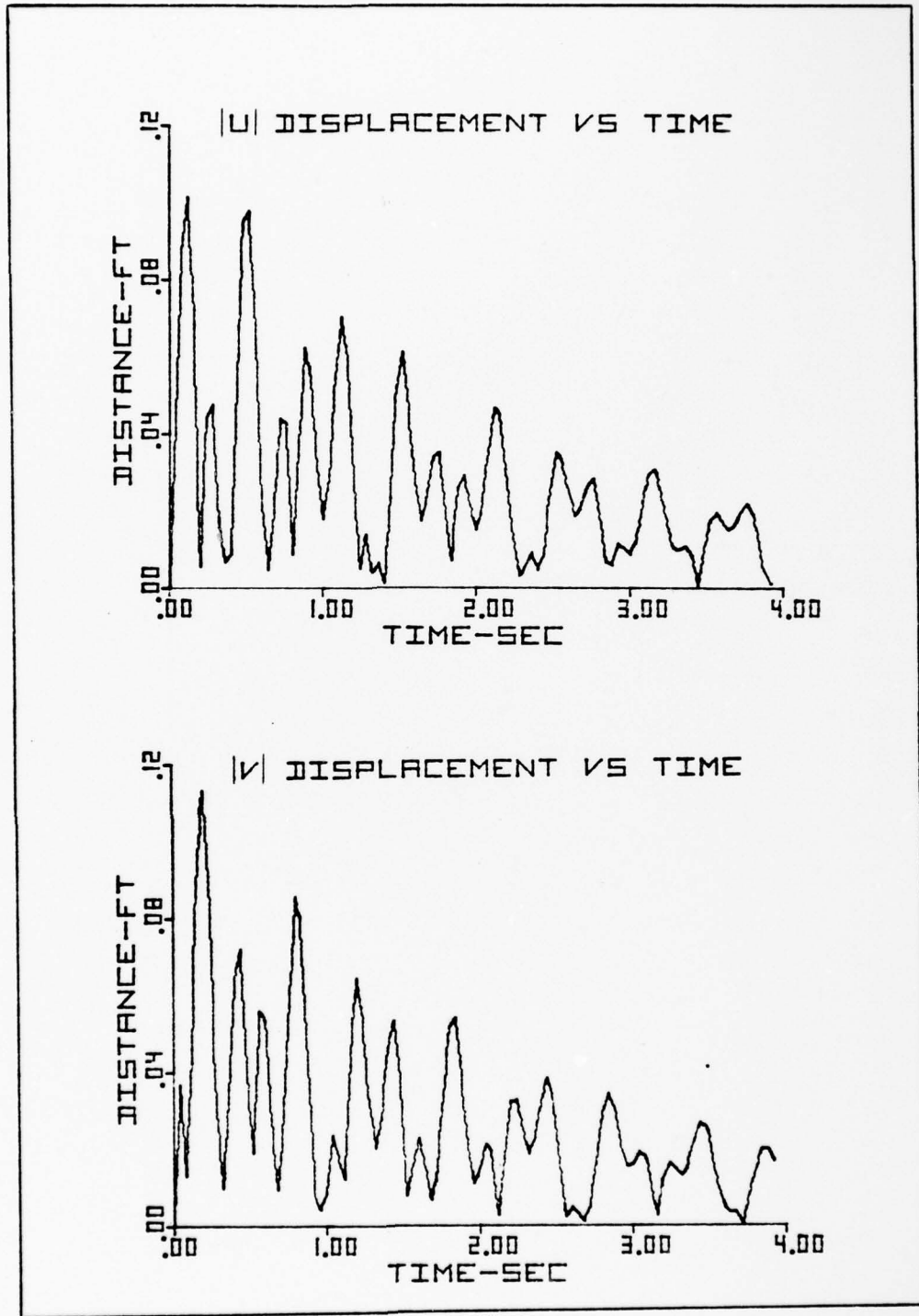
Figure 18.   Uncontrolled Magnitude of Antenna Modal Motion

54

Table III.

Modal Feedback Matrix

	Col 1	Col 2	Col 3	Col 4	Col 5	Col 6	Col 7
Row 1	-4.4616E+02	-2.7734E-05	-2.5912E+01	4.4038E-01	1.1418E+02	-1.1989E+02	4.7521E+00
Row 2	-2.7734E-05	-5.5071E+02	5.8072E-06	3.9216E-05	3.9204E-06	-2.3392E-06	-5.6464E-06

	Col 8	Col 9	Col 10	Col 11	Col 12	Col 13	Col 14
Row 1	6.5266E+02	-7.5227E+02	6.9208E+02	1.0007E+00	-1.4872E-01	7.2695E-03	6.9414E-02
Row 2	5.8153E-05	-9.8977E-05	5.8236E-05	-1.8357E-01	9.8347E-01	3.6369E-08	-2.2787E-08

	Col 15	Col 16	Col 17	Col 18	Col 19	Col 20
Row 1	1.9977E-02	-2.0048E-02	1.1033E-01	4.3745E-01	-8.1584E-01	7.3383E-01
Row 2	-5.2146E-09	8.9877E-10	1.3796E-07	-2.0146E-07	-3.0046E-09	2.3180E-09

55

With the feedback gains applied to the system differential equations of motion, the control required on the angular velocities $\dot{\theta}_1$ and $\dot{\theta}_2$ was obtained. The resulting controlled motion of θ_1 and θ_2 is depicted in Figure 19. The controlled motion of the first four modes is as illustrated in Figures 20 through 23. Figure 24 shows the overall magnitude of the antenna motion as a function of time. Comparing the uncontrolled to the controlled motion, that is, Figure 13 to Figure 19 and Figure 18 to Figure 24, it can be seen that the desired null orientation of the system is rapidly achieved. The control in angular velocity rates required to obtain this orientation is plotted in Figures 25 and 26. Figure 25 shows that the controller is active for only a short period. Figure 26 more clearly illustrates the magnitude of control required during the more active stage. This figure also illustrates that the controlled angular velocity rates are nearly zero after a time of one-tenth of a second. If the actual mechanism imparting control was known, these control angular velocity rates could be transformed into some thrust requirement or momentum exchange requirement.

Recall that earlier in this thesis the assumption was made that the results obtained by the continuous modal method would be considered an exact representation of the satellite system. Later in this thesis, the results obtained by applying integral coordinate feedback gains to the continuous modal system will be compared to the results just presented.

56
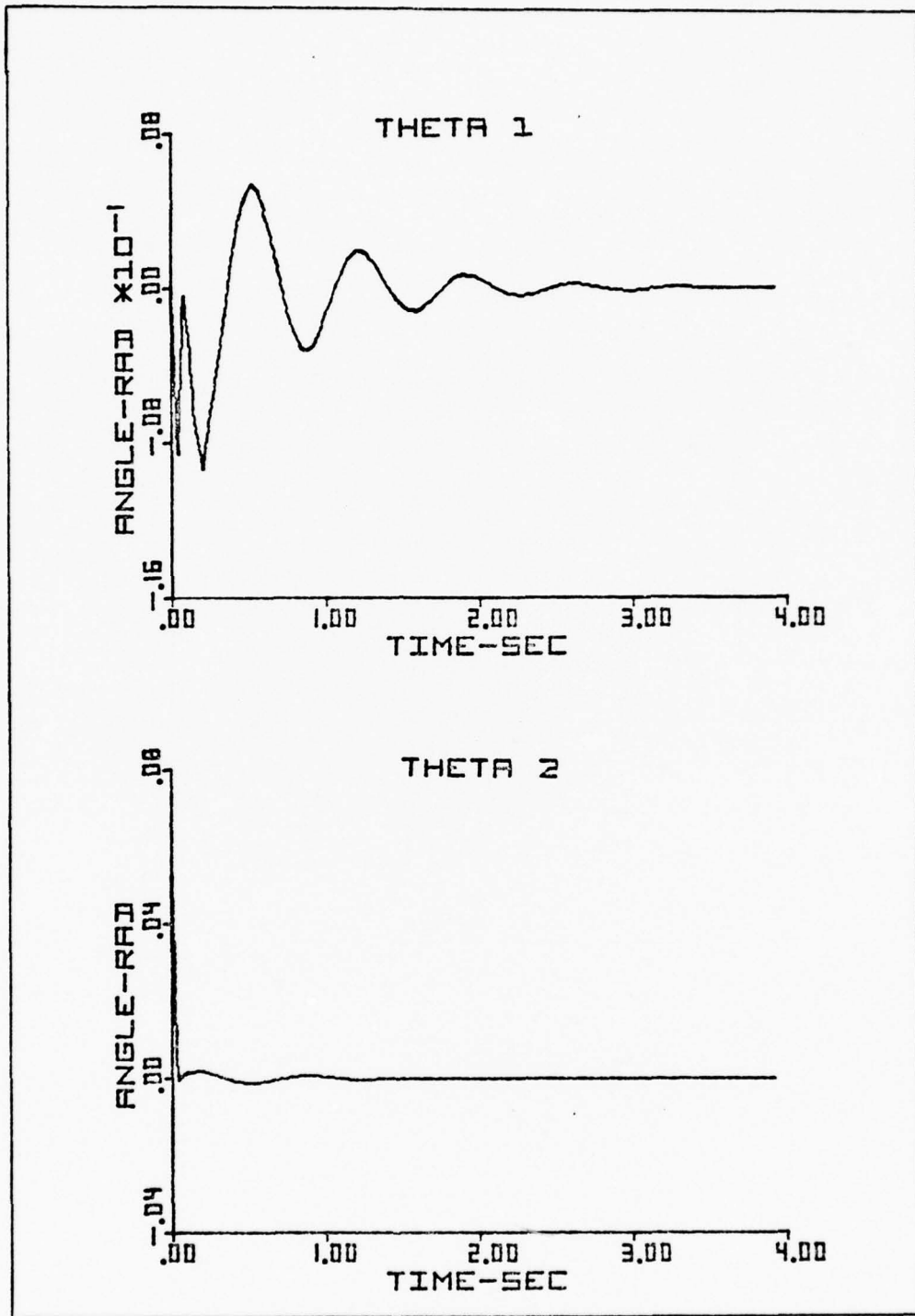
Figure 19.   Controlled Angular Motion - Modal Analysis

57
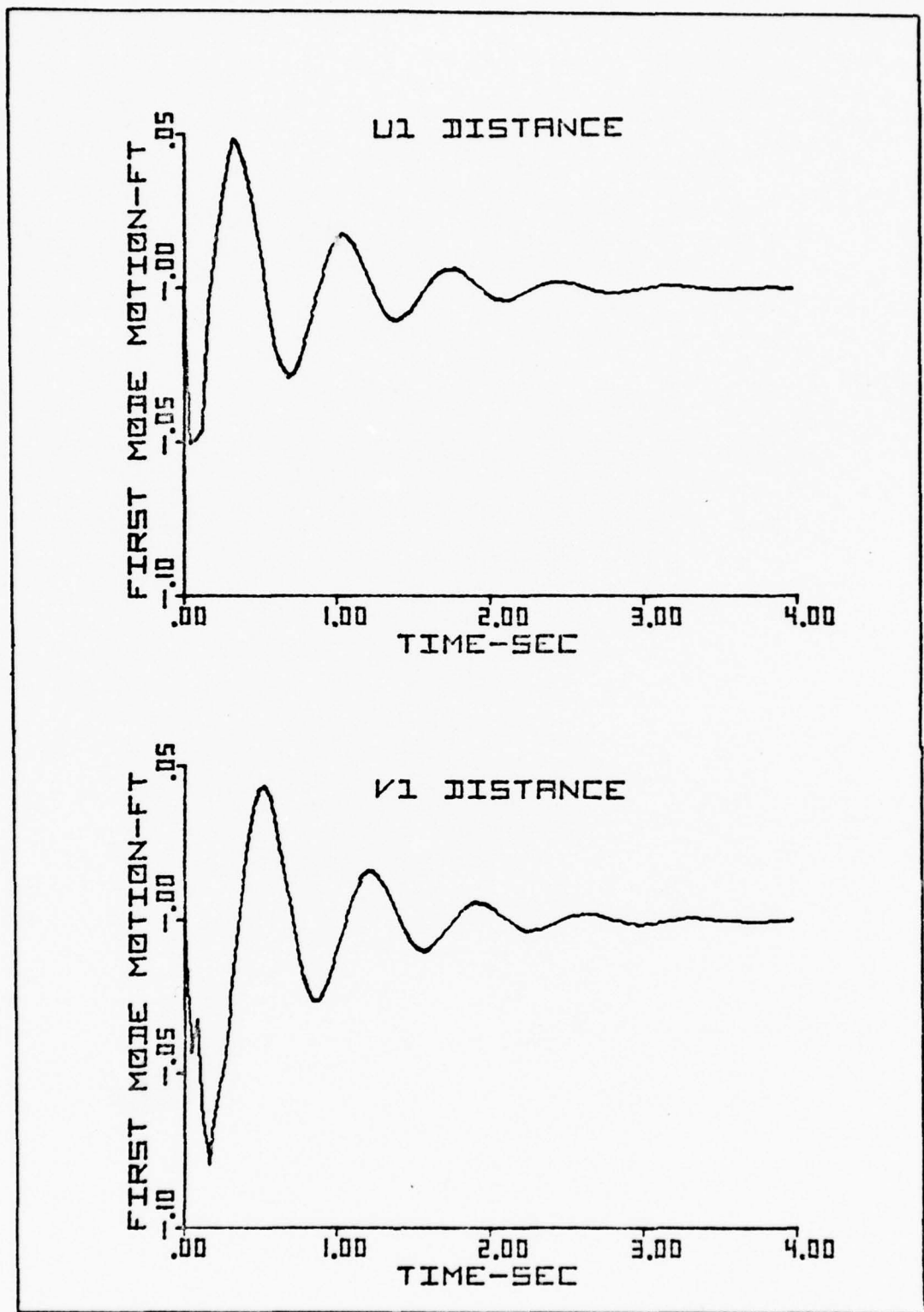
Figure 20.   Controlled First Mode Antenna Motion

58
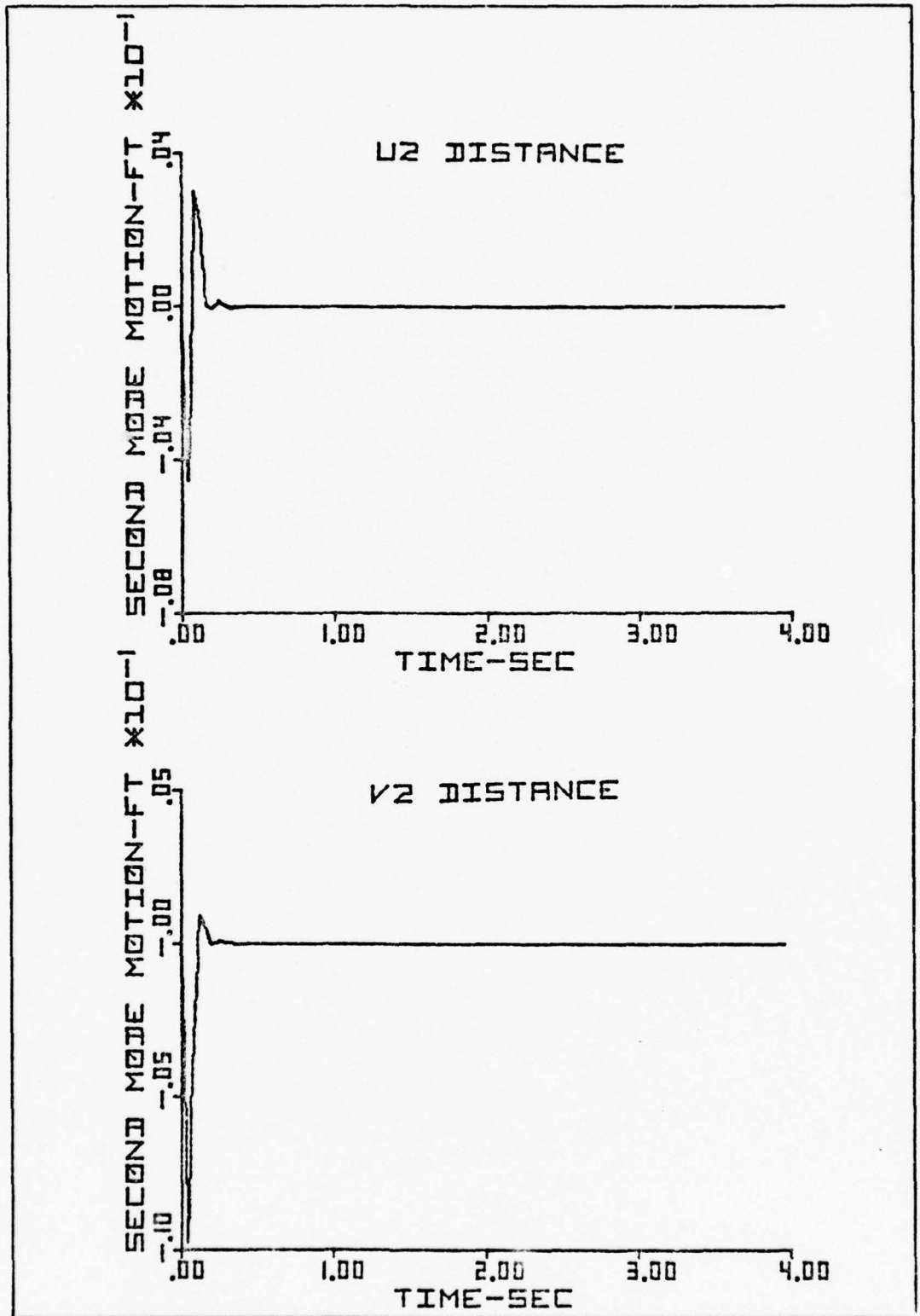
Figure 21. Controlled Second Mode Antenna Motion

59
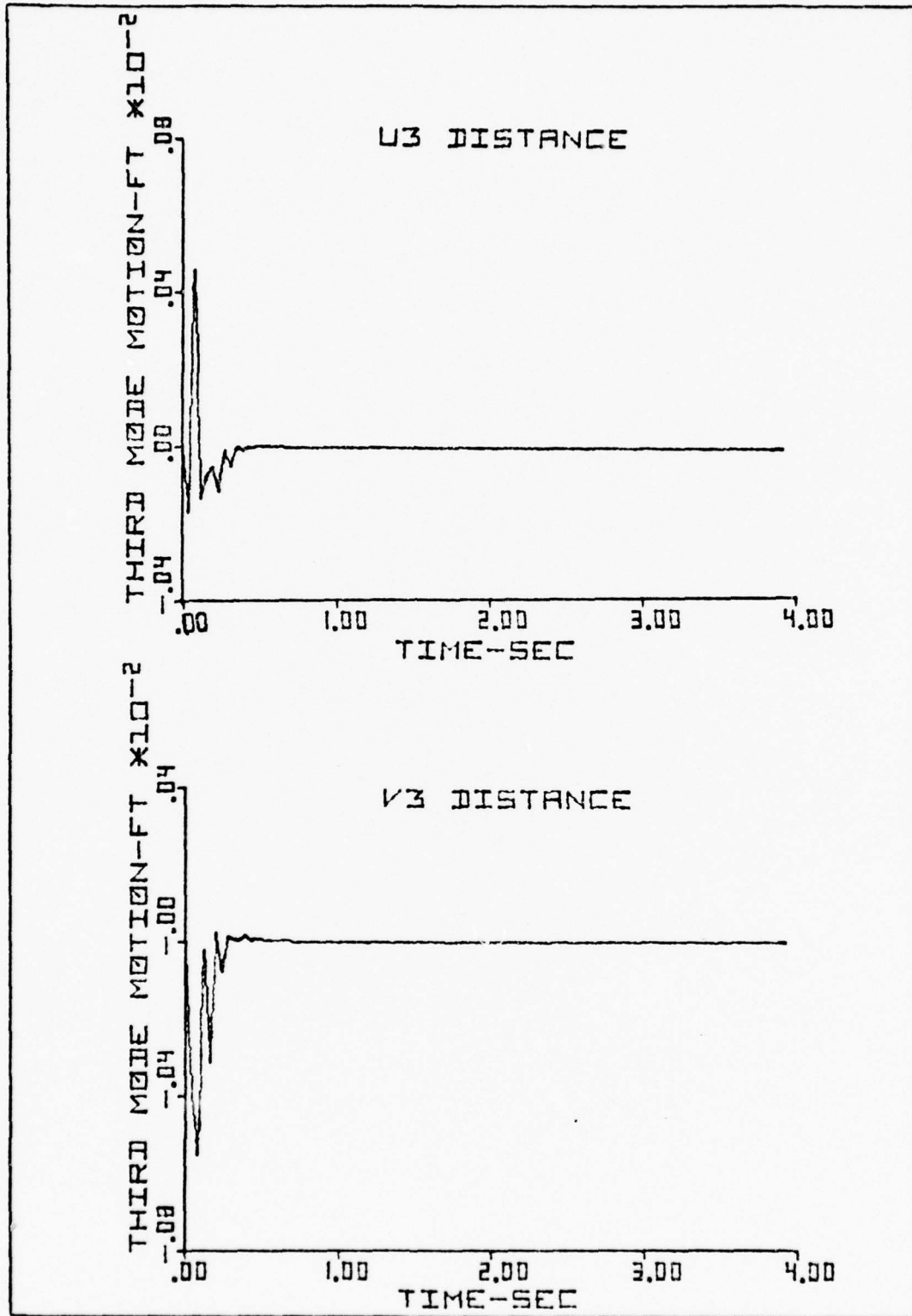
Figure 22.   Controlled Third Mode Antenna Motion
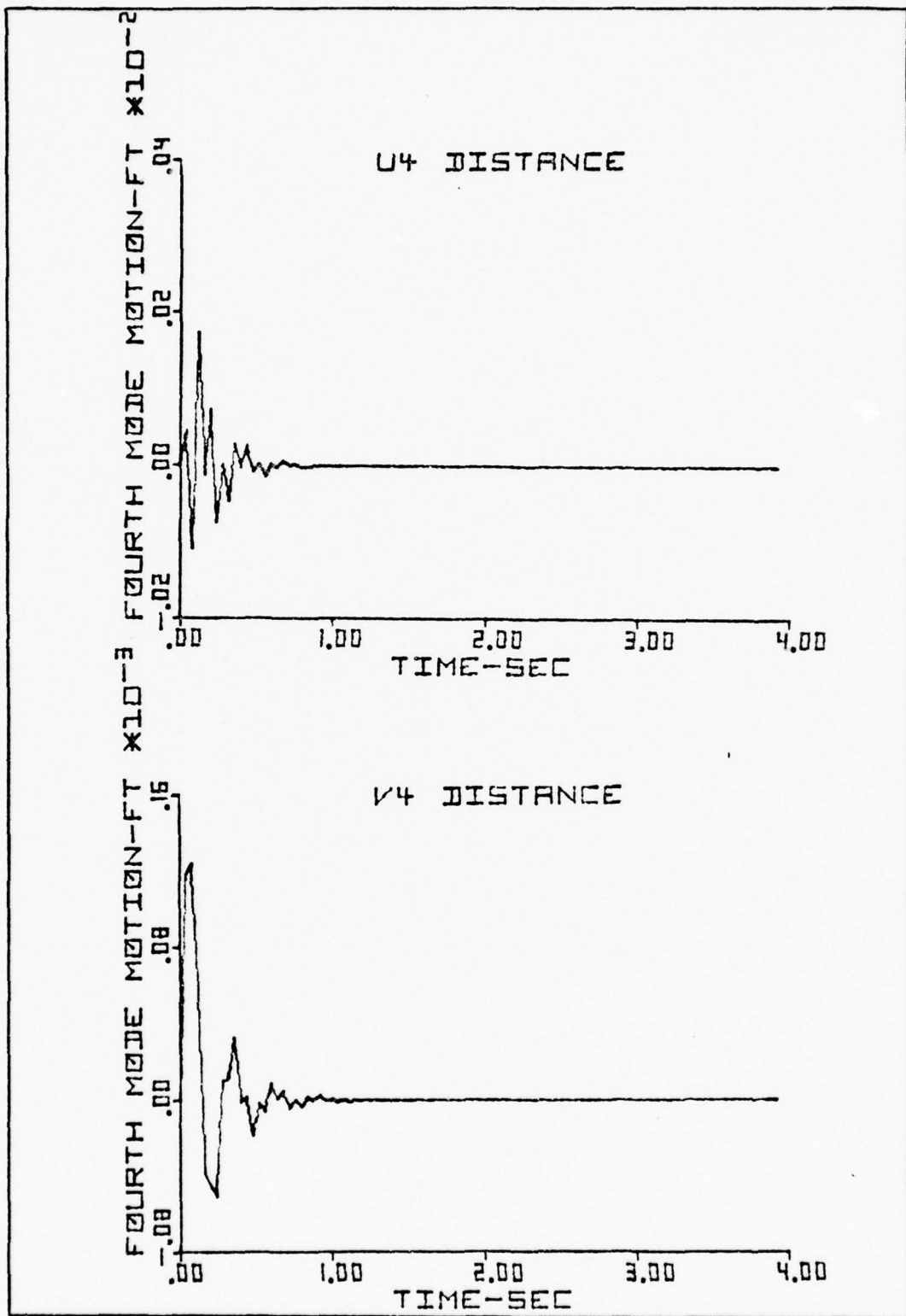
Figure 23.   Controlled Fourth Mode Antenna Motion

61
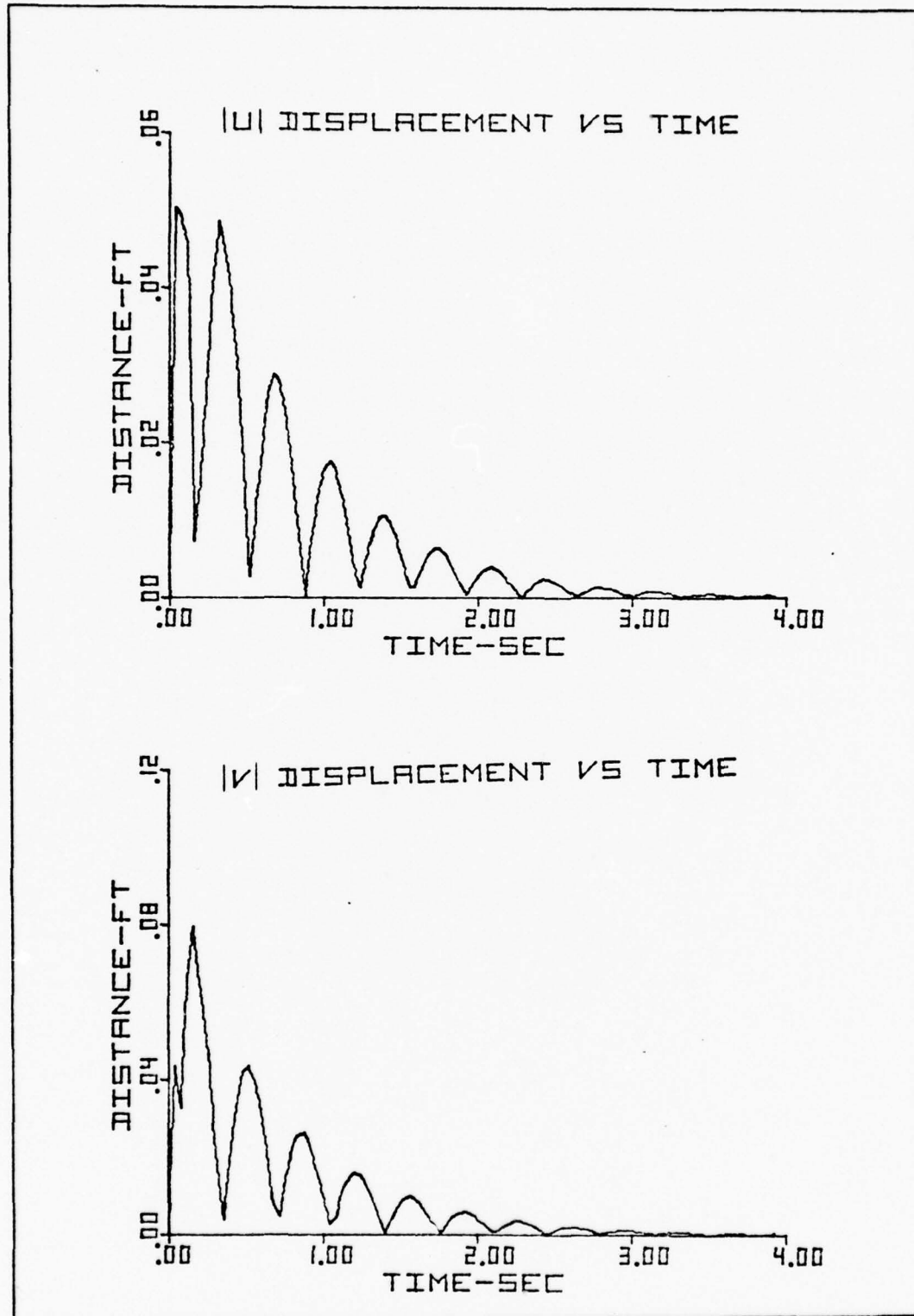
Figure 24. Controlled Magnitude of Antenna Modal Motion

62
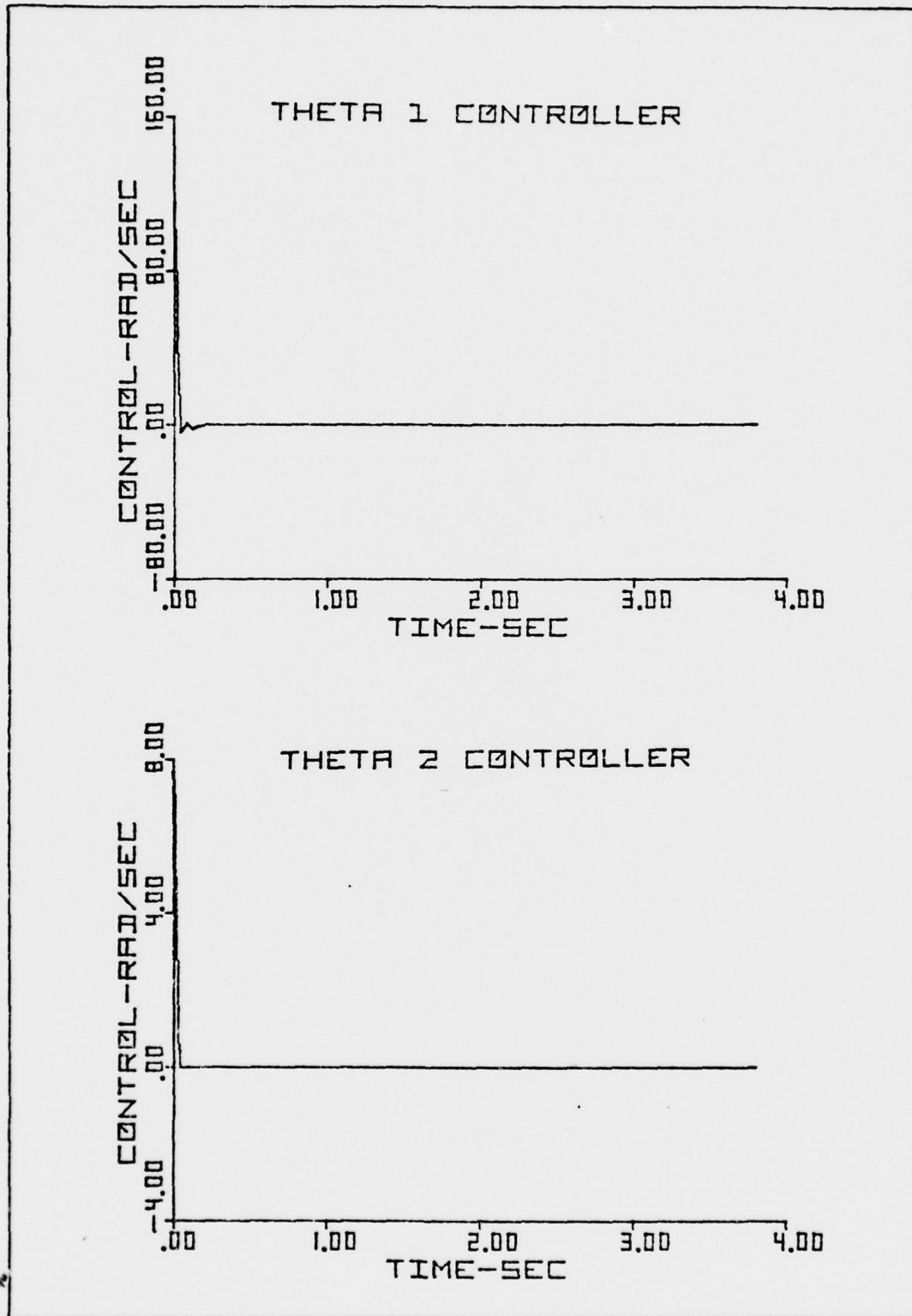
Figure 25.   Control Requirements - Modal Analysis
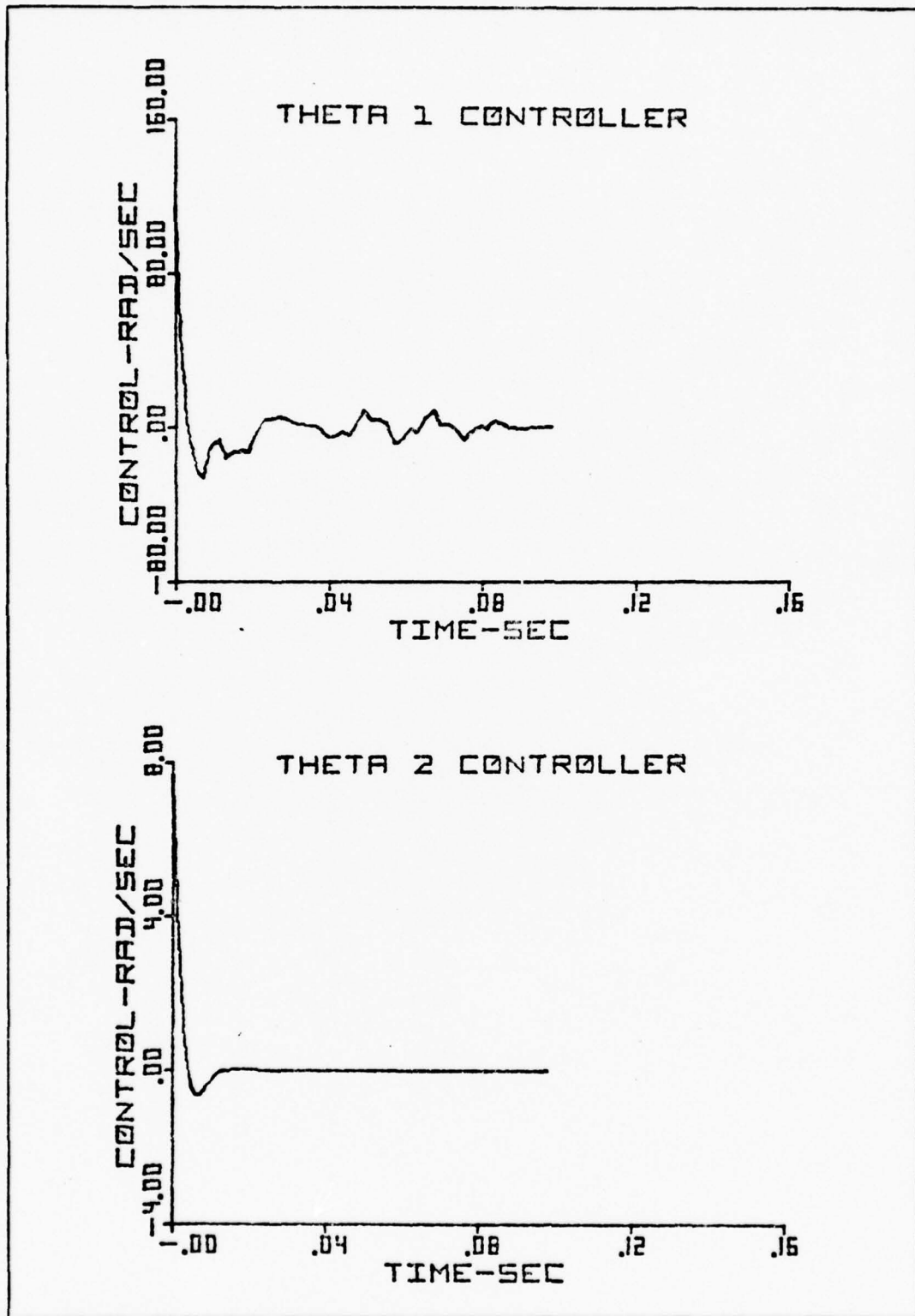
Figure 26.   Control Requirements - Modal Analysis

Integral Coordinate Results

For the continuous system, using integral coordinate techniques, the uncontrolled system motion is as depicted in Figures 27 and 28. Note that the antenna motion is again naturally damped out. Additionally, Figure 28 shows that the satellite's spin axis is again repositioning itself away from the nominal spin axis direction. To establish the control required to reorient the satellite's spin axis, feedback gains were obtained from Subprogram OPTCON. These feedback gains were verified by using the Subroutine MRIC to determine required gains. The resulting feedback gains obtained by both methods were identical and appear in Table IV.

Table IV.

Integral Coordinate Feedback Matrix

	Col 1	Col 2	Col 3	Col 4
Row 1	-3.7814E+02	-3.5142E+01	-2.3539E-05	-3.2541E+00
Row 2	-2.3539E-05	3.0379E-05	-5.4318E+02	2.9721E-06

	Col 5	Col 6	Col 7	Col 8
Row 1	9.8671E-01	-1.6621E-01	-1.2605E-01	5.1639E-01
Row 2	-1.8106E-01	1.3820E-07	9.8347E-01	-5.4437E-07
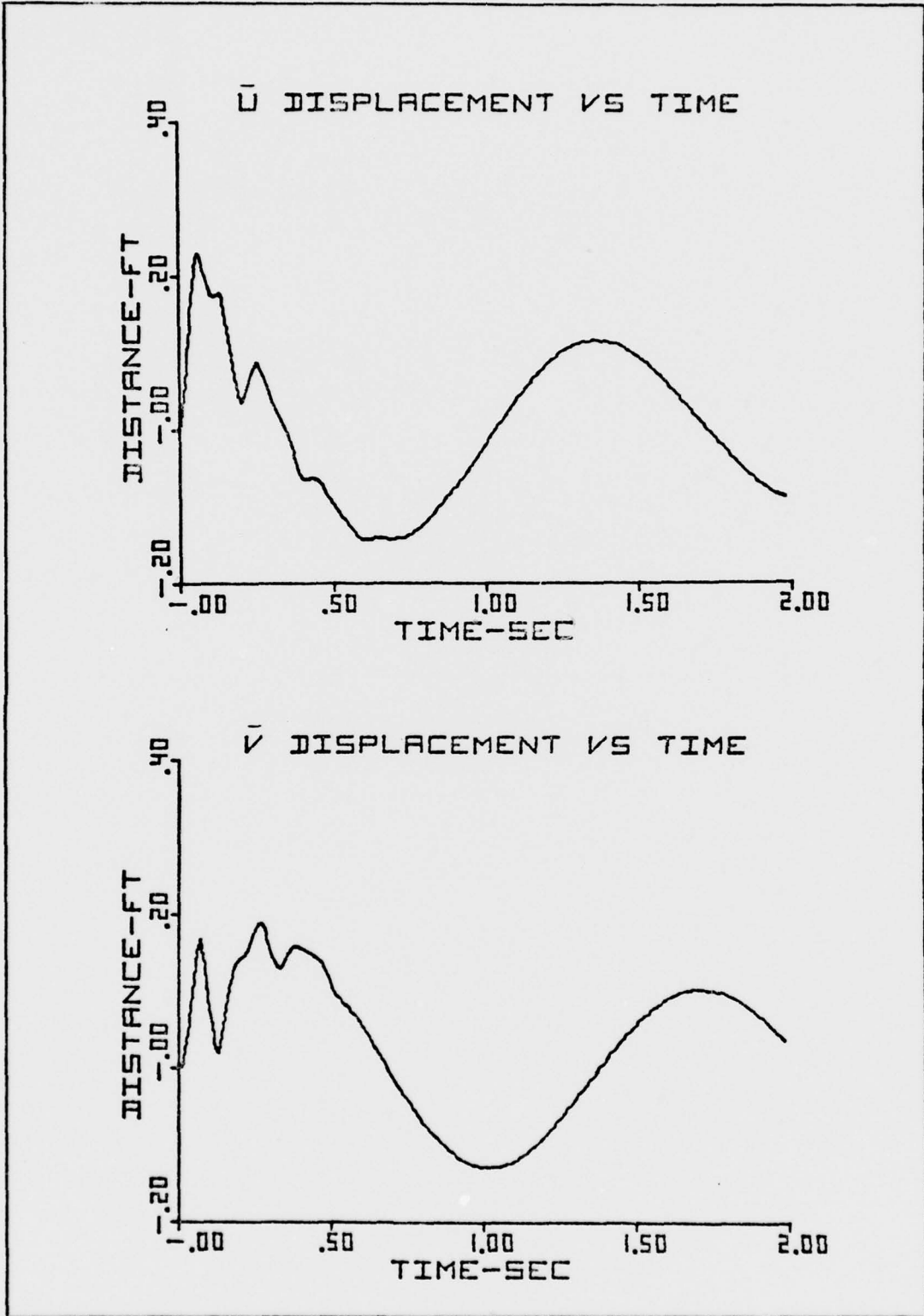
Figure 27.   Uncontrolled Antenna Motion - Integral Coordinates

66
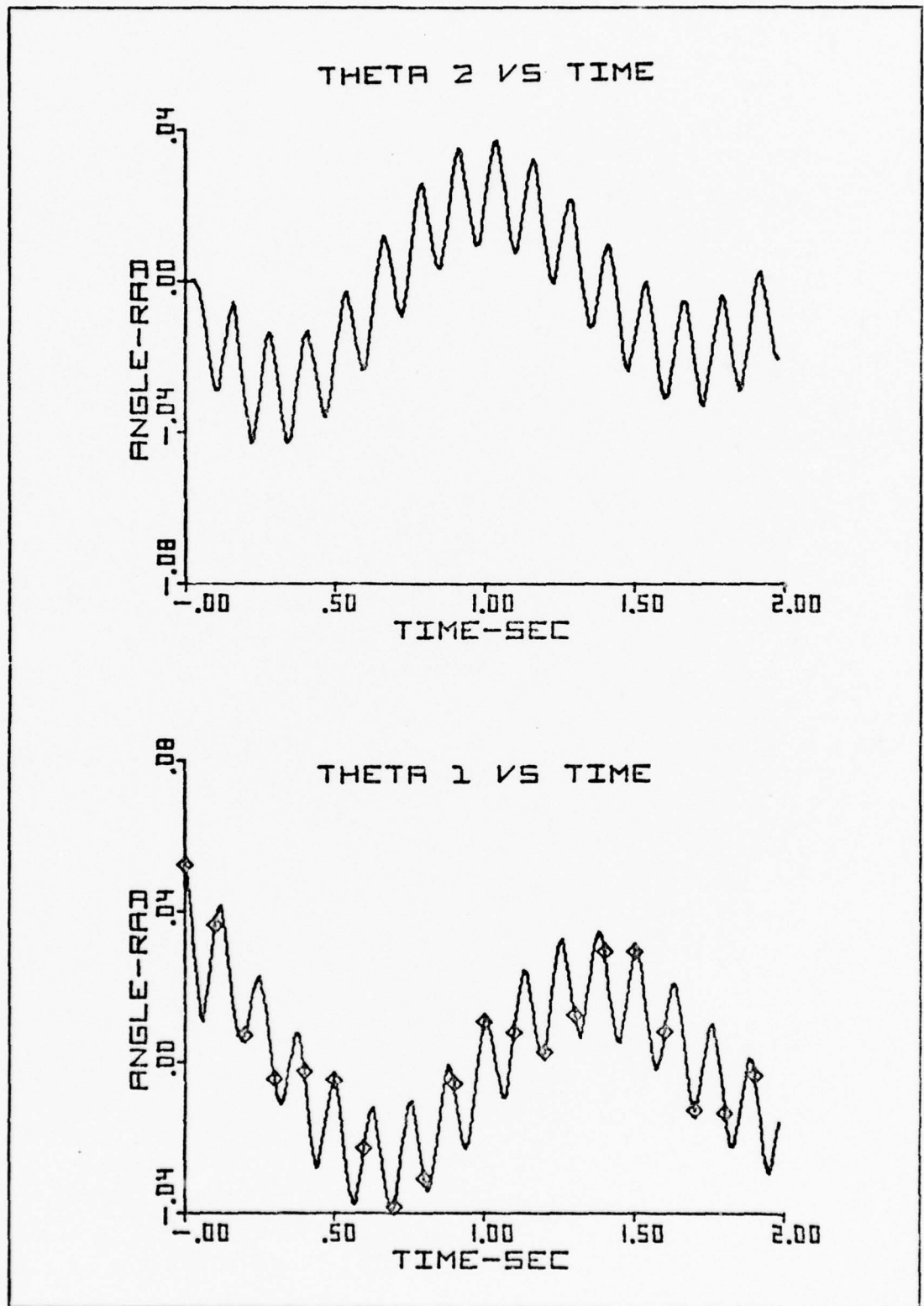
Figure 28.   Uncontrolled Angular Motion - Integral Coordinates

67

As in the previous techniques, the required control was found by performing the matrix multiplication of equation (55). For the integral coordinate method, the states were defined in the following order:

$$\overline{x}(t) = \begin{array}{rcl} x_1 &=& \theta_1 \\ x_2 &=& \overline{v} \\ x_3 &=& \theta_2 \\ x_4 &=& \overline{u} \\ x_5 &=& P_{\theta_1} \\ x_6 &=& P_{\overline{v}} \\ x_7 &=& P_{\theta_2} \\ x_8 &=& P_{\overline{u}} \end{array} \qquad (58)$$

Figure 29 depicts the controlled states θ_1, θ_2, $\overline{u}$, and $\overline{v}$ versus time for the integral coordinate technique as obtained by the AFIT Subprogram OPTCON. Figures 30 and 31 illustrate these same states as obtained by integrating the integral coordinate equations of motion forward with control included in the system. As these figures indicate, the satellite returns to the desired attitude in approximately one second. Figure 32 depicts the amount of control required using integral coordinate techniques. A more descriptive illustration of this control is given in Figure 33. By comparing Figure 33 to Figure 26, it can be noted that control requirements for the integral coordinate and modal techniques are nearly identical. The all negative eigenvalues appearing in Table V indicate the stability of the integral coordinate method for this satellite configuration.

Figure 29. Controlled States - Integral Coordinates
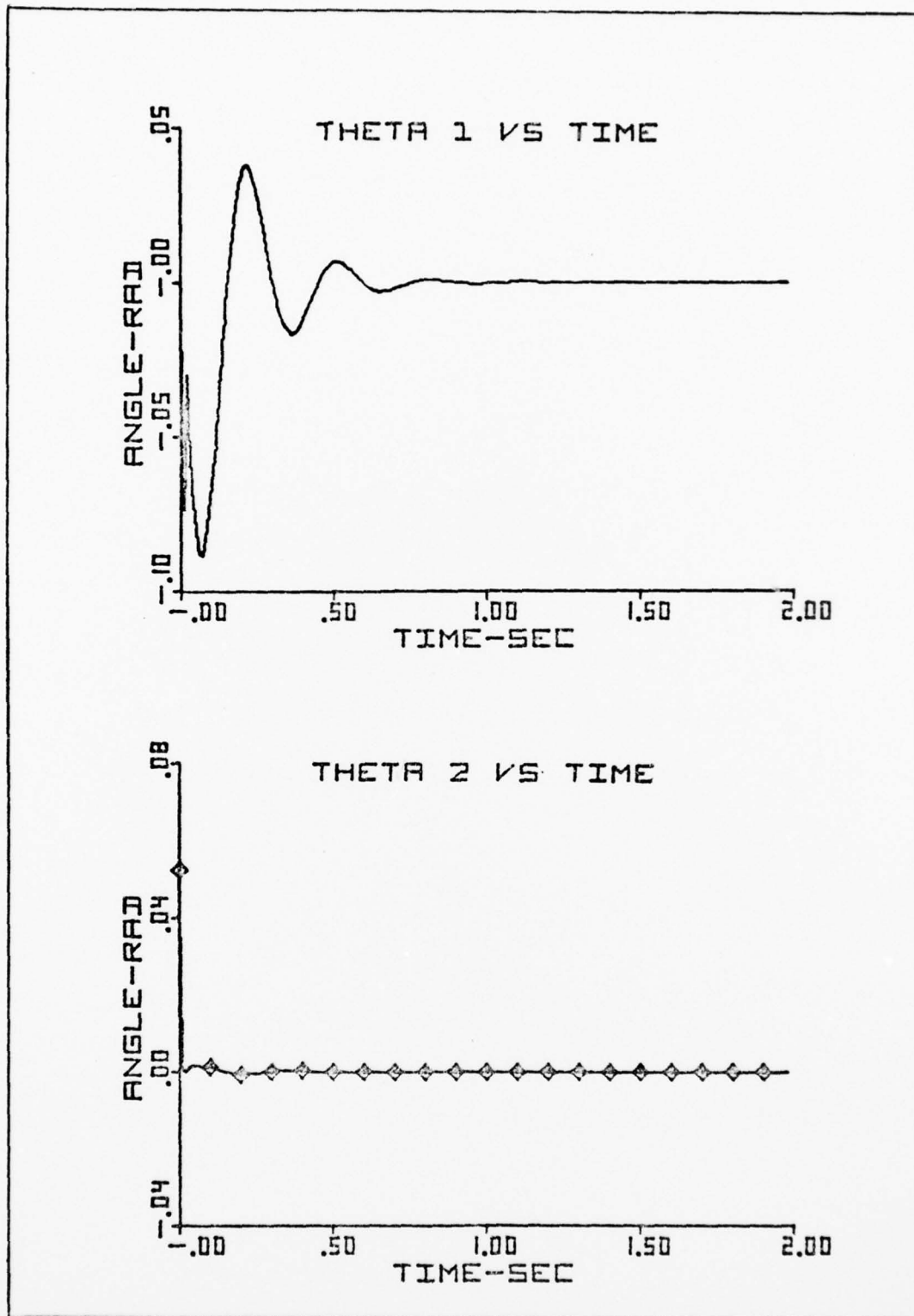
Figure 30. Controlled Angular Motion - Integral Coordinates

70
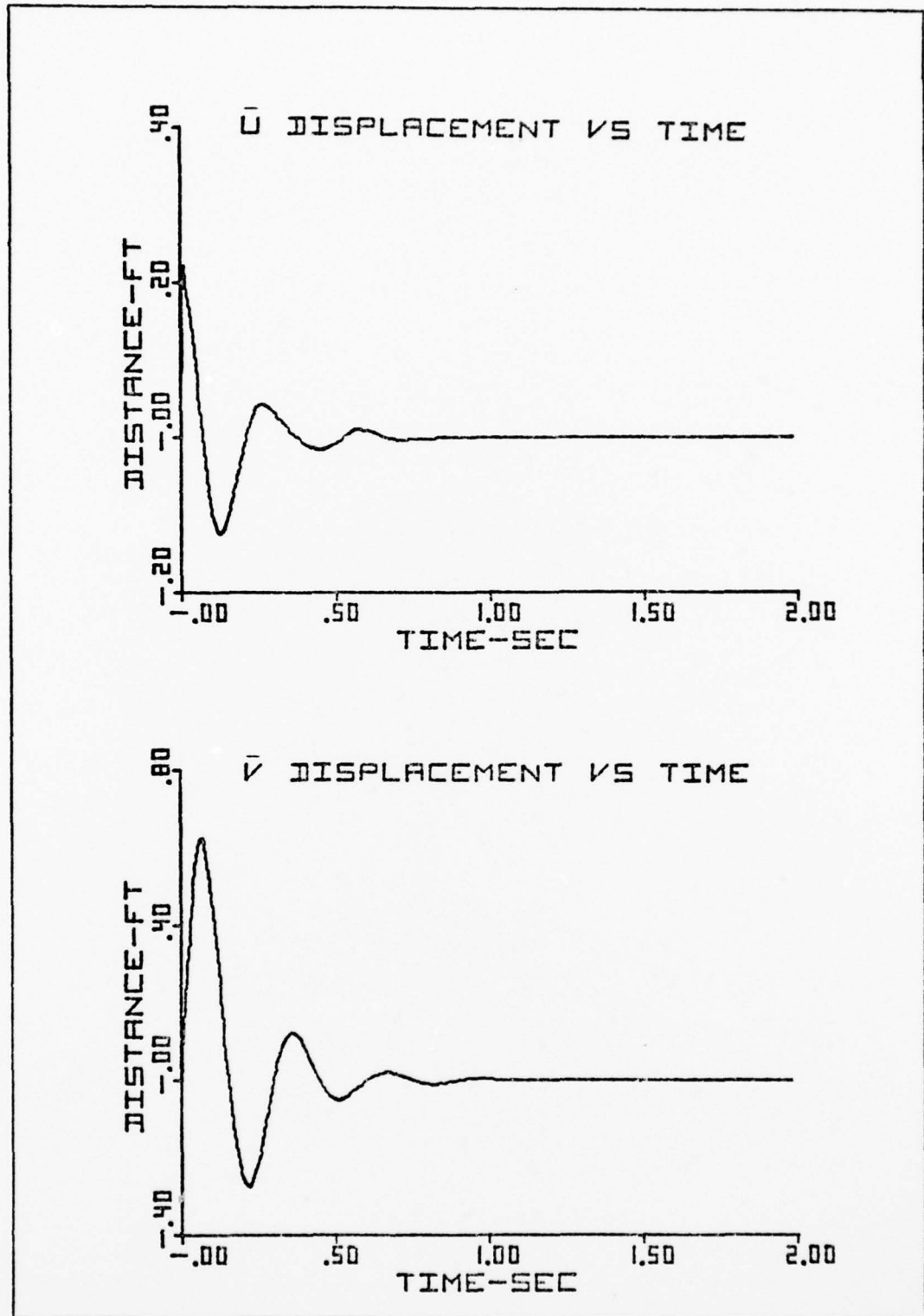
Figure 31.   Controlled Antenna Motion - Integral Coordinates

71
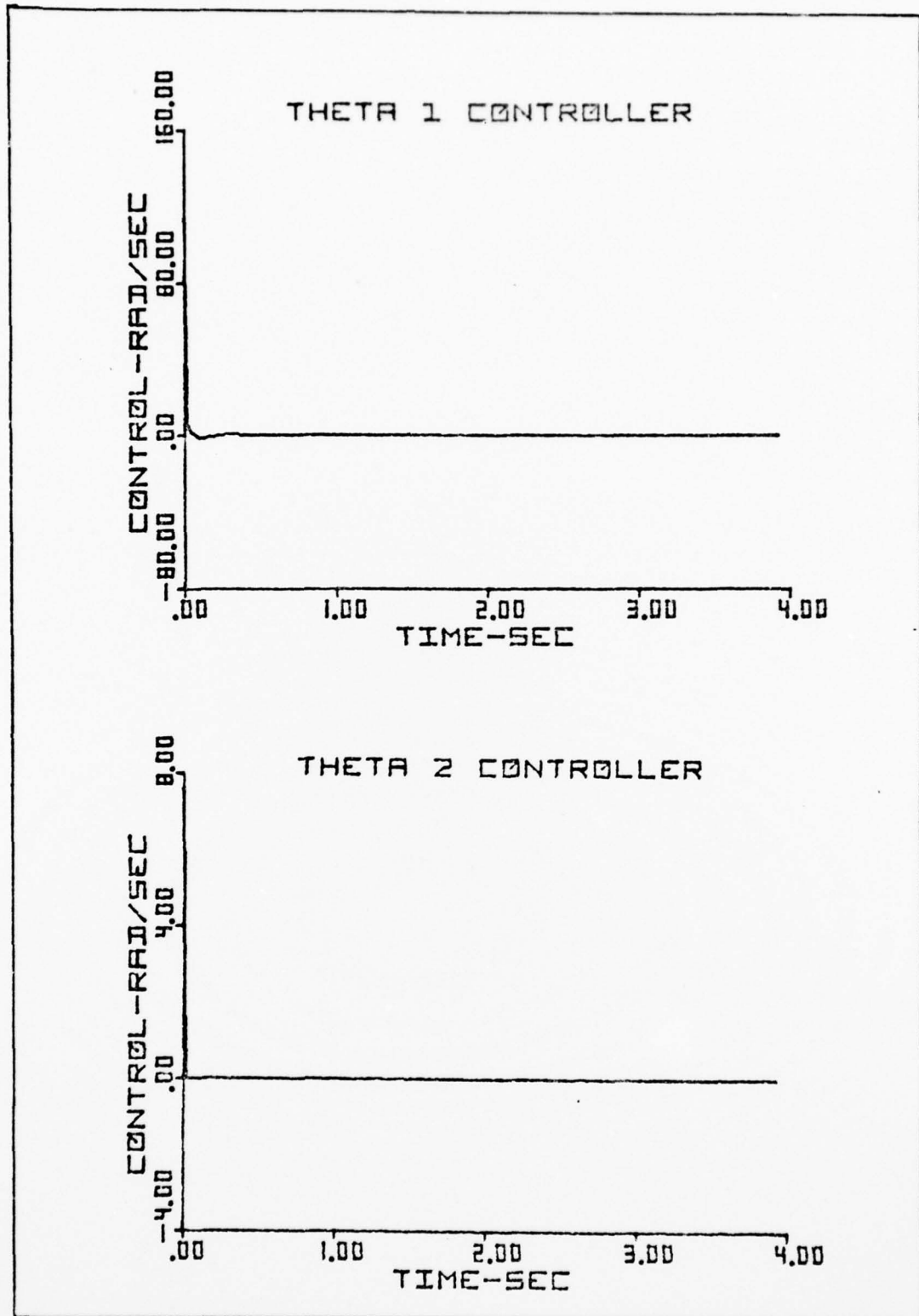
Figure 32.   Control Requirements - Integral Coordinates

72
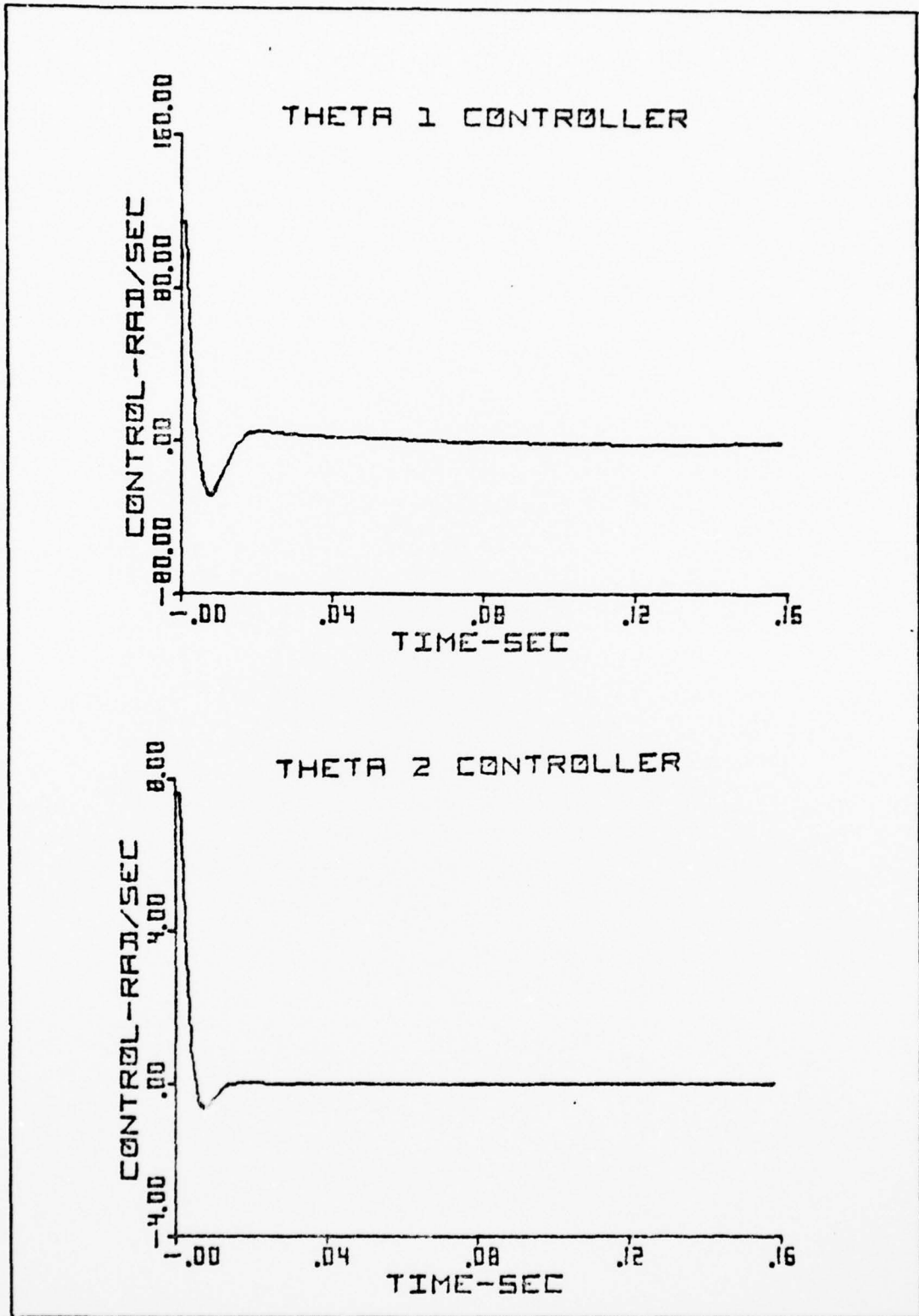
Figure 33.   Control Requirements - Integral Coordinates

73

Table V.

Integral Coordinate Closed-Loop Eigenvalues

Real	Imaginary
-.47474E+01	-.33747E+02
-.47474E+01	.33747E+02
-.56459E+01	-.21147E+02
-.56459E+01	.21147E+02
-.18968E+03	-.19868E+03
-.18968E+03	.19868E+03
-.27159E+03	-.27615E+03
-.27159E+03	.27615E+03

Analysis

The results to this point have shown that regardless
of which of the three techniques is choosen to investigate
the system, some feedback gains can be determined which
return the modelled satellite's attitude back to a desired
orientation. Although the integral coordinate method is
apparently a viable technique for controlling a satellite
system, further investigation must be made to determine its
effectiveness in providing feedback gains which could con-
trol an actual satellite system.

Recall the assumption that the continuously modelled
modal analysis investigation represents the physical sat-
ellite system. Hence, the effectiveness of the integral

74

coordinate technique can be determined by applying integral
coordinate feedback gains to the continuous modal invest-
igation and seeing if the satellite does, in fact, return
to a desired orientation. To this end, modal displacements
were related to integral coordinate displacements by the
following:

$$\bar{u} = \int_{h}^{h+1} pzudz \quad - \text{ integral coordinate}$$

$$U = \sum_{i=1}^{4} \Phi_i u_i \quad - \text{ modal analysis}$$

or

$$\bar{u} = \int_{h}^{h+1} \sum_{i=1}^{4} \Phi_i u_i pzdz = \sum_{i=1}^{4} (ml^2)^{\frac{1}{2}} S_{z_i} u_i$$

Similarly,

$$\bar{v} = \sum_{i=1}^{4} (ml^2)^{\frac{1}{2}} S_{z_i} v_i$$

$$P_{\bar{u}} = \frac{2\dot{\bar{u}}}{RI} + 2\dot{\theta}_2 + 2\theta_1 \Omega$$

$$P_{\bar{v}} = \frac{2\dot{\bar{v}}}{RI} - 2\dot{\theta}_1 + 2\theta_2 \Omega \tag{59}$$

Basically, the control was determined by first equating modal
states to integral coordinate states. After this, the re-
sulting integral coordinate displacements were multiplied
by the previously obtained integral coordinate feedback gains,
which yielded the required control. Numerical integration
of the now modified modal system provided the following
results. Figure 34 illustrates that the satellite does
return to a desired pointing attitude, as evidenced by θ_1
and θ_2 returning to zero radians. Comparing Figure 34 to

75

Figure 19, it can be seen that the integral coordinate feedback gains do control the system almost as well as the optimal feedback gains obtained for the purely modal analysis investigation. Figures 35 through 38 depict mode displacements, and again, the control is such that the antennas return to a nominal position. Figure 39 presents the magnitude of antenna displacements for the continuous modal system using integral coordinate feedback gains. If Figure 39 is compared to Figure 24, it can be noted that the magnitude of antenna motion for the continuous modal system, using integral coordinate feedback gains, is nearly as controlled as the pure continuous modal analysis. The control required to return the satellite to the desired orientation is depicted in Figures 40 and 41. These control results are comparable to the results obtained in Figures 25 and 26 for the pure modal investigation. The above analysis has shown that integral coordinate feedback gains do control the satellite system almost as well as feedback gains obtained by modal techniques. This supports the supposition that the integral coordinate method is a viable technique for estimating optimal control feedback gains for an actual satellite system.

Other example problems were investigated with the results being basically the same as those presented above. As long as the satellite system was inherently stable, integral coordinate feedback gains could be found and verified by applying them to the continuous modal system.

For satellite systems which were inherently unstable, either the integral coordinate technique or the modal method could control the satellite. However, when integral coordinate feedback gains were substituted into the modal system, the system would not control as desired. This was apparently due to the fact that the control on the antenna, which was pervasive in nature, was unable to keep up with the inherent instabilities of the system.
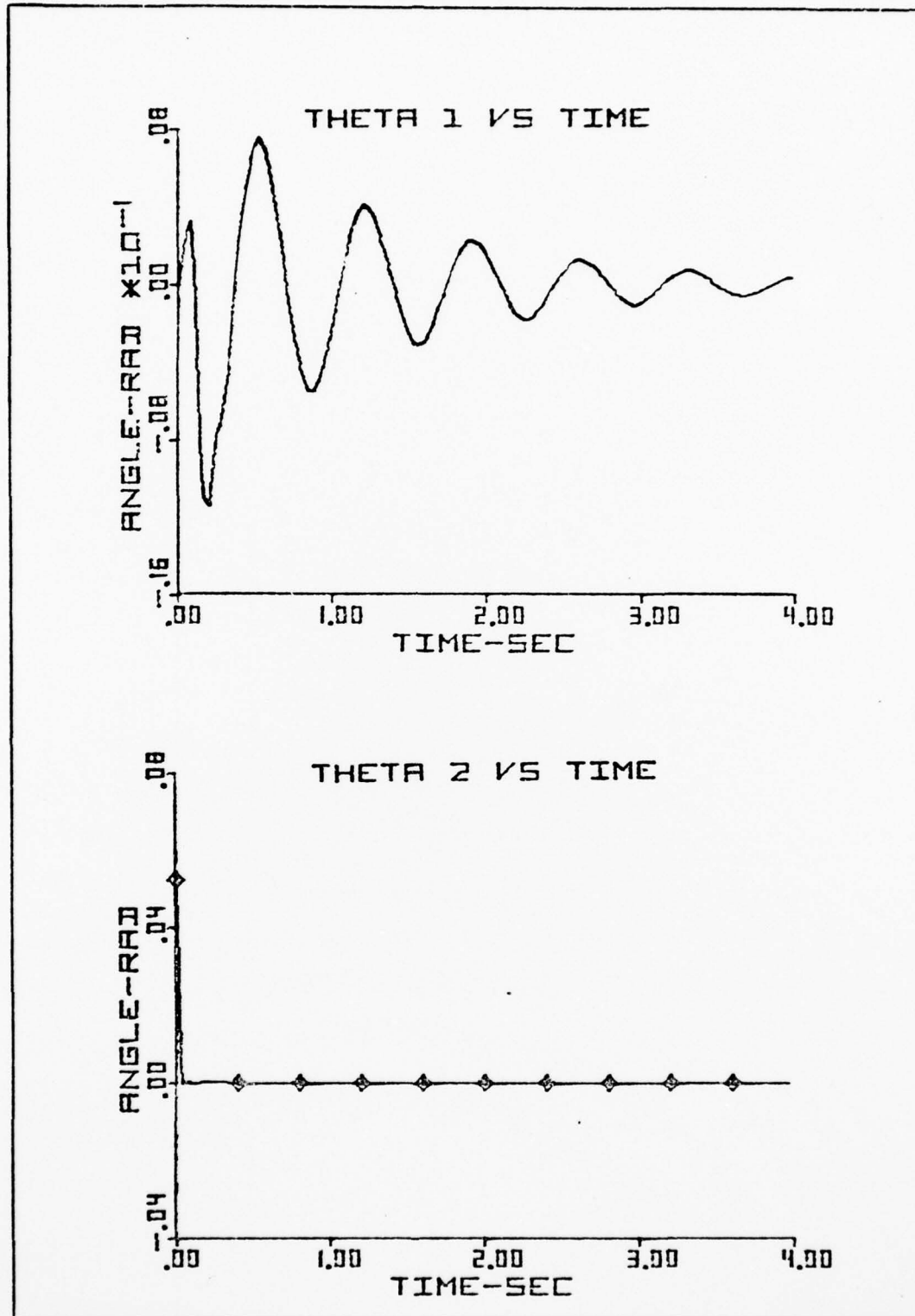
Figure 34. Controlled Angular Motion Using Integral
Coordinate Feedback Gains in Modal System

78
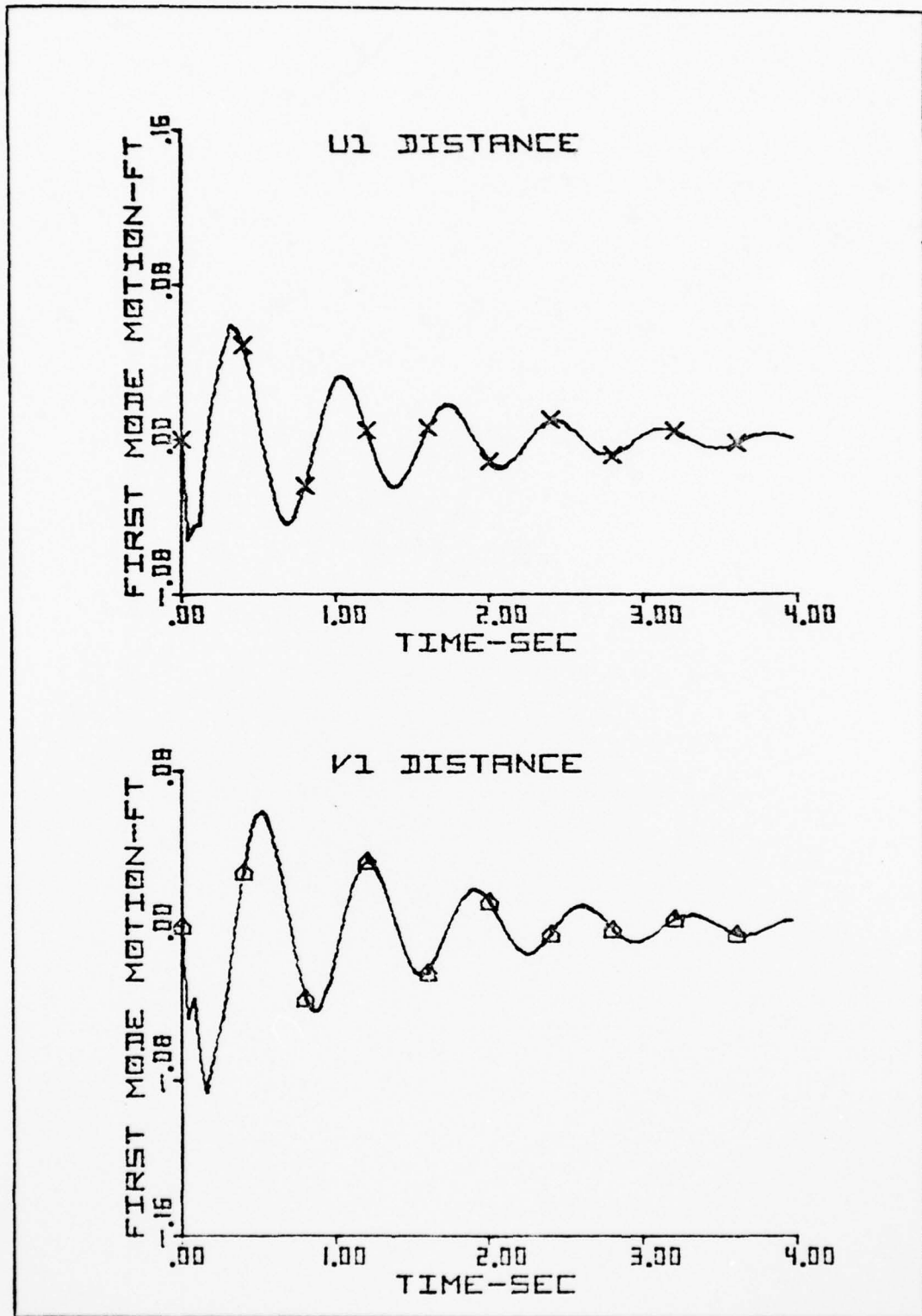
Figure 35. Controlled First Mode Antenna Motion Using
Integral Coordinate Feedback Gains in Modal System
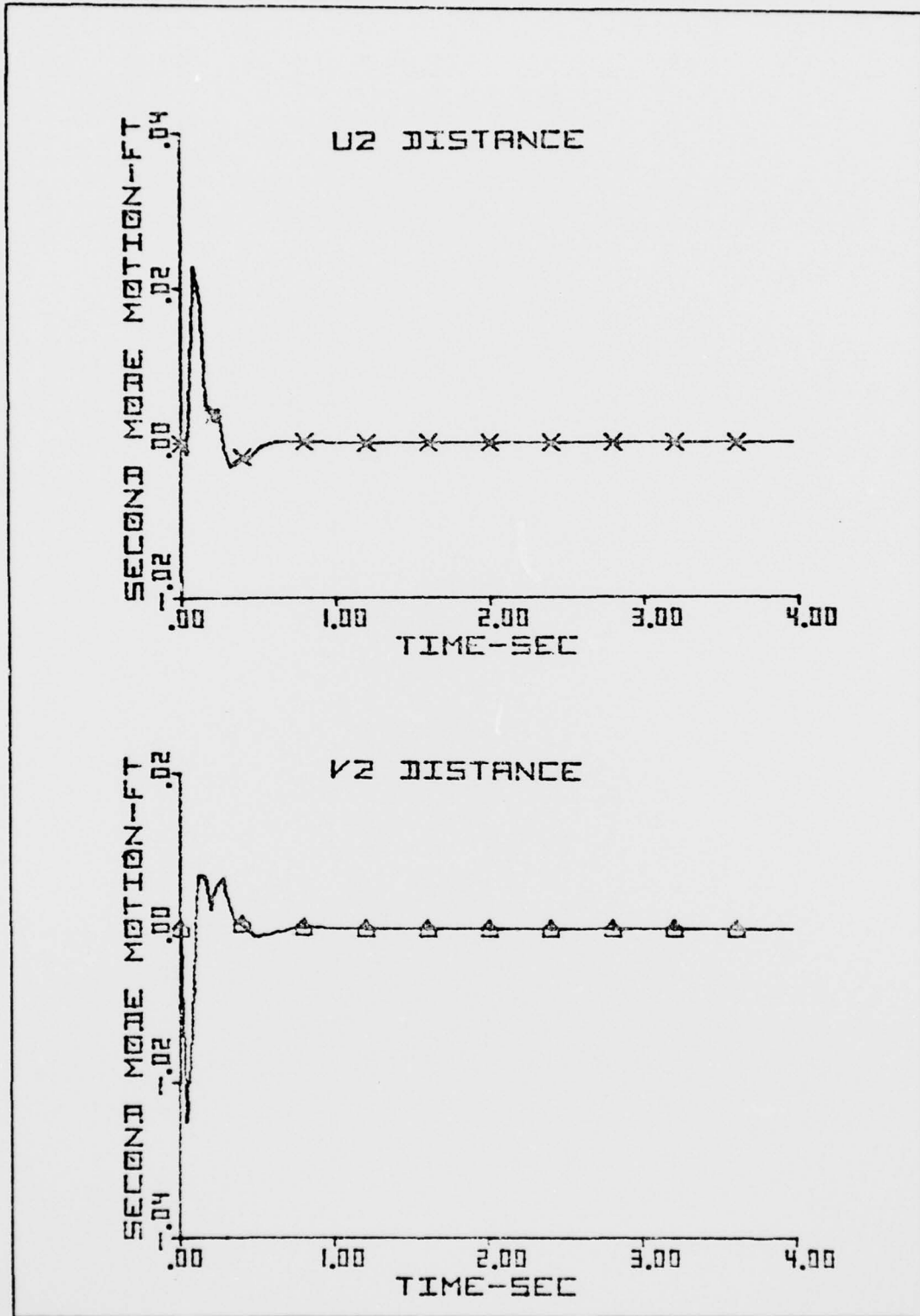
Figure 36. Controlled Second Mode Antenna Motion Using Integral Coordinate Feedback Gains in Modal System

80
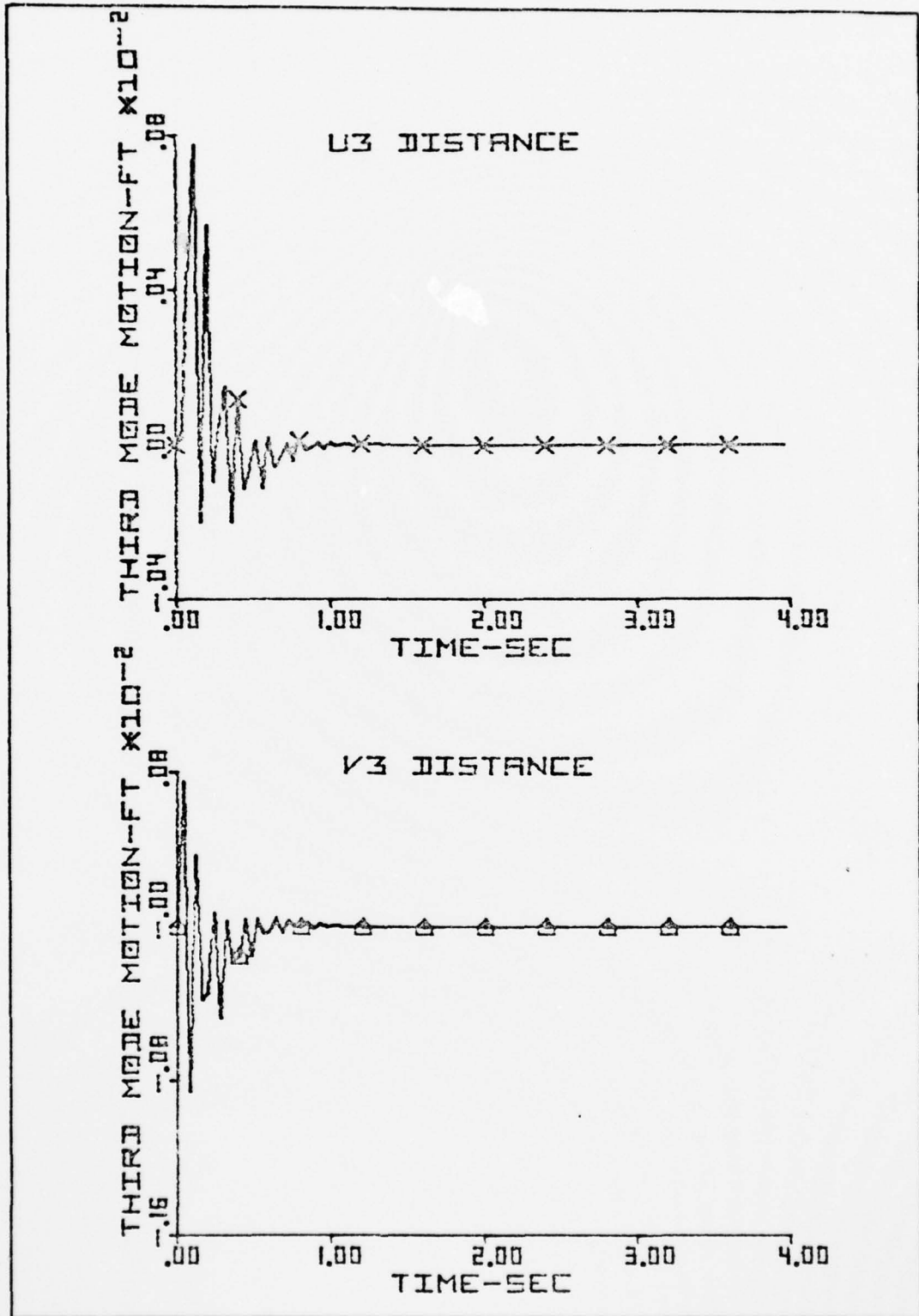
Figure 37. Controlled Third Mode Antenna Motion Using
Integral Coordinate Feedback Gains in Modal System

81
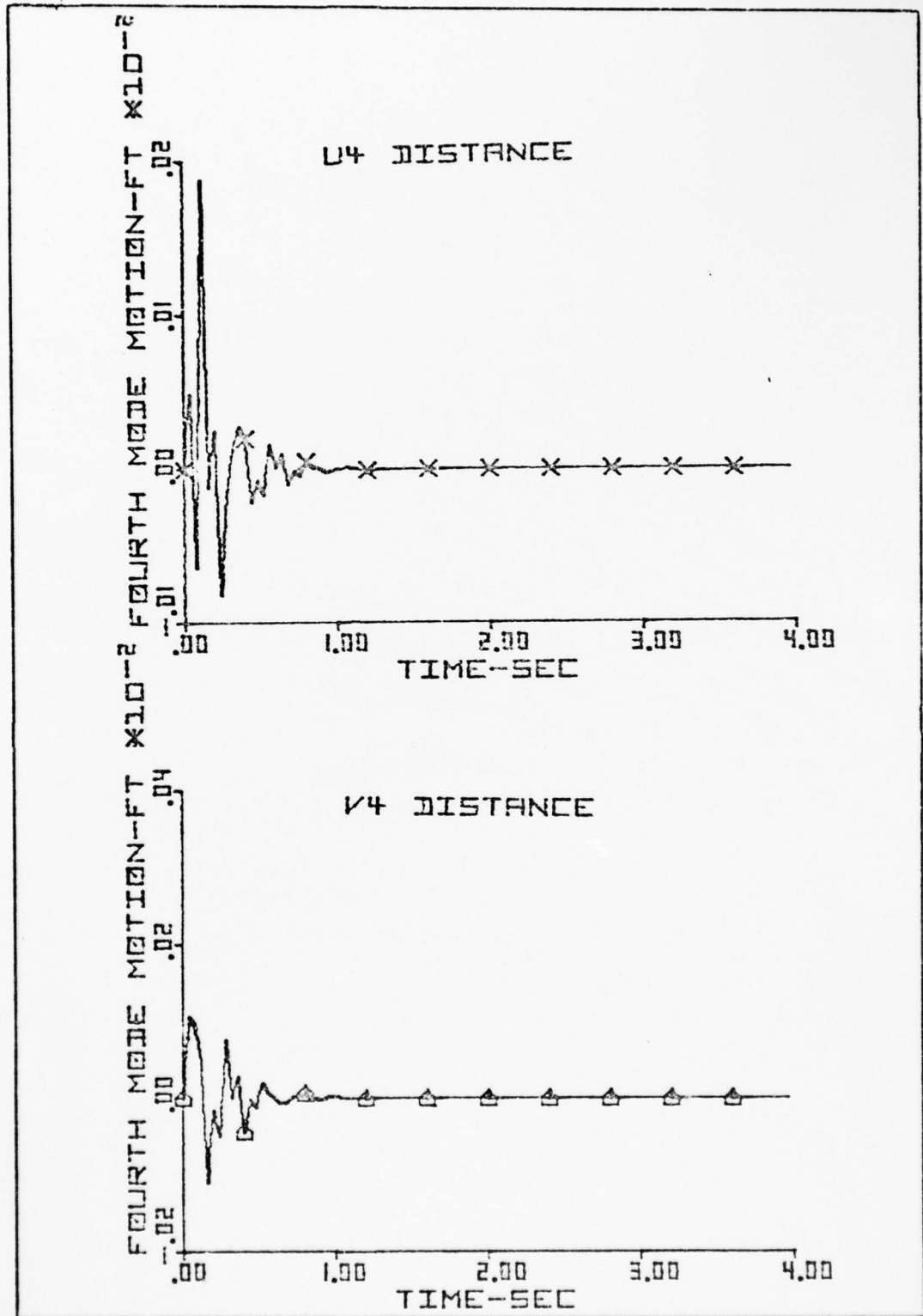
Figure 38. Controlled Fourth Mode Antenna Motion Using Integral Coordinate Feedback Gains in Modal System

82

Figure 39. Controlled Magnitude of Antenna Modal Motion With
Integral Coordinate Feedback Gains in Modal System
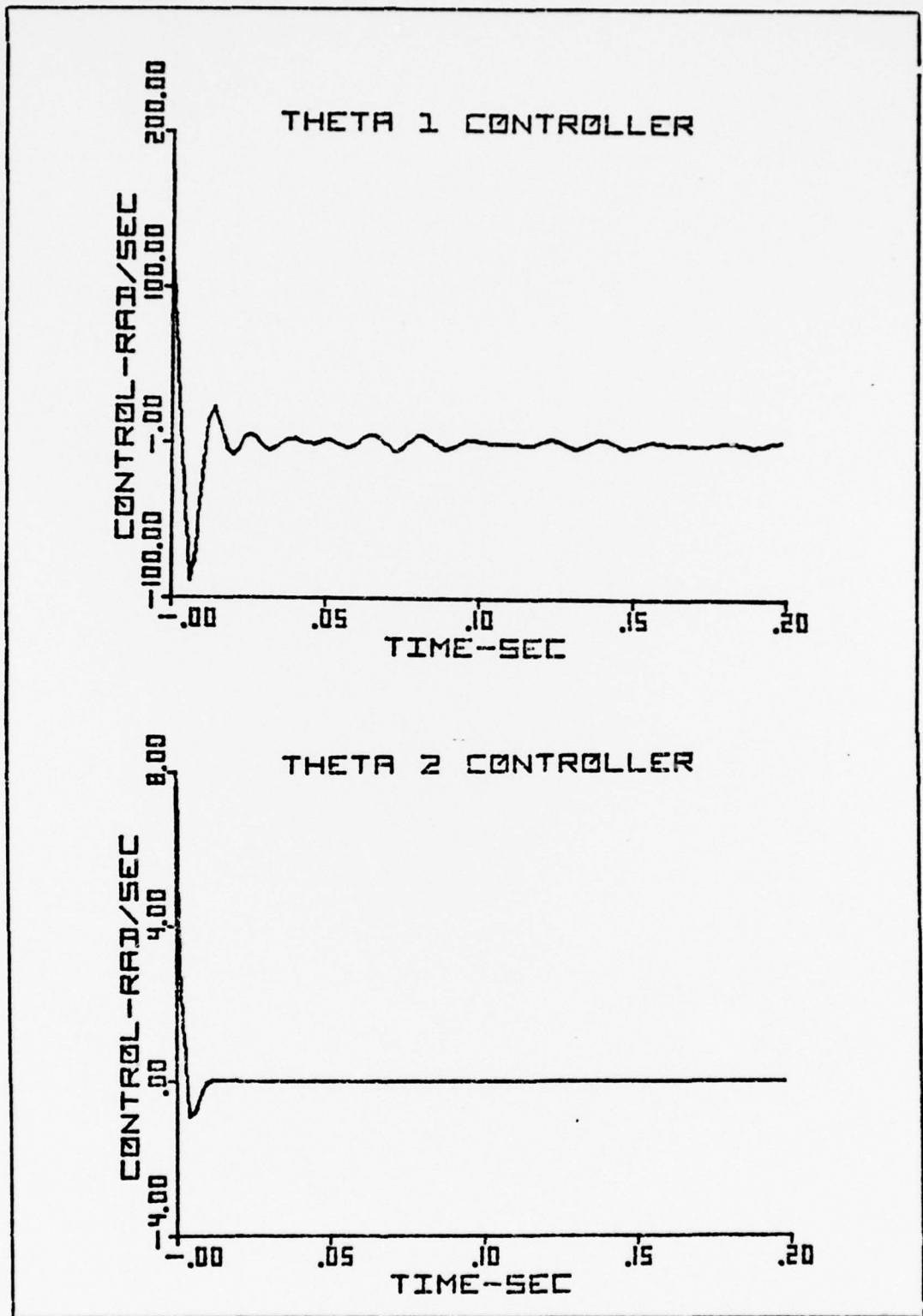
Figure 40. Control Requirements Using Integral Coordinate Feedback Gains in Modal System

84
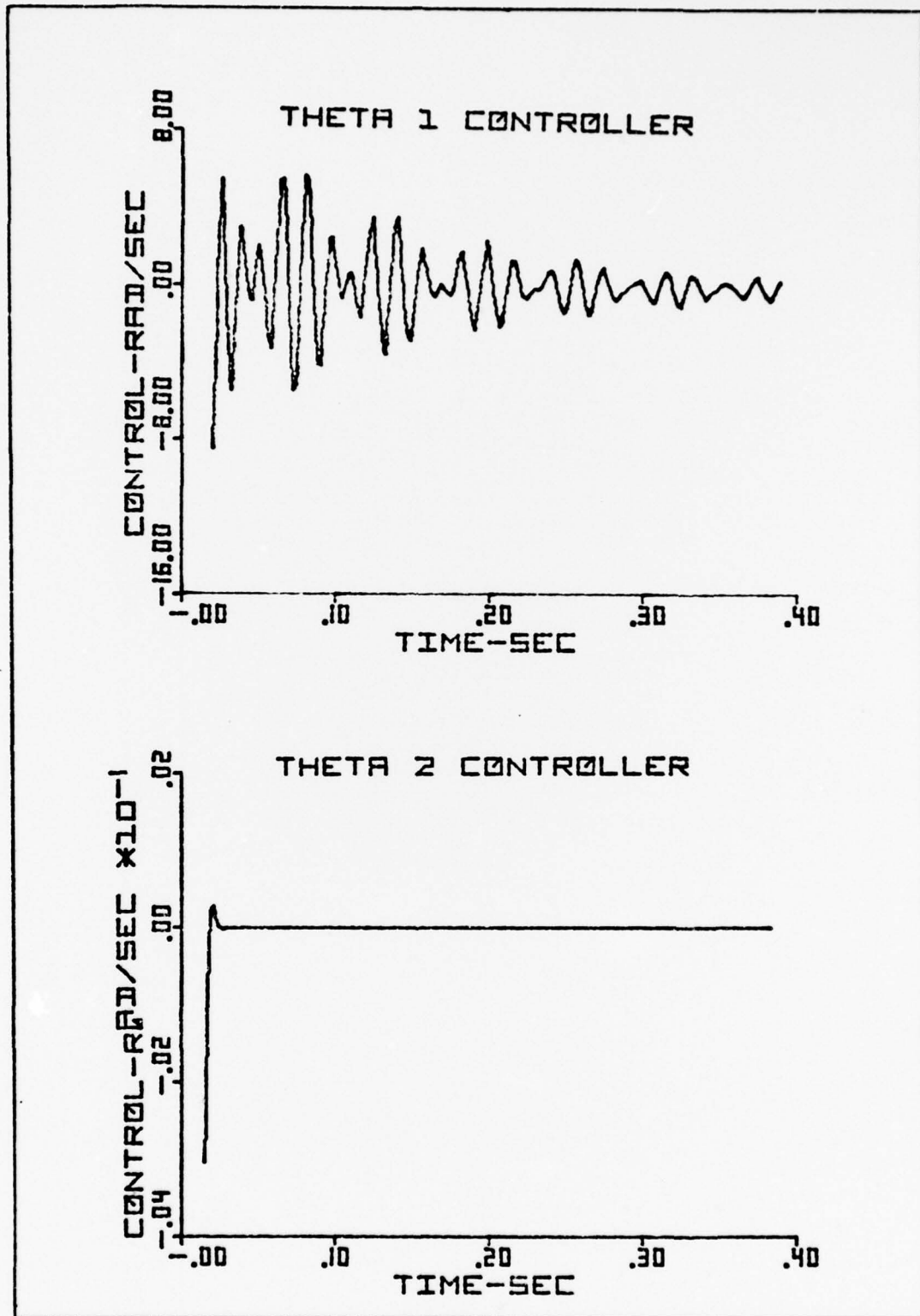
Figure 41. Control Requirements Using Integral Coordinate
Feedback Gains in Modal System

V. Conclusions

By analyzing the results to example 1, several conclusions may be made regarding the utility of the three methods investigated. A discussion of these conclusions is presented below.

The discrete system analysis was the simplest to perform. However, the results obtained by this method are least useful to the satellite designer. The method was simple in that only eight first order differential equations of motion needed to be solved to describe the attitude of the satellite. This required minimal programming effort and minimal computer time in obtaining a solution to the control problem. The method lacked utility in that the continuous antennas were crudely discretized and could not be easily related to an actual physical satellite. Since the model did not have the completeness of the continuous system model, a designer would lack confidence in his ability to obtain optimal control feedback gains which approximated those required for the true system.

The purely continuous modal technique offers a reversed situation from that of the discrete method. The modal analysis technique offers a means of obtaining realistic feedback gains, however, the method is rather complex to easily employ. Even for this rather simple satellite, having only two flexible antennas, the method required the solution of the fixed-free beam eigenvalue problem and the solution of twenty first order differential equations. The computer

86

programming effort was considerably greater than that required for the discrete analysis, and computer execution times were approximately five times greater. Although time consuming, this method adequately models the satellite system and is often used by the designer to obtain feedback gains and the associated optimal control requirements.

To determine control requirements for a satellite in the early stages of design, a spacecraft designer would like to have at his disposal a technique which combines the attributes of the discrete and modal investigations. The results obtained for the integral coordinate method indicate that this technique could provide the designer with such a design tool. The method was generally simple, requiring the solution of the same number of differential equations as the discrete system. Problem formulation was further simplified since the beam eigenvalue problem did not have to be solved. Programming effort and computer execution times were approximately the same as the discrete system analysis. As shown, the satellite's controlled motion with integral coordinate feedback gains applied to the continuous modal system was almost identical to that of the pure modal method. This tends to verify the fact that a designer can obtain realistic estimates of control requirements by using the simplified integral coordinate techniques developed in this thesis.

VI. Summary and Recommendations

Summary

This thesis investigated three methods for obtaining control feedback gains of satellites containing flexible appendages. These methods included a discrete system analysis, continuous modal analysis, and a new integral coordinate analysis. For each of the techniques considered, equations of motion describing the satellite's attitude were developed. Active control was applied to the satellite by an arbitrary mechanism capable of providing angular velocity inputs. Control was required in the system to keep the attitude of the satellite at a desired null orientation. A sample problem was investigated and an analysis of the results for the three techniques was performed. The discrete method was found to be simple, but lacking in utility for obtaining realistic control estimates. The modal analysis obtained valid control results, however, the method involved rather complex mathematical formulations. The results obtained for the integral coordinate method indicate that it is a simple, time saving, and valid means for obtaining estimated control requirements for satellites with flexible appendages.

Recommendations

Having completed this investigation, it is recommended that the integral coordinate method be used for obtaining control requirements for the specific type of satellite

discussed in this thesis. This recommendation is based on three reasons. For one, it is easy to employ during early stages of design. Secondly, it avoids involved numerical procedures. And finally, the effect of changing various system parameters can be easily assessed. Although the utility of the integral coordinate technique was generally established in this investigation, it is also recommended that this method be further examined. In particular, other satellite configurations or other spacecraft in general should be investigated to determine the utility of the integral coordinate technique for estimating optimal control requirements. If shown effective for a wider classification of space vehicles, the spacecraft designer would realize an enormous savings in time and effort in obtaining estimated optimal control requirements.

Bibliography

1. Meirovitch, L., and R. Calico. "The Stability of Motion of Satellites With Flexible Appendages." <u>NASA Contractor Report</u>, NASA CR-1978 (Feburary 1972).

2. ...... "A Comparative Study of Stability Methods for Flexible Satellites." <u>AIAA Journal</u>, <u>11</u>:91-98 (January 1973).

3. Sohoni, V., and D. Guild. "Optimal Attitude Control System for Spinning Aerospace Vehicles." <u>Journal of Astronautical Sciences</u>, <u>18</u>:86-100 (September 1970).

4. Meirovitch, L., and H. Nelson. "On the High-Spin Motion of a Satellite Containing Elastic Parts." <u>Journal of Spacecraft and Rockets</u>, <u>3</u>:1597-1602 (November 1966).

5. Meirovitch, L. "Bounds on the Extension of Antennas for Stable Spinning Satellites." <u>Journal of Spacecraft and Rockets</u>, <u>11</u>:202-204 (March 1974).

6. Meirovitch, L., and J. Juang. "Effects of the Mass Center Shift for Force-Free Flexible Spacecraft." <u>AIAA Journal</u>, <u>13</u>:1535-1536 (November 1975).

7. Meirovitch, L. <u>Methods of Analytical Dynamics</u>, McGraw-Hill, Inc., New York, 1975.

8. ...... <u>Elements of Vibration Analysis</u>, McGraw-Hill, Inc., New York, 1975.

9. Hurty, W., and M. Rubinstein. <u>Dynamics of Structures</u>, Prentice-Hall, Inc., New Jersey, 1964.

10. Bryson, A., and Y. Ho. <u>Applied Optimal Control</u>, John Wiley and Sons, New York, 1975.

11. Wilt, Mirmak, and Ray. <u>Solution of Linear-Quadratic Optimal Control Problem (OPTCON)</u>. Air Force Institute of Technology Computer Program Library, 1974 (Revised January 1976).

12. Kleinman, D. <u>Computer Programs Useful in Linear Systems Studies (MRIC)</u>. ARML Subroutine, SCI Technical Memorandum. Palo Alto, California: Systems Control, Inc., December 1971.

13. Shampine, L., and M. Gordon. <u>Computer Solution of Ordinary Differential Equations The Initial Value Problem (ODE)</u>. CC6600 Computer Program Library

Appendix A

Kinetic Energy Derivation

The following is a derivation of the kinetic energy expression given by equation (2).
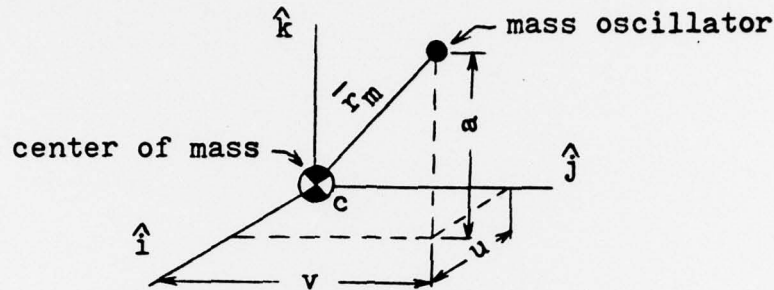
The velocity of the rigid body less the mass oscilators is given by

$$\overline{V}_{B-m} = \overline{V}_c + \overline{\omega} \times \overline{r} \qquad (A-1)$$

The velocity of the mass oscillators is given by

$$\overline{V}_m = \overline{V}_c + \overline{\omega} \times \overline{r}_m + \dot{u}\hat{i} + \dot{v}\hat{j} \qquad (A-2)$$

Therefore, the kinetic energy expression given by equation (1) can be written as

$$T = \frac{1}{2}\int_{B-m}(\overline{V}_{B-m}\cdot\overline{V}_{B-m})dm + \frac{1}{2}\int_m(\overline{V}_m\cdot\overline{V}_m)dm \qquad (A-3)$$

or

$$T = \frac{1}{2}\int_{B-m}(\overline{V}_c + \overline{\omega} \times \overline{r})\cdot(\overline{V}_c + \overline{\omega} \times \overline{r})dm + \frac{1}{2}\int_m(\overline{V}_c + \overline{\omega} \times \overline{r}_m$$

$$+ \dot{u}\hat{i} + \dot{v}\hat{j})\cdot(\overline{V}_c + \overline{\omega} \times \overline{r}_m + \dot{u}\hat{i} + \dot{v}\hat{j})dm$$

$$= \frac{1}{2}M\overline{V}_c\cdot\overline{V}_c + \frac{1}{2}\overline{\omega}^T I_{B-m}\overline{\omega} + m\overline{V}_c\cdot\overline{V}_c + \frac{1}{2}\overline{\omega}^T I_m\overline{\omega} + m(\dot{u}^2 + \dot{v}^2)$$

$$+ 2m(\overline{\omega} \times \overline{r}_m)(\dot{u}\hat{i} + \dot{v}\hat{j}) + \text{terms which go to zero}$$

$$(A-4)$$

91

where

$$I_{B-m} \equiv \begin{bmatrix} A & 0 & 0 \\ 0 & B & 0 \\ 0 & 0 & C \end{bmatrix} \tag{A-5}$$

and

$$I_m = \begin{bmatrix} a^2 + v^2 & -uv & -au \\ -uv & a^2 + u^2 & -av \\ -au & -av & u^2 + v^2 \end{bmatrix} \tag{A-6}$$

Substituting equations (A-5) and (A-6) into equation (A-4) yields

$$\begin{aligned}
T =\ & \tfrac{1}{2}M\overline{V}_c\cdot\overline{V}_c + \tfrac{1}{2}(A\Omega_x^2 + B\Omega_y^2 + C\Omega_z^2) + m\overline{V}_c\cdot\overline{V}_c \\
& + m\Big[(a^2 + v^2)\Omega_x^2 + (a^2 + u^2)\Omega_y^2 + (u^2 + v^2)\Omega_z^2 \\
& - 2uv\Omega_x\Omega_y - 2au\Omega_x\Omega_z - 2av\Omega_y\Omega_z\Big] + 2m\Big[u\dot{v}\Omega_z - \dot{u}v\Omega_z \\
& \qquad\qquad - a\dot{v}\Omega_x + a\dot{u}\Omega_y\Big] + m(\dot{u}^2 + \dot{v}^2) \tag{A-7}
\end{aligned}$$

Combining constant terms and letting $A' = A + 2ma^2$ and $B' = B + 2ma^2$ yields

$$\begin{aligned}
T =\ & \tfrac{1}{2}A'\Omega_x^2 + \tfrac{1}{2}B'\Omega_y^2 + \tfrac{1}{2}C\Omega_z^2 + m\Big[\dot{u}^2 + \dot{v}^2 + v^2\Omega_x^2 \\
& + u^2\Omega_y^2 + (u^2 + v^2)\Omega_z^2 - 2a\dot{v}\Omega_x + 2a\dot{u}\Omega_y - 2(\dot{u}v \\
& - u\dot{v})\Omega_z - 2uv\Omega_x\Omega_y - 2av\Omega_y\Omega_z - 2au\Omega_x\Omega_z\Big] + \text{Const} \tag{A-8}
\end{aligned}$$

Equation (A-8) is in agreement with the kinetic energy expression obtained in Ref. 4 for the same satellite system.

Appendix B

Transformation

The following is a transformation from orbitally referenced angular velocities to body referenced angles and angular rates.
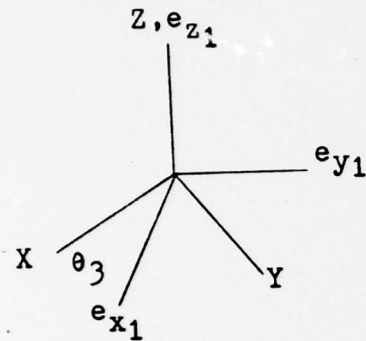
$$C_{1/X} = \begin{bmatrix} \cos\theta_3 & \sin\theta_3 & 0 \\ -\sin\theta_3 & \cos\theta_3 & 0 \\ 0 & 0 & 1 \end{bmatrix}$$

$$\text{(B-1)}$$
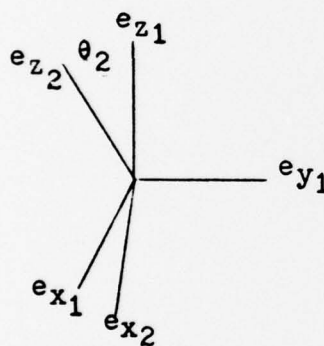
$$C_{2/1} = \begin{bmatrix} \cos\theta_2 & 0 & -\sin\theta_2 \\ 0 & 1 & 0 \\ \sin\theta_2 & 0 & \cos\theta_2 \end{bmatrix}$$

$$\text{(B-2)}$$
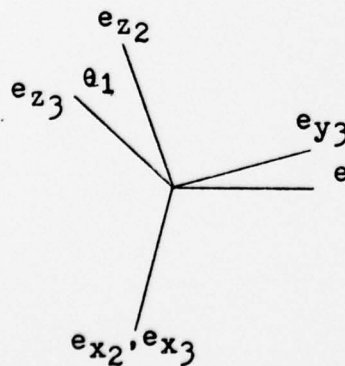
$$C_{3/2} = \begin{bmatrix} 1 & 0 & 0 \\ 0 & \cos\theta_1 & \sin\theta_1 \\ 0 & -\sin\theta_1 & \cos\theta_1 \end{bmatrix}$$

$$\text{(B-3)}$$

93

The angular velocity of the satellite can be described by the vector

$$\bar{\omega} = \dot{\theta}_3 e_{z_1} + \dot{\theta}_2 e_{y_2} + \dot{\theta}_1 e_{x_3} \qquad \text{(B-4)}$$

From equations (B-1), (B-2), and (B-3) it can be shown that

$$\begin{bmatrix} e_{x_2} \\ e_{y_2} \\ e_{z_2} \end{bmatrix} = \begin{bmatrix} 1 & 0 & 0 \\ 0 & \cos\theta_1 & -\sin\theta_1 \\ 0 & \sin\theta_1 & \cos\theta_1 \end{bmatrix} \begin{bmatrix} e_{x_3} \\ e_{y_3} \\ e_{z_3} \end{bmatrix} \qquad \text{(B-5)}$$

and

$$\begin{bmatrix} e_{x_1} \\ e_{y_1} \\ e_{z_1} \end{bmatrix} = \begin{bmatrix} \cos\theta_2 & \sin\theta_1 \sin\theta_2 & \cos\theta_1 \sin\theta_2 \\ 0 & \cos\theta_1 & -\sin\theta_1 \\ -\sin\theta_2 & \sin\theta_1 \cos\theta_2 & \cos\theta_1 \cos\theta_2 \end{bmatrix} \begin{bmatrix} e_{x_3} \\ e_{y_3} \\ e_{z_3} \end{bmatrix}$$

$$\cdot \qquad \text{(B-6)}$$

Substituting the appropriate expressions from equations (B-5) and (B-6) into equation (B-4) yields

$$\bar{\omega} = (\dot{\theta}_1 - \sin\theta_2 \, \dot{\theta}_3)e_{x_3} + (\sin\theta_1 \cos\theta_2 \, \dot{\theta}_3 + \cos\theta_1 \, \dot{\theta}_2)e_{y_3}$$

$$+ (\cos\theta_1 \cos\theta_2 \, \dot{\theta}_3 - \sin\theta_1 \, \dot{\theta}_2)e_{z_3} \qquad \text{(B-7)}$$

Hence,

$$\bar{\omega} = \begin{bmatrix} \Omega_x \\ \Omega_y \\ \Omega_z \end{bmatrix} = \begin{bmatrix} 1 & 0 & -\sin\theta_2 \\ 0 & \cos\theta_1 & \sin\theta_1 \cos\theta_2 \\ 0 & -\sin\theta_1 & \cos\theta_1 \cos\theta_2 \end{bmatrix} \begin{bmatrix} \dot{\theta}_1 \\ \dot{\theta}_2 \\ \dot{\theta}_3 \end{bmatrix} \qquad \text{(B-8)}$$

94

Appendix C

Derivation of Discrete System Equations of Motion

The following is a brief description of the derivation of the equations of motion for the discrete system by applying equations (13) and (14) to the system Hamiltonian and Lagrangian. From equation (13)

$$P_{\theta_1} = \frac{\partial L}{\partial \dot{\theta}_1} = A'\dot{\theta}_1 - 2ma\dot{v} - A'\theta_2\Omega - 2mau\Omega \qquad (C-1)$$

$$P_{\theta_2} = \frac{\partial L}{\partial \dot{\theta}_2} = B'\dot{\theta}_2 + 2ma\dot{u} + B'\theta_1\Omega - C\theta_1\Omega - 2mav\Omega \qquad (C-2)$$

$$P_{\theta_3} = \frac{\partial L}{\partial \dot{\theta}_3} = C\dot{\theta}_3 + C\Omega \qquad (C-3)$$

$$P_u = \frac{\partial L}{\partial \dot{u}} = 2m\dot{u} + 2ma\dot{\theta}_2 + 2ma\theta_1\Omega - 2mv\Omega \qquad (C-4)$$

$$P_v = \frac{\partial L}{\partial \dot{v}} = 2m\dot{v} - 2ma\dot{\theta}_1 + 2ma\theta_2\Omega + 2mu\Omega \qquad (C-5)$$

Equations (C-1) through (C-5) where solved simultaneously for $\dot{\theta}_1$, $\dot{\theta}_2$, $\dot{\theta}_3$, $\dot{u}$, and $\dot{v}$. From equation (14)

$$\dot{P}_{\theta_1} = (B' - C)\Omega\dot{\theta}_2 + (B' - C)\Omega^2\theta_1 + 2ma\Omega(\dot{u} - v\Omega) \qquad (C-6)$$

$$\dot{P}_{\theta_2} = -A'\Omega\dot{\theta}_1 + 2ma\Omega(\dot{v} + u\Omega) + (A' - C)\Omega^2\theta_2 \qquad (C-7)$$

$$\dot{P}_{\theta_3} = 0 \qquad (C-8)$$

$$\dot{P}_u = (2m\dot{v} - 2ma\dot{\theta}_1)\Omega + (2mu + 2ma\theta_2)\Omega^2 - 2Ku - 2D\dot{u} \qquad (C-9)$$

$$\dot{P}_v = -(2m\dot{u} + 2ma\dot{\theta}_2)\Omega + (2mv - 2ma\theta_1)\Omega^2 - 2Kv - 2D\dot{v} \qquad (C-10)$$

Substituting in the relations obtained from equations (C-1) through (C-5) into equations (C-6) through (C-10), and after much simplification, the expressions of equation (15) may be obtained.

Appendix D

Derivation of Modal Analysis Equations of Motion

The following is a brief description of the derivation of the equations of motion for the modal analysis method by applying equations (37) and (38). From equation (37)

$$P_{\theta_1} = A'\dot{\theta}_1 - 2 \sum_{i=1}^{4} S_{z_i}\dot{v}_i(ml^2)^{\frac{1}{2}} - A'\theta_2\Omega$$

$$- 2\Omega \sum_{i=1}^{4} S_{z_i}u_i(ml^2)^{\frac{1}{2}} \qquad (D-1)$$

$$P_{\theta_2} = B'\dot{\theta}_2 + 2 \sum_{i=1}^{4} S_{z_i}\dot{u}_i(ml^2)^{\frac{1}{2}} + B'\theta_1\Omega$$

$$- C\theta_1\Omega - 2\Omega \sum_{i=1}^{4} S_{z_i}v_i(ml^2)^{\frac{1}{2}} \qquad (D-2)$$

$$P_{\theta_3} = C\dot{\theta}_3 + C\Omega \qquad (D-3)$$

$$P_{u_j} = 2\dot{u}_j + 2\dot{\theta}_2 S_{z_j}(ml^2)^{\frac{1}{2}} + 2\theta_1\Omega S_{z_j}(ml^2)^{\frac{1}{2}}$$

$$- 2\Omega v_j \qquad j = 1,---,4 \qquad (D-4)$$

$$P_{v_j} = 2\dot{v}_j - 2\dot{\theta}_1 S_{z_j}(ml^2)^{\frac{1}{2}} + 2\theta_2\Omega S_{z_j}(ml^2)^{\frac{1}{2}}$$

$$+ 2\Omega u_j \qquad j = 1,---,4 \qquad (D-5)$$

Equations (D-1) through (D-5) where solved simultaneously for $\dot{\theta}_1$, $\dot{\theta}_2$, $\dot{\theta}_3$, $\dot{u}_{1,2,3,4}$, and $\dot{v}_{1,2,3,4}$. From equation (38)

$$\dot{P}_{\theta_1} = (B' - C)\Omega\dot{\theta}_2 + (B' - C)\Omega^2\theta_1 + 2\Omega \sum_{i=1}^{4} S_{z_i}\dot{u}_i(ml^2)^{\frac{1}{2}}$$

$$- 2\Omega^2 \sum_{i=1}^{4} S_{z_i}v_i(ml^2)^{\frac{1}{2}} \qquad (D-6)$$

96

$$\dot{P}_{\theta_2} = -A'\Omega\dot{\theta}_1 + (A' - C)\Omega^2\theta_2 + 2\Omega \sum_{i=1}^{4} S_{zi}\dot{v}_i(ml^2)^{\frac{1}{2}}$$

$$+ 2\Omega^2 \sum_{i=1}^{4} S_{zi}u_i(ml^2)^{\frac{1}{2}} \qquad \text{(D-7)}$$

$$\dot{P}_{\theta_3} = 0 \qquad \qquad \text{(D-8)}$$

$$\dot{P}_{u_j} = 2\Omega\dot{v}_j - 2(ml^2)^{\frac{1}{2}}\Omega S_{zj}(\dot{\theta}_1 - \Omega\theta_2) + 2\Omega^2 u_j - 2\omega_j^2 u_j$$

$$- \frac{2d}{p}\left[\frac{P_{u_j}}{2} - \frac{S_{zj}(ml^2)^{\frac{1}{2}}}{D_b}(P_{\theta_2} + C\theta_1\Omega) + \Omega v_j\right.$$

$$\left. + \frac{S_{zj}ml^2}{D_b} \sum_{i=1}^{4} S_{zi}P_{u_i}\right] \quad j = 1,---,4 \quad \text{(D-9)}$$

$$\dot{P}_v = -2\Omega\dot{u}_j - 2(ml^2)^{\frac{1}{2}}\Omega S_{zj}(\dot{\theta}_2 + \Omega\theta_1) + 2\Omega^2 v_j - 2\omega_j^2 v_j$$

$$- \frac{2d}{p}\left[\frac{P_{v_j}}{2} + \frac{S_{zj}(ml^2)^{\frac{1}{2}}}{D_a}P_{\theta_1} + \frac{S_{zj}ml^2}{D_a} \sum_{i=1}^{4} S_{zi}P_{v_i}\right.$$

$$\left. - \Omega u_j\right] \quad j = 1,---,4 \quad \text{(D-10)}$$

where

$$D_a = A' - 2ml^2 \sum_{i=1}^{4} S_{zi}^2$$

$$D_b = B' - 2ml^2 \sum_{i=1}^{4} S_{zi}^2 \qquad \text{(D-11)}$$

Substituting the relations obtained from equations (D-1) through (D-5) into equation (D-6) through (D-10), and after much simplification, the expressions of equation (39) may be obtained.

97

Appendix E

Derivation of Integral Coordinate Equations of Motion

The following is a brief description of the derivation of the equations of motion for the integral coordinate method by applying equations (13) and (14) to the system Hamiltonian and Lagrangian. From equation (13)

$$P_{\theta_1} = A'\dot{\theta}_1 - 2\dot{\bar{v}} - A'\theta_2\Omega - 2\Omega\bar{u} \qquad (E-1)$$

$$P_{\theta_2} = B'\dot{\theta}_2 + 2\dot{\bar{u}} + B'\theta_1\Omega - C\theta_1\Omega - 2\Omega\bar{v} \qquad (E-2)$$

$$P_{\theta_3} = C\dot{\theta}_3 + C\Omega \qquad (E-3)$$

$$P_{\bar{u}} = \frac{2\dot{\bar{u}}}{RI} + 2\dot{\theta}_2 + 2\theta_1\Omega \qquad (E-4)$$

$$P_{\bar{v}} = \frac{2\dot{\bar{v}}}{RI} - 2\dot{\theta}_1 + 2\theta_2\Omega \qquad (E-5)$$

where

$$RI = \int_{h}^{h+1} pz^2 dz \qquad (E-6)$$

Equations (E-1) through (E-5) where solved simultaneously for $\dot{\theta}_1$, $\dot{\theta}_2$, $\dot{\theta}_3$, $\dot{\bar{u}}$, and $\dot{\bar{v}}$. From equation (14)

$$\dot{P}_{\theta_1} = (B' - C)\Omega\dot{\theta}_2 + 2\Omega\dot{\bar{u}} + (B' - C)\Omega^2\theta_1 - 2\Omega^2\bar{v} \qquad (E-7)$$

$$\dot{P}_{\theta_2} = -A'\Omega\dot{\theta}_1 + 2\Omega\dot{\bar{v}} + (A' - C)\Omega^2\theta_2 + 2\Omega^2\bar{u}$$

$$\dot{P}_{\theta_3} = 0$$

$$\dot{P}_{\bar{u}} = -2\Omega\dot{\theta}_1 + 2(\Omega^2 - \omega_1^2)\frac{\bar{u}}{RI} + 2\Omega^2\theta_2 - \frac{2d}{pRI}\dot{\bar{u}} \qquad (E-10)$$

$$\dot{P}_{\bar{v}} = -2\Omega\dot{\theta}_2 + 2(\Omega^2 - \omega_1^2)\frac{\bar{v}}{RI} - 2\Omega^2\theta_1 - \frac{2d}{pRI}\dot{\bar{v}} \qquad (E-11)$$

Substituting the relations in equations (E-1) through (E-5) into equations (E-7) through (E-11), and after simplification, the expressions of equation (48) may be obtained.

Vita

Vincent Thomas Cilmi was born on 19 January 1948 in Manhattan, New York. He graduated from Sewanhaka High School, Floral Park, New York in 1966 and attended the Georgia Institute of Technology in Atlanta, Georgia from which he received the degree of Bachelor of Aerospace Engineering in September 1970. He received a commission in the Air Force through ROTC and entered pilot training in December 1970. He earned his wings in November 1971 and was subsequently assigned to Mather AFB, California. While at Mather, he served as a T-29 and T-43 Aircraft Commander in the 454th Flying Training Squadron. He entered the School of Engineering, Air Force Institute of Technology, in June 1976.

Permanent address: 1521 Kiefer Avenue
                    Elmont, New York 11003

REPORT DOCUMENTATION PAGE		READ INSTRUCTIONS BEFORE COMPLETING FORM
1. REPORT NUMBER AFIT/GA/AA/77D-1 ✓	2. GOVT ACCESSION NO.	3. RECIPIENT'S CATALOG NUMBER
4. TITLE (and Subtitle) OPTIMAL CONTROL OF AN ORBITING SATELLITE CONTAINING FLEXIBLE APPENDAGES		5. TYPE OF REPORT & PERIOD COVERED MS Thesis
		6. PERFORMING ORG. REPORT NUMBER
7. AUTHOR(s) Vincent T. Cilmi Captain		8. CONTRACT OR GRANT NUMBER(s)
9. PERFORMING ORGANIZATION NAME AND ADDRESS ✓ Air Force Institute of Technology(AFIT-EN) Wright-Patterson AFB, Ohio 45433		10. PROGRAM ELEMENT, PROJECT, TASK AREA & WORK UNIT NUMBERS
11. CONTROLLING OFFICE NAME AND ADDRESS		12. REPORT DATE December 1977
		13. NUMBER OF PAGES 114
14. MONITORING AGENCY NAME & ADDRESS(if different from Controlling Office)		15. SECURITY CLASS. (of this report) Unclassified
		15a. DECLASSIFICATION/DOWNGRADING SCHEDULE

16. DISTRIBUTION STATEMENT (of this Report)

Approved for public release; distribution unlimited

17. DISTRIBUTION STATEMENT (of the abstract entered in Block 20, if different from Report)

18. SUPPLEMENTARY NOTES

Approved for public release; IAW AFR 190-17

JERRAL F. GUESS
Director of Information

19. KEY WORDS (Continue on reverse side if necessary and identify by block number)

Optimal Control
Satellites
Flexible Appendages
Integral Coordinates

20. ABSTRACT (Continue on reverse side if necessary and identify by block number)

This thesis investigated three methods for obtaining
optimal control requirements for satellites having flexible
appendages. A discrete method, modal method, and a new
integral coordinate method for obtaining control require-
ments were examined. Mathematical formulation was performed
on a satellite configuration consisting of a symmetrical
rigid body with two flexible antennas extending in opposite

DD FORM 1473   EDITION OF 1 NOV 65 IS OBSOLETE
1 JAN 73

20. Cont

directions along the spin axis. System equations of motion were derived using Hamilton's equations. Modern optimal control theory, involving the minimization of a quadratic cost functional and the numerical solution to the steady state matrix Riccati equation, was applied to the system. An example problem was presented and numerically solved. The resulting controlled states and control requirements for each method were compared and a discussion of the advantages and disadvantages of the different techniques was presented. The results of this thesis indicate that the integral coordinate technique provides a valid and useful means of obtaining realistic estimates of control requirements for the class of satellites under consideration. The report goes on to recommend further investigation of the integral coordinate method for other spacecraft and satellite configurations.